2022

Frayed connections: How long-term nitrogen additions disrupt plant-soil interactions and the carbon cycle of a temperate forest

Brooke A. Eastman
West Virginia University, be0011@mix.wvu.edu

Frayed connections: How long-term nitrogen additions disrupt plant-soil interactions and the carbon cycle of a temperate forest

Brooke Eastman

Dissertation submitted to
the Eberly College of Arts and Sciences
at West Virginia University

in partial fulfillment of the requirement for the degree of

Doctor of Philosophy in
Biology

William T. Peterjohn, Ph.D., chair
Mary Beth Adams, Ph.D.
Edward Brzostek, Ph.D.
Brenden McNeil, Ph.D.
Ember Morrissey, Ph.D.
Richard Thomas, Ph.D.

Department of Biology

Morgantown, West Virginia

2022

Keywords: carbon cycling; nitrogen deposition; temperate deciduous forest; ecosystem modelling; soil organic matter

Abstract

Frayed connections: How long-term N additions disrupt plant-soil interactions and the carbon cycle of a temperate forest

Brooke A. Eastman

Forests are expected to mitigate some of the negative effects of climate change by sequestering anthropogenic carbon (C) from the atmosphere, but the degree to which they drawn down C will depend on the availability of key nutrients, such as nitrogen (N). There is a fair amount of uncertainty in the future of the forest C sink, mostly owing to the fate of soil organic matter (SOM) and soil heterotrophic respiration to future conditions. In N limited systems, plants allocate a significant amount of their photosynthate belowground for the acquisition of nutrients, but under conditions of chronic N deposition, plants may shift their allocation and nutrient acquisition strategies to favor aboveground production. In turn, this shift in C allocated belowground can cause a chain reaction of response in the soil, influencing the soil C stocks and persistence of soil C under future global changes. In this dissertation, I explore how the tightly coupled C and N cycles influence one another and the C storage potential of a temperate deciduous forest under conditions of elevated N deposition. I employ three diverse methodologies to determine how N availability controls C cycling and storage: a long-term, whole-watershed N addition experiment at the Fernow Experimental Forest; a short-term, targeted experiment of litter decomposition and SOM characterization; and a soil biogeochemical model comparison. These three methodologies allowed me to answer three broad questions: (1) How do potential changes in nutrient acquisition strategies due to chronic N additions impact the forest C sink? (2) What effects does over 25 years of N additions have on the decomposition and formation of SOM? (3) To what extent does soil biogeochemical model structure (first-order decay dynamics versus microbially explicit) impact model representation of C cycle responses to N additions? For question 1, I constructed C and N budgets for the fertilized and a reference watershed in the long-term N addition experiment. I found that over 25 years of N additions led to a shift in C allocation to favor woody biomass production over belowground C flux and increased the soil C stock and C:N ratio of SOM. For question 2, I measured leaf litter decomposition rates for two years in the fertilized and reference watershed, as well as assessed the composition of the SOM. Leaf litter decay rates were slower in the fertilized watershed, especially for low-quality litter (high C:N and lignin:N ratios). Also, there was an accumulation of particulate organic matter, or undecomposed plant-like SOM, in the fertilized watershed, which was positively related to the bulk soil C:N ratio. Finally, for questions 3, I performed a N perturbation experiments using two structurally distinct soil models and compared these results to data from the Fernow Experimental Forest N addition experiment. This comparison allowed us to identify key mechanisms that models do not include, such as enzyme inhibition and shifting vegetation allocation with N additions, which led the models to miss some key observed responses, especially the reduction in soil respiration. Altogether, this dissertation highlights the importance of plant-soil interactions in the cycling of C and N in forest ecosystems, and how elevated N inputs can cause some disconnects between plant and soil processes that control the storage and sequestration of C.

Acknowledgments

I sincerely thank my research advisor, Dr. Bill Peterjohn, for being a great teacher and friend. Your patience, caring demeanor, and big picture mindset guided me through this transformative experience. I also thank my committee members for their guidance and input. Particularly, I thank Dr. Eddie Brzostek for always having an open door as you helped direct both this thesis and my career development; Dr. Mary Beth Adams for advocating for me, introducing me to new opportunities, and helping me to navigate the Fernow Experimental Forest and its wealth of data; Dr. Brenden McNeil for your positive encouragement and the unique perspective you always offered on my research projects and results; Dr. Richard Thomas for keeping it real and having words of wisdom during this challenging life experience; and Dr. Ember Morrissey for teaching me new techniques and always being willing to philosophize about ecology. Also, I am so thankful for the mentorship of Dr. Will Wieder: you taught me so much about ecosystem and earth system models, and your patience, positivity, and trust in me make you an incredible mentor. I thank Dr. Melannie Hartman for your invaluable and continued support of the Fernow modelling project. Thank you, Dr. Jim McGraw, for being an accessible mentor and teaching me about experimental design, statistics, and scientific writing. Above all, this achievement would never have been possible without the immense love and support from my husband, Gerardo Patron-Cano, who helped in the field and kept me fed with organic roasted veggies. And I have tremendous appreciation and love for my son, Omar, who is a daily reminder of why this research is important to me and was a huge force of motivation behind this dissertation. Thank you to my family: Mom, Dad, Chris, Ryan, Nicole, Angela, Lindsay, Mariana, and Ricardo for your bottomless love and support through this journey and always. I am so grateful to Jenny Bardwell and Dr. Sandy Leibhold for providing the supportive friendship, community, and home that allowed me to thrive. And to Molly Martin for the help with baby Omar while I wrote the final chapters of this dissertation. I will always appreciate my fellow grad students for the camaraderie and guidance, especially Roshan Abeyratna, Nannette Raczka, Chansotheary Dang, Joe Carrara, Mark Burnham, Chris Walter, and Justin Mathias. I thank Dr. Joan Centrella, Dr. Debbie Stine, and Dr. Jay Cole for introducing me to science policy and empowering me to pursue opportunities and a career in this field. I thank the many undergrads who helped with field and lab work including Matthew Marsh, Hannah Walls, Liz Matejczyk, Misty Wilson, Andrea Blankenship, Matt Green, Hannah Minihan, and Rachel McCoy. Thank you to the Department of Biology for the generous support during my tenure. Thank you to the staff at the Fernow Experimental Forest for supporting the long-term research experiments, especially Chris Cassidy, Freddie Wood, Melissa Thomas-Van Gundy. This research was funded by the National Science Foundation Long-Term Research in Environmental Biology (LTREB) program (DEB). Further support came from the National Center for Atmospheric Research (NCAR) Advanced Study Program, NCAR supercomputing allocation award, West Virginia University STEM dissertation completion grant, the Anthony J. Haefner Memorial Scholarship, the Professor Charles H. Baer Graduate Scholarship, and the Department of Biology.

“We need to have a whole cultural shift, where it becomes our culture to take care of the Earth, and in order to make this shift, we need storytelling about how the Earth takes care of us and how we can take care of her.”

- Xiye Bastida

Table of Contents

List of Tables

List of Figures

Chapter 1. Introduction and Main Objectives

Forests provide many ecosystem services including storing about 45% of all terrestrial carbon (C) and sequestering up to 25% of anthropogenic carbon dioxide (CO_2) emissions (Bonan, 2008; Pan *et al.*, 2011a). Of all of earth's forests, temperate forests in the northern hemisphere appear to be a particularly significant component of the global land C sink (Ollinger *et al.*, 2008; Pan *et al.*, 2011a), in part because of their relatively young age that lends to greater rates of C storage (Amiro *et al.*, 2010; Besnard *et al.*, 2018). However, forest ecosystems are facing various rapid changes, and predicting their response to complex changes and their interactions has proved challenging (Friedlingstein *et al.*, 2014). Global changes, such as shifts in precipitation regimes, elevated atmospheric CO_2, and variations in nitrogen (N) and sulfur (S) deposition interact in complex ways that will influence the magnitude of forest C sequestration in the future (Terrer *et al.*, 2017b; Mathias & Thomas, 2018; Walker *et al.*, 2020).

One such change, enhanced N deposition, has amplified N availability in many forest ecosystems, with implications for the global C cycle (Galloway *et al.*, 2004). Primarily through the burning of fossil fuels and high temperature combustion, emissions of nitrogen oxides ($NO_{x)}$ and subsequent increases in N deposition (a key component of acid rain) has elevated N availability in large regions of temperate forest. This additional N deposition affects forest ecosystems in many ways: by acidifying soil, causing eutrophication in streams and downstream water bodies, increasing plant productivity, and reducing plant diversity – especially in the herbaceous layer (Lovett *et al.*, 2009; Gilliam, 2019). Because temperate forests are historically limited, or co-limited, by N availability, enhanced inputs of N releases forests from N limitation and enhances the forest C sink by stimulating plant growth (Vitousek & Howarth, 1991; Elser *et al.*, 2007; Thomas *et al.*, 2010; Du & de Vries, 2018).

In addition to enhanced vegetation production, N deposition can have additional direct and indirect impacts on forest C cycling, especially belowground. Directly, augmented N in forest soils may inhibit soil enzymes that degrade lignin, a C-rich, N-poor, recalcitrant plant compound abundant in woody material (Carreiro *et al.*, 2000; Treseder, 2004). Indirectly, N deposition can shift microbial communities and their function, leading to cascading effects on the decomposition and formation of soil organic carbon stocks (Ramirez *et al.*, 2012; Morrison *et al.*, 2016; Moore *et al.*, 2021). Furthermore, plant-soil interactions can be altered by N additions, such as the potential for shifts in plant tissue C:N ratios to influence microbial biochemistry (Midgley & Phillips, 2016), or the ability of reduced total belowground carbon flux by trees to increase C limitation of soil microbes (Gill & Finzi, 2016). These shifts in plant-soil interactions with N additions typically result in lower rates of organic matter decomposition by soil microbes, and reduced soil CO_2 efflux to the atmosphere (Janssens *et al.*, 2010).

Despite our general understanding of how soils respond to experimental N additions over short periods of time, how soils will respond to prolonged changes in the global environment are highly uncertain, with estimates ranging from soils being a net C sink to becoming a net C source (Todd-Brown *et al.*, 2013; Bond-Lamberty *et al.*, 2018). To advance our understanding, we need to integrate observational data, long-term experiments, and theoretical models to determine functional relationships between soil C cycling processes and global change drivers. Since soils contain more than twice the amount of C as vegetation (Quéré *et al.*, 2018), and because this C stock may be particularly sensitive to future environmental changes (Melillo *et al.*, 2017; Craine *et al.*, 2018; Ofiti *et al.*, 2021), improving our predictive capabilities of future C stocks in soils is of high priority for developing efficient climate change policy and forest management strategies.

Although rare, there are a few locations where long-term observations and experiments can provide insights into the effects that environmental changes can have on the response of critical

ecosystem processes that occur over decadal time scales. One such location is the Fernow Experimental Forest (Fernow) in West Virginia, USA (39.03° N, 79.67° W) where a 30-year, whole-watershed, N-fertilization experiment provides a unique opportunity to examine the persistent effects of enhanced N additions on C and N cycling in the temperate forests of the Central Appalachian Mountains—a region of historically high levels on atmospheric N deposition.

The Fernow whole-watershed fertilization experiment consists of two forested catchments. The treatment watershed (+N WS3; 34 ha) has received 35.4 kg N ha^{-1} $year^{-1}$ as $(NH_4)_2SO_4$ via helicopter or airplane since 1989. An adjacent watershed (Ref WS7; 24 ha) with a similarly aged stand of trees serves as a reference (Adams et al., 2006). The +N WS3 was most recently clear-cut between 1969-1970, leaving a shade strip along the stream channel until 1972 when the shade strip was also cut, and the forest was allowed to regrow naturally. Ref WS7 was clear-cut in two sections: the upper half in 1963-1964 and the lower half in 1966-1967. Following cutting, both sections of Ref WS7 were kept barren with herbicides until 1969 when the forest was allowed to regrow naturally.

For this study I synthesized a diversity of long- and short-term measurements from these watersheds to examine the effects that decades of elevated N inputs had on C storage and partitioning in a temperate forest ecosystem. Most observations for this synthesis were made at one of three sets of plots in each watershed: (1) “Dendrometer plots”: 10 plots per watershed used to measure the growth since 2011 of four dominant tree species, as well other recent observations of soil respiration, bulk density, organic horizon mass, litterfall, and N mineralization; (2) “Permanent growth plots”: 25 locations in each watershed used to monitor long-term tree growth, tree mortality, and litterfall; and (3) “Soil pits”: 15 locations per watershed where a ~ 30 x 30 cm area of soil was excavated and samples collected from the

organic horizon, and mineral horizon depths of 0-10 cm, 10-20 cm, 20-30 cm, and 30-45 cm. I also used the "Dendrometer plots" to conduct a targeted, short-term (2-year), reciprocal litter transplant experiment in order to better understand the effect of long-term N additions on the dynamics of leaf litter decay and the storage of soil carbon in various soil organic matter fractions that have become the focus of an emerging theoretical understanding of soil organic matter formation (Schmidt *et al.,* 2011; Cotrufo *et al.,* 2015; Lehman & Kleber, 2015).

Although valuable, the scarcity of long-term observations and experiments limits our ability to assess their broader implications for many questions surrounding changes in the global environment, such as global climate change. Thus, as goals and policies for greenhouse gas emissions are created to mitigate and adapt to climate change, we depend on modelled projections of the magnitude of the land C sink over the next century. But, computational models can also aid in scientific discovery by: 1) offering the opportunity to test our hypotheses and theoretical framing of how ecosystems are structured and function; 2) allowing us to assess the broader implications of experimental findings at various spatial and temporal scales; and 3) predicting future conditions as well as ecosystem responses to those future conditions.

In response to concerns about our changing climate, recent model development efforts have focused on capturing the response of the land C sink to global change – especially for forest ecosystems (Wieder *et al.,* 2013; Fisher *et al.,* 2014; Wieder *et al.,* 2015; Brzostek *et al.,* 2017). Forests are currently expected to slow the rate at which anthropogenic CO_2 emissions will accumulate in the atmosphere through C sequestration, thereby mitigating global warming to some extent (Ainsworth & Long, 2005; Arora *et al.*, 2013). However, the magnitude and longevity of this effect is uncertain, and while we expect N limitation to constrain the positive CO_2-fertilization effect on the forest growth (Norby *et al.*, 2010a; Craine *et al.,* 2018; Groffman *et al.,* 2018; Terrer *et al.,* 2019b), we have not thoroughly developed and validated how Earth

System Models represent N cycling (Thomas *et al.*, 2015; Meyerholt *et al.*, 2020). Most Earth System Models now incorporate the N cycle and some of the key processes by which N and C cycles interact. But despite these efforts, the land C sink, especially soil C stocks and belowground microbial C-N interactions, remain the greatest sources of uncertainty in global C cycle models (Fisher *et al.*, 2014; Arora *et al.*, 2020).

Despite the apparent need to add microbially explicit soil biogeochemical processes to Earth System Models, doing so introduces additional uncertainty associated with how critical processes are represented and parameterized. Thus, to determine whether model refinements are worth the added uncertainty and computational cost, we need to assess the performance of more complex models by comparing their outputs against observational benchmarks, especially against long-term experimental data that may simulate future conditions (Wieder *et al.*, 2019a). Tests against long-term data are critical because they allow us to determine whether models can capture the influence of important processes that are slow to respond, such as changes in soil C stocks or shifts in species composition (Harden *et al.*, 2018). Thus, integrating results from long-term experiments, like those from the Fernow, with heuristic models will allow us to identify the most important processes driving C cycling, and determine which processes are most sensitive to environmental change.

In this dissertation I utilized a variety of approaches to enhance our understanding and prediction of forest ecosystem responses to N deposition, including long-term experiments, targeted short-term experiments, and the testing and refinement of existing computational models. In *Chapter 2*, I synthesize over 25 years of observational data to create C and N budgets from a long-term, whole-watershed, N fertilization experiment at the Fernow Experimental Forest. In *Chapter 3*, I build off the main findings and knowledge gaps from this synthesis to determine the difference in leaf litter decomposition rates and soil organic matter characteristics

between the fertilized and reference watersheds of the long-term N addition experiment. Finally, in *Chapter 4*, I use a unique soil biogeochemical model testbed to evaluate how model structure (i.e., microbially implicit vs. microbially explicit decay dynamics) impacts model predictions of forest ecosystem responses to N additions, and I compare these predictions with data from the long-term N addition experiment at the Fernow and use these comparisons to guide model refinements. Altogether, the diverse methods used for my dissertation allowed us to fill in gaps in our understanding of how long-term N additions impact forest C cycling, especially the formation and decomposition of soil organic matter.

Main objectives

In this dissertation, I used three approaches to enhance our understanding of how forest ecosystems can respond to enhanced N inputs. The main goal of this dissertation was to examine how N deposition impacts plant-soil interactions and the implications this has for the land-atmosphere exchange of C.

In **Chapter 2**, I took advantage of the extensive observations at the Fernow long-term N addition experiment to synthesize the ecosystem C and N cycle responses to over 25 years of N fertilization to address the question:

> *How do potential changes in nutrient acquisition strategies due to chronic N additions impact the forest C sink?*

In **Chapter 3**, I used the results from my synthesis to design a targeted field experiment to examine the question:

> *What effects does over 25 years of N additions have on the decomposition and fate of soil organic matter?*

And finally, in **Chapter 4** I tested and compared the performance of two structurally different soil biogeochemical models using observations from the Fernow to answer the question:

> *To what extent does soil biogeochemical model structure (first-order decay dynamics vs. microbially explicit) impact model performance in response to N additions?*

Literature cited

Adams MB, DeWalle DR, Hom JL eds. 2006. The Fernow Watershed Acidification Study. Dordrecht, the Netherlands: Springer.

Ainsworth EA, Long SP. 2005. What have we learned from 15 years of free-air CO_2 enrichment (FACE)? A meta-analytic review of the responses of photosynthesis, canopy properties and plant production to rising CO2. *New Phytologist* **165**: 351–372.

Amiro BD, Barr AG, Barr JG, Black TA, Bracho R, Brown M, Chen J, Clark KL, Davis KJ, Desai AR, *et al.* 2010. Ecosystem carbon dioxide fluxes after disturbance in forests of North America. *Journal of Geophysical Research: Biogeosciences* **115:** G00K02.

Arora VK, Boer GJ, Friedlingstein P, Eby M, Jones CD, Christian JR, Bonan G, Bopp L, Brovkin V, Cadule P, *et al.* 2013. Carbon-concentration and carbon-climate feedbacks in CMIP5 earth system models. *Journal of Climate* **26**: 5289–5314.

Arora VK, Katavouta A, Williams RG, Jones CD, Brovkin V, Friedlingstein P, Schwinger J, Bopp L, Boucher O, Cadule P, *et a*l. 2020. Carbon-concentration and carbon-climate feedbacks in CMIP6 models and their comparison to CMIP5 models. *Biogeosciences* **17**: 4173–4222.

Besnard S, Carvalhais N, Arain MA, Black A, De Bruin S, Buchmann N, Cescatti A, Chen J, Clevers JGPW, Desai AR, *et al.* 2018. Quantifying the effect of forest age in annual net forest carbon balance. *Environmental Research Letters* **13:** 124018.

Bonan GB. 2008. Forests and climate change: Forcings, feedbacks, and the climate benefits of forests. *Science* **320**: 1444–1449.

Bond-Lamberty B, Bailey VL, Chen M, Gough CM, Vargas R. 2018. Globally rising soil heterotrophic respiration over recent decades. *Nature* **560**: 80–83.

Brzostek ER, Rebel, K., Smith, K.R., Phillips, R.P. 2017. Chapter 26 - Integrating mycorrhizae into global scale models: A journey toward relevance in the Earth's climate system. In: Johnson, N.C., Gehring, C., Jansa, J., eds. *Mycorrhizal mediation of soil: fertility, structure, and carbon storage.* Elsevier, 479-499.

Carreiro MM, Sinsabaugh RL, Repert DA, Parkhurst DF. 2000. Microbial Enzyme Shifts Explain Litter Decay Responses to simulated nitrogen deposition. *Ecology* **81**: 2359–2365.

Cotrufo MF, Soong JL, Horton AJ, Campbell EE, Haddix ML, Wall DH, Parton WJ. 2015. Formation of soil organic matter via biochemical and physical pathways of litter mass loss. *Nature Geoscience* **8**: 776–779.

Craine JM, Elmore AJ, Wang L, Aranibar J, Bauters M, Boeckx P, Crowley BE, Dawes MA, Delzon S, Fajardo A, et al. 2018. Isotopic evidence for oligotrophication of terrestrial ecosystems. *Nature Ecology and Evolution* **2**: 1735–1744.

Du E, de Vries W. 2018. Nitrogen-induced new net primary production and carbon sequestration in global forests. *Environmental Pollution* **242**: 1476–1487.

Elser JJ, Bracken MES, Cleland EE, Gruner DS, Harpole WS, Hillebrand H, Ngai JT, Seabloom EW, Shurin JB, Smith JE. 2007. Global analysis of nitrogen and phosphorus limitation of primary producers in freshwater, marine and terrestrial ecosystems. *Ecology Letters* **10**: 1135–1142.

Fisher JB, Huntzinger DN, Schwalm CR, Sitch S. 2014. Modeling the Terrestrial Biosphere. *Annual Review of Environment and Resources* **39**: 91–123.

Friedlingstein P, Meinshausen M, Arora VK, Jones CD, Anav A, Liddicoat SK, Knutti R. 2014. Uncertainties in CMIP5 climate projections due to carbon cycle feedbacks. *Journal of Climate* **27**: 511–526.

Galloway JN, Dentener FJ, Capone DG, Boyer EW, Howarth RW, Seitzinger SP, Asner GP, Cleveland CC, Green PA, Holland EA, *et al*. 2004. Nitrogen cycles: Past, present, and future. *Biogeochemistry* **70**: 153-226.

Gill AL, Finzi AC. 2016. Belowground carbon flux links biogeochemical cycles and resource-use efficiency at the global scale. *Ecology Letters* **19**: 1419–1428.

Gilliam FS. 2019. Excess nitrogen in temperate forest ecosystems decreases herbaceous layer diversity and shifts control from soil to canopy structure. *Forests* **10**, 66.

Groffman PM, Driscoll CT, Durán J, Campbell JL, Christenson LM, Fahey TJ, Fisk MC, Fuss C, Likens GE, Lovett G, *et al.* 2018. Nitrogen oligotrophication in northern hardwood forests. *Biogeochemistry* **141:** 523–539.

Harden JW, Hugelius G, Ahlström A, Blankinship JC, Bond-Lamberty B, Lawrence CR, Loisel J, Malhotra A, Jackson RB, Ogle S, *et al.* 2018. Networking our science to characterize the state, vulnerabilities, and management opportunities of soil organic matter. *Global Change Biology* **24**: e705–e718.

Janssens IA a., Dieleman W, Luyssaert S, Subke J, Reichstein M, Ceulemans R, Ciais P, Dolman AJ, Grace J, Matteucci G, *et al.* 2010. Reduction of forest soil respiration in response to nitrogen deposition. *Nature Geoscience* **3**: 315–322.

Kochenderfer JN. 2006. Fernow and the Appalachian Hardwood Region. In: Adams MB, DeWalle DR, Hom JL, eds. The Fernow Watershed Acidification Study. Springer, 17–39.

KC. 2009. Effects of Air Pollution on Ecosystems and Biological Diversity in the Eastern United States. *Annals of the New York Academy of Sciences* **1162**: 99–135.

Lehmann J, Kleber M. 2015. The contentious nature of soil organic matter. Nature 528: 60–68.

Lovett GM, Tear TH, Evers DC, Findlay SEG, Cosby BJ, Dunscomb JK, Driscoll CT, Weathers KC. 2009. Effects of Air Pollution on Ecosystems and Biological Diversity in the Eastern United States. *Annals of the New York Academy of Sciences* **1162**: 99–135.

Mathias JM, Thomas RB. 2018. Disentangling the effects of acidic air pollution, atmospheric CO_2, and climate change on recent growth of red spruce trees in the Central Appalachian Mountains. *Global Change Biology* **24**: 3938–3953.

Melillo JM, Frey SD, DeAngelis KM, Werner WJ, Bernard MJ, Bowles FP, Pold G, Knorr MA, Grandy AS. 2017. Long-term pattern and magnitude of soil carbon feedback to the climate system in a warming world. *Science* **358**: 101-105.

Meyerholt, J, Sickel, K, Zaehle, S. 2020. Ensemble projections eludicate effects of uncertainty in terrestrial nitrogen limitation on future carbon uptake. *Global Change Biology* **26:** 3978-3996.

Midgley MG, Phillips RP. 2016. Resource stoichiometry and the biogeochemical consequences of nitrogen deposition in a mixed deciduous forest. *Ecology* **97**: 3369–3377.

Moore JAM, Anthony MA, Pec GJ, Trocha LK, Trzebny A, Geyer KM, van Diepen LTA, Frey SD. 2021. Fungal community structure and function shifts with atmospheric nitrogen deposition. *Global Change Biology* **27**: 1349–1364.

Morrison EW, Frey SD, Sadowsky JJ, van Diepen LTA, Thomas WK, Pringle A. 2016. Chronic nitrogen additions fundamentally restructure the soil fungal community in a temperate forest. *Fungal Ecology* **23**: 48–57.

Norby RJ, Warren JM, Iversen CM, Medlyn BE, McMurtrie RE. 2010. CO_2 enhancement of forest productivity constrained by limited nitrogen availability. *Proceedings of the National Academy of Sciences* **107**: 19368–19373.

Ofiti NOE, Zosso CU, Soong JL, Solly EF, Torn MS, Wiesenberg GLB, Schmidt MWI. 2021. Warming promotes loss of subsoil carbon through accelerated degradation of plant-derived organic matter. *Soil Biology & Biochemistry* **156**: 108185.

Ollinger S V, Richardson AD, Martin ME, Hollinger DY, Frolking SE, Reich PB, Plourde LC, Katul GG, Munger JW, Oren R, *et al*. 2008. Canopy Nitrogen, Carbon Assimilation, and Albedo in Temperate and Boreal Forests: Functional Relations and Potential Climate Feedbacks. *Proceedings of the National Academy of Sciences* **105**: 19336–19341.

Pan Y, Birdsey RA, Fang J, Houghton R, Kauppi PE, Kurz WA, Phillips OL, Shvidenko A, Lewis SL, Canadell JG, *et al*. 2011. A large and persistent carbon sink in the world's forests. *Science* **333**: 988–993.

Quéré C, Andrew R, Friedlingstein P, Sitch S, Hauck J, Pongratz J, Pickers P, Ivar Korsbakken J, Peters G, Canadell J, *et al.* 2018. Global Carbon Budget 2018. *Earth System Science Data* **10**: 2141–2194.

Ramirez KS, Craine JM, Fierer N. 2012. Consistent effects of nitrogen amendments on soil microbial communities and processes across biomes. *Global Change Biology* **18**: 1918–1927.

Schmidt MWI, Torn MS, Abiven S, Dittmar T, Guggenberger G, Janssens I a., Kleber M, Kögel-Knabner I, Lehmann J, Manning D a. C, *et al.* 2011. Persistence of soil organic matter as an ecosystem property. *Nature* **478**: 49–56.

Terrer C, Jackson RB, Prentice IC, Keenan TF, Kaiser C, Vicca S, Fisher JB, Reich PB, Stocker BD, Hungate BA, *et al.* 2019. Nitrogen and phosphorus constrain the CO_2 fertilization of global plant biomass. *Nature Climate Change* **9:** 684–689.

Terrer C, Vicca S, Stocker BD, Hungate BA, Phillips RP, Reich PB, Finzi AC, Prentice IC. 2017. Ecosystem responses to elevated CO_2 governed by plant-soil interactions and the cost of nitrogen acquisition. *New Phytologist* **217**: 347–355.

Thomas RQ, Brookshire ENJ, Gerber S. 2015. Nitrogen limitation on land: How can it occur in Earth system models? *Global Change Biology* **21**: 1777–1793.

Thomas RQ, Canham CD, Weathers KC, Goodale CL. 2010. Increased tree carbon storage in response to nitrogen deposition in the US. *Nature Geoscience* **3**: 13–17.

Todd-Brown KEO, Randerson JT, Post WM, Hoffman FM, Tarnocai C, Schuur EAG, Allison SD. 2013. Causes of variation in soil carbon simulations from CMIP5 Earth system models and comparison with observations. *Biogeosciences* **10**: 1717–1736.

Treseder KK. 2004. A meta-analysis of mycorrhizal responses to nitrogen, phosphorus, and atmospheric CO_2 in field studies. *New Phytologist* **164**: 347–355.

Vitousek PM, Howarth RW. 1991. Nitrogen Limitation on Land and in the Sea : How Can It Occur? *Biogeochemistry* **13**: 87–115.

Walker AP, De Kauwe MG, Bastos A, Belmecheri S, Georgiou K, Keeling RF, McMahon SM, Medlyn BE, Moore DJP, Norby RJ, *et al*. 2020. Integrating the evidence for a terrestrial carbon sink caused by increasing atmospheric CO_2. *New Phytologist* **229:** 2413–2445.

Wieder WR, Bonan GB, Allison SD. 2013. Global soil carbon projections are improved by modelling microbial processes. *Nature Climate Change* **3**: 909–912.

Wieder WR, Cleveland CC, Smith WK, Todd-Brown K. 2015. Future productivity and carbon storage limited by terrestrial nutrient availability. *Nature Geoscience* **8**: 441–444.

Chapter 2. Altered plant carbon partitioning enhanced forest ecosystem carbon storage after 25 years of nitrogen additions

"If humans are to help reverse global warming, we will need to step into the flow of the carbon cycle in new ways, stopping our excessive exhale of carbon dioxide and encouraging the winded ecosystems of the planet to take a good long inhale as they heal. It will mean learning to help the helpers, those microbes, plants, and animals that do the daily alchemy of turning carbon into life."

- **Janine Benyus**

Reprinted from

Eastman, B.A., Adams, M.B., Brzostek, E.R., Burnham, M.B., Carrara, J.E., Kelly, C., McNeil, B.E., Walter, C.A., Peterjohn, W.T., 2021. Altered plant carbon partitioning enhanced forest ecosystem carbon storage after 25 years of nitrogen additions. *New Phytologist* **230:** 1435–1448.

2.1 Abstract

Decades of atmospheric nitrogen (N) deposition in the northeastern USA have enhanced this globally important forest carbon (C) sink by relieving N limitation. While many N fertilization experiments found increased forest C storage, the mechanisms driving this response at the ecosystem scale remain uncertain. Following the optimal allocation theory, augmented N availability may reduce belowground C investment by trees to roots and soil symbionts. To test this prediction and its implications on soil biogeochemistry, we constructed C and N budgets for a long-term, whole-watershed N fertilization study at the Fernow Experimental Forest, WV, USA. N fertilization increased C storage by shifting C partitioning away from belowground components and towards aboveground woody biomass production. Fertilization also reduced the C cost of N acquisition, allowing for greater C sequestration in vegetation. Despite equal fine litter inputs, the C and N stocks and C : N ratio of the upper mineral soil were greater in the fertilized watershed, likely due to reduced decomposition of plant litter. By combining aboveground and belowground data at the watershed scale, this study demonstrates how plant C allocation responses to N additions may result in greater C storage in both vegetation and soil.

2.2 Introduction

Historically high rates of nitrogen (N) deposition across temperate forests in the northern hemisphere (Galloway *et al.*, 2008; Fowler *et al.*, 2013) often alleviated N-limitation (LeBauer & Treseder 2008) and enhanced this important terrestrial carbon (C) sink (Pan *et al.*, 2011; Schulte-Uebbing & de Vries 2017; O'Sullivan *et al.*, 2019). Experimental N additions to aggrading temperate forests typically cause greater biomass accumulation, decreased soil respiration, and enhanced soil C (Xia & Wan 2008; Janssens *et al.*, 2010; Liu & Greaver 2010; Lovett *et al.*, 2013; Frey *et al.*, 2014; de Vries *et al.*, 2014). However, few N addition experiments have persisted long enough and at an ecologically relevant spatial scale to allow a more complete expression of mechanisms that enhance woody biomass or the feedback of plant responses

to soil biogeochemistry. Plant-microbial interactions significantly shape the biogeochemistry of ecosystems through the exchange of C for N between plants and microbes, which modulates plant NPP and alters the stabilization and mineralization of soil C (Chapman *et al.*, 2006; Drake *et al.*, 2011; Phillips *et al.*, 2013a; Terrer *et al.*, 2016). Thus, quantifying the responses of both above- and below-ground ecosystem components to experimental N additions is needed to determine the mechanisms underlying these responses, and to predict how these ecosystems will respond to reduced N inputs and other environmental changes (Schmidt *et al.*, 2011; Averill & Waring 2017; Zak *et al.*, 2017).

Such widely observed responses to experimental N additions (e.g. enhanced aboveground biomass and reduced soil respiration) are generally consistent with the optimal allocation theory of Bloom, Chapin, and Mooney (1985), in which plants adjust to optimally partition resources for the acquisition of the most limiting resource. Given this theory, 'subsidies' of N to a N-limited ecosystem should reduce the C cost of N acquisition by lessening N limitation, allowing plants to partition C towards acquiring other limiting resources (e.g. light; Johnson *et al.*, 1997; Mohan *et al.*, 2014). Consequently, we expect elevated N inputs to shift plant C flux away from belowground N acquisition and towards aboveground productivity. Given recent research highlighting the importance of belowground C inputs in fueling decomposition (Sulman *et al.*, 2017), this allocation shift could initiate a plant-soil feedback in which less C flux to mycorrhizae and microbial priming of soil organic matter (SOM) decomposition may increase soil C stocks (Gill & Finzi, 2016; Carrara *et al.*, 2018) and ultimately reduce mineralization rates of essential plant nutrients. An important assumption of optimal resource allocation theory is that resource availability changes slowly through synchronous changes in C and N fluxes, and it is uncertain whether the theory applies at the whole-ecosystem scale and in ecosystems experiencing fairly rapid changes in the environment—such as N additions (Bloom *et al.* 1985; Phillips *et al.* 2013).

Unsurprisingly, many gaps in our empirical knowledge of ecosystem responses to N deposition are mirrored in Earth system models (ESMs), at times leading to uncertain predictions of the future C sink. Recent model improvements have used observational benchmarks to improve the representation of C-N

dynamics (Thornton *et al.*, 2007; Wieder *et al.* 2015; Terrer *et al.* 2019), and plant-microbe interactions (Shi *et al.*, 2016, 2019). Yet, these models do not capture the commonly observed reduction in soil respiration with N additions (Janssens *et al.*, 2010). Specifically, the current generation of ESMs often respond to elevated N deposition with increased NPP to all plant components and an accumulation of soil C through greater plant litter inputs, as opposed to a shift in C partitioning and subsequent decrease in decomposition rates (Ise *et al.*, 2010; Bellassen *et al.*, 2011; Todd-Brown *et al.*, 2013; Fernández-Martínez *et al.*, 2016; Montané *et al.*, 2017; Sulman *et al.*, 2017). One reason models cannot capture these widespread ecosystem responses to N deposition is that their structures lack the plant-microbe interactions controlling these patterns (e.g. reduced belowground C flux slowing microbial decomposition; Fisher *et al.*, 2019; Meyerholt *et al.*, 2020). Thus, long-term experimental data are invaluable for clarifying mechanisms behind ecosystem responses and restructuring models to better capture the N impacts on global C cycling (Wieder *et al.*, 2019; Davies-Barnard *et al.*, 2020).

In this study, we utilized data from the whole-watershed N addition study at the Fernow Experimental Forest (Fernow) in West Virginia, USA, to examine the effects of 25+ years of elevated N inputs on ecosystem C storage and partitioning. The abundant and long-term data from this site provide a rare opportunity to assess how N additions influence C and N interactions in a temperate deciduous forest over decadal time scales, and help clarify mechanisms that may influence the terrestrial C sink and constrain global C models. We constructed C and N budgets for two adjacent watersheds after 25+ years of ammonium sulfate ($(NH_4)_2SO_4$) additions to one watershed. From these budgets, we synthesized the C and N stocks and fluxes of major forest ecosystem components, estimated changes in plant C allocation and identified some potential mechanisms behind the ecosystem response to chronic N additions. More specifically, we used these budgets to explore three questions: (1) How do N additions affect tree C allocation and ultimately impact productivity over the long term?; (2) Does a reduction in the C cost of N acquisition act as an important mechanism driving changes in the plant C pools and fluxes with N additions?; and (3) What are the impacts of the tree responses to N addition on soil biogeochemistry?

2.3 Materials and Methods

Study site

Located in the Allegheny Mountain region of the Central Appalachian Mountains, the Fernow Experimental Forest, near Parsons, WV (39.03° N, 79.67° W), hosts over 80 years of ecological monitoring and experimentation, including a whole-watershed N addition experiment (Adams *et al.*, 2012). Elevations range from 530-1,115 m, and slopes are typically between 20-50%. Soils are shallow (<1 m) and predominantly Calvin channery silt loam (*Typic Dystrochrept*), underlain with fractured sandstone and shale. Mean monthly air temperatures range from ~ -2.8°C in January to ~ 20°C in July, with a growing season from May through October (Table 2-1; Young *et al.*, 2019). Mean annual precipitation is ~146 cm and evenly distributed across seasons.

The whole-watershed N addition experiment consists of two adjacent watersheds in a broadleaf deciduous forest (Fig. 2-1). From January 1989 through October 2019, one watershed (+N WS3; 34 ha) received 3.5 g N m^{-2} y^{-1} as $(NH_4)_2SO_4$, which was about double the rate of ambient N in throughfall at the start of the experiment (Helvey & Kunkle, 1986) and about quadruple the rate of N deposition at the end of the experiment (NADP site WV18; CASTNET site PAR107). Fertilizer treatments were distributed in three unequal applications per year that roughly mimicked the temporal pattern of ambient deposition. An adjacent watershed (Ref WS7; 24 ha) serves as a reference to the fertilized watershed (Adams *et al.*, 2006). Forest stands in the watersheds were ~18-19 years old when the experiment began (1989; Table 2-1). Differences in land use history are summarized in Table 2-1, with a major difference being that Ref WS7 was maintained barren with herbicides for 3-6 years prior to recovery, which likely contributed to the greater baseline streamwater nitrate (NO_3^-) flux prior to treatment (Fig. S2-5; see also Kochenderfer & Wendel, 1983; Kochenderfer, 2006). Tree species are similar in both watersheds, however their relative abundance differs slightly, with +N WS3 dominated by *Prunus serotina* and *Acer rubrum* and Ref WS7 dominated by *Liriodendron tulipifera*, *P. serotina*, and *Betula lenta* (Fig. S2-1). One N-fixing tree,

Robinia pseudoacacia, is present in both watersheds and, according to tree censuses in 2016 and 2018, makes up <7% of the basal area in the Ref WS7 and <1% in +N WS3.

Assessing the impacts of N additions on watershed C and N budgets

In this study, we synthesized a variety of data collected by several researchers over the course of the experiment to: 1) construct watershed-level C and N budgets; 2) gain insight into the response of biogeochemical cycles to chronic N additions; and 3) assess the implications for the temperate forest C sink. These data were collected over various time scales and locations (Fig. 2-1), and the budgets provided an integrated picture of the C and N stocks after 25+ years of N additions (typically from data collected between 2012-2019). Below we describe the methods used to determine major C and N pools (e.g., aboveground biomass, fine root biomass, and soil stocks) and fluxes (e.g. aboveground net primary productivity (ANPP), foliar N resorption, fine root production, soil respiration, and inorganic N discharge). The budgets were also used to examine how N additions influence plant resource economics (e.g. C partitioning & the C cost of N acquisition). The C and N concentrations of many ecosystem components were determined using standard methods, especially Dumas combustion using an elemental analyzer (e.g., NA 1500 Series 2, Carlo Erba Instruments). When combining datasets across various years or plots, standard errors were propagated analytically (Methods S2-1; Lehrter & Cebrian, 2010). Additional details on data collection are found in the Supplementary Information.

Aboveground biomass and productivity

Aboveground woody biomass was estimated from permanent growth plot data collected by the USFS Northern Research Station (Fig. 2-1; Adams *et al.*, 2006). Briefly, all trees >2.54 cm in diameter at breast height (DBH) were measured and permanently tagged at 25 randomly located 405-m^2 plots established in 1990 (+N WS3) or 1991 (Ref WS7). All trees were re-measured during the dormant seasons of 1996, 1999, 2003, 2009, and the summer of 2018. DBH was converted to biomass increments using species-specific allometric equations (Brenneman *et al.*, 1978; M.B. Adams, unpublished data). For species

without specific allometric parameters, we used parameters from tree species with similar wood densities (Miles & Smith, 2009).

To estimate total aboveground woody C and N pools, wood C and N concentrations were applied to the 2018 growth-plot biomass estimates. Wood C and N concentrations of the outer 1 cm of bole wood were measured in the summer of 2016 from 10 trees of each of the four dominant tree species in both watersheds (Table S2-1). Because wood N concentrations are often greater in the outer 1 cm of bole wood, we multiplied N content by a heartwood:sapwood ratio of 0.76 to obtain conservative estimates of wood N stocks (Meerts, 2003). For unsampled tree species, the watershed average wood C and N concentrations were used.

Mean annual rates of net aboveground wood C and N accumulation were calculated using the difference between pools of two consecutive DBH censuses (growth + ingrowth – mortality) divided by the number of years between measurements. To estimate total ANPP, annual leaf litterfall mass data (1989-2015, n=25) were converted into C flux estimates and added to net wood C increments (see Adams, 2008). Neither species composition nor nutrient concentrations of the long-term litterfall data were measured, so the C and N inputs of fine litter were estimated from 10 additional litter-collection plots in the autumns of 2015-2017 (Fig. 2-1; Methods S2-2; Table S2-2). Assuming litter mass varied more from year-to-year than litter C concentrations, we applied the mean of all plot-level litter C concentrations (total g of C per g of leaf litter) across three years (n=30) to the long-term litterfall mass data (n=25). Total ANPP was estimated for each plot then averaged to determine the mean watershed ANPP (n=25), and error was propagated analytically (Methods S2-1).

Fine root pools, production, and turnover

Methods of fine root measurements are detailed in Table S2-3. Briefly, fine root biomass was measured in the organic horizon in the summers of 2012, 2013, and 2015. In 2012 and 2013, two subsamples of fine roots in the organic horizon were measured at seven plots (Fig. 2-1; W.T. Peterjohn, unpublished data); in 2015, one organic horizon sample was collected from the same plots plus three

additional plots per watershed (see Carrara *et al.* 2018). Fine root biomass was measured in the mineral horizon in 1991, 2013, 2015, and 2016 to depths of 45, 15, 15, and 10 cm, respectively (Adams, 2016; W,T, Peterjohn, unpublished data; Carrara *et al.*, 2018; B.A. Eastman and W.T. Peterjohn, unpublished data). In 2016, fine roots in the mineral soil (10 cm) were measured at 60 locations (six subsamples x 10 plots) per watershed. Fine roots collected in 2012, 2013, and 2016 were analyzed for C and N concentration. To compare fine root C and N stocks between years, the mean C and N concentrations of fine roots measured in 2012, 2013, 2016 were applied to 1991 and 2015 fine root biomass. To adjust for the shallower depth of sampling in 2016 (0-10 versus 0-15 cm), the 2016 mass estimates were increased 150% when performing statistical analysis across years.

Fine root production and turnover were measured for two 1-year periods from 2016-2018 in the top 10 cm of mineral soil using cylindrical, 2-mm mesh, in-growth cores filled with homogenized, root-free, mineral soil (B.A. Eastman & W.T. Peterjohn, unpublished data). Four in-growth cores were deployed in 10 plots for one year, after which cores were removed, soil and roots collected, and new mineral soil put into the cores for the second year. Fine roots (<2 mm) were hand-picked, rinsed with deionized water, and dried at 65^{o}C for > 48 hours prior to mass determination. Fine root turnover was estimated from the annual rates of root ingrowth measured in 2016-2018 divided by the root biomass stock measured in 2016. Fine root C and N concentrations from 2016 were applied to biomass production and turnover.

Annual N uptake and foliar N resorption

To examine how chronic N additions impacted the N acquisition strategies of trees, we estimated N uptake and its components. For this study, N uptake is defined as the total flux of soil N to fine roots and aboveground plant tissues, minus foliar N resorption, which simplifies to:

$$N\ uptake = N_{wood} + N_{litter} + N_{froot} \quad \text{Eq. 1}$$

Where N_{wood} is the N content of the annual increment of aboveground woody biomass (2009-2018); N_{litter} is the annual amount of N returned to the soil in leaf litter (2015-2017), which assumes resorption from green leaves to litter is in steady state; and N_{froot} is the amount of N associated with annual fine root N production (0-10 cm; 2016-2018). We calculated N uptake for each watershed using mean watershed values of wood, litter and fine root production, and standard error was propagated analytically (Methods S2-1).

N concentrations of canopy leaves were measured in July 2012 on three leaves from each of four dominant tree species in 10 plots (Methods S2-3). In July 2016, an additional 8-11 trees of another species (*Quercus rubra*) were sampled for foliar N concentration, and watershed means from these data were combined with the 2012 data. For species not selected for foliar N analysis (<15% of total leaf litter mass) we randomly sampled from the grand mean and standard deviation of N concentrations for each watershed. Foliage mass was estimated from plot-level leaf litter mass (from 2016-2018). We accounted for mass loss during senescence by multiplying litter mass by 1.27, the mean temperate deciduous ratio of green to senesced leaf mass (Van Heerwaarden *et al.*, 2003). This correction avoids large bias in underestimating foliar resorption and resorption efficiency. To estimate the total foliar N pool ($N_{foliage}$), mean N concentrations by species were multiplied by corrected foliage mass by species at the plot level, and then averaged for each watershed.

N retranslocation ($N_{foliage} - N_{litter}$) and N resorption efficiency ($(N_{foliage} - N_{litter}) / N_{foliage}$) were estimated at the plot level, using data from the years available (foliage in 2012 and 2016, and litter in 2015-2017).

Soil C and N stocks

In 2016, soil C and N concentrations were measured at 15 soil pits (30.5 x 30.5 cm; Fig. 2-1) per watershed. Soil samples were collected from the organic horizon and 0-10, 10-20, 20-30, and 30-45 cm depths of the mineral soil. Samples were sieved to 2 mm, air-dried in a greenhouse, and ground prior to C and N analysis. Fine earth bulk density (coarse fragment-free; g m^{-3}) was measured for the 0-5 cm depth

of mineral soil at 100 locations per watershed in 2011 (Gilliam *et al.*, 2018), and for the 15 to 45-cm depth at three quantitative soil pits at a nearby site in the Fernow (Adams *et al.*, 2004). These measured bulk densities were regressed on soil depth to calculate values for each depth at which C and N concentration were measured (Fig. S2-2). To account for differences in the volume of coarse fragments between watersheds, we corrected the fine earth bulk density estimates for coarse fragment volume by horizon as measured in both watersheds (n=25; Adams, 2016). Specifically, fine earth bulk densities of each soil depth were corrected using the mean proportion of coarse fragments of the corresponding soil horizon. Total C and N stocks for mineral soils were calculated for each depth increment as the product of soil C or N concentrations, depth increment, and corrected bulk density.

The mean mass of the organic horizon (g m^{-2}) was estimated from two (25 x 25 cm) measurements at seven plots in June of 2012 and 2013 (Fig. 2-1). For both watersheds, C and N concentrations of the organic horizon measured in 2016 (n=15) were multiplied by the mean organic horizon mass per area measured in 2012 & 2013 to estimate the total C and N stocks. Error in these estimates represents plot-to-plot variability in both the C and N concentrations and organic horizon mass.

Soil and stream C and N fluxes

Total belowground C flux (TBCF) consists of the C flux to fine root production and maintenance, mycorrhizal associations, and root exudates often directed to the acquisition of N (Hobbie, 2006; Hobbie & Hobbie, 2008; Högberg *et al.*, 2010). We estimated TBCF at 10 plots per watershed (Fig. 2-1) using a mass balance approach (Raich & Nadelhoffer, 1989):

$$TBCF = R_s - \text{leaf litter C} \qquad \text{Eq. 2}$$

Where annual C inputs from leaf litter (2015) were subtracted from annual soil CO_2 efflux (R_s), assuming that the annual change in the soil C pool and soil C leaching losses were negligible (Giardina & Ryan, 2002). In 2016-2017, soil respiration, temperature, and moisture were measured weekly during the growing season and biweekly-monthly during the winter in the same plots where litterfall-C was collected

(Fig. 2-1; Methods S2-4). Annual soil CO_2 efflux was estimated from an Arrhenius model of soil respiration versus soil temperature (van't Hoff, 1898; Lloyd & Taylor, 1994), applied to data from hourly soil temperature measurements from the same plots (Methods S2-4).

C losses through leaching were difficult to estimate due to a lack of measurements, although intermittent measurements of dissolved organic C (DOC) concentrations in streamwater are available from 2007 (W.T. Peterjohn, unpublished data; Edwards & Wood, 2011). Streamwater DOC concentrations were measured 12 times in +N WS3 and eight times in Ref WS7 in March-November of 2007, and a rough estimate of DOC discharge was obtained by multiplying the mean of all concentrations for each watershed by the annual stream discharge of water.

Soil N inputs from leaf litterfall were measured in 10 plots per watershed in 2015 and 2016 along with litter C inputs, as described above. N inputs from wet and dry atmospheric deposition were measured at NADP and CASTNET sites WV18 and PAR107. The +N WS3 also received 3.5 g N m^{-2} y^{-1} from experimental fertilizations of $(NH_4)_2SO_4$ (Table 2-1).

N losses in stream water were estimated from continuous streamflow measurements and streamwater chemistry sampled weekly or biweekly since 1983 by the USFS Northern Research Station near weirs at the base of each watershed (Edwards & Wood, 2011). Volume-weighted monthly means of streamwater NO_3^- and NH_4^+ concentrations from January 1984 through December 2017 were multiplied by the corresponding total monthly streamwater discharge to calculate export rates from each watershed. Monthly N export values were summed to arrive at annual estimates of dissolved inorganic N discharge. Because we lack consistent measurements of particulate or dissolved organic N in streamwater, we were unable to estimate dissolved organic N export.

We did not include gaseous N losses in our budget, and from the few measurements of production rates and emissions of N-containing trace gases (NO and N_2O) in these watersheds (Peterjohn *et al.,* 1996; Venterea *et al.,* 2004), it seems unlikely that their combined flux would exceed ~ 0.1 g N m^{-2} yr^{-1}.

However, gaseous N losses are difficult to measure and unmeasured N_2 losses could account for a portion of budget imbalances.

C partitioning and C cost of N acquisition

To determine if trees shift their C partitioning to favor aboveground versus belowground C flux under chronic N additions, we compared C fluxes to ANPP versus TBCF. We also estimated the C cost of soil N acquisition (Nacq) for each watershed using a previously published formula (Fisher *et al.*, 2010; Brzostek *et al.*, 2014; Shi *et al.*, 2019):

$$\text{C cost of Nacq (g C g N}^{-1}) = \frac{\text{TBCF (g C m}^{-2}\text{ yr}^{-1})}{\text{Nacq (g N m}^{-2}\text{ yr}^{-1})} \quad \text{Eq. 3}$$

Although TBCF can be expended for other purposes (e.g., uptake of other resources, and protection from aluminum toxicity), N is typically the most limiting nutrient in forests of this region. Thus, our calculations assume this TBCF is directed for N acquisition, and these estimates may be conservatively considered an upper estimate for the C cost of Nacq.

Statistical Analysis

To control for initial differences in aboveground C stocks, an analysis of covariance (ANCOVA) tested for watershed differences in biomass C, using 1991 estimates of basal area as an independent covariate. As wood N stock estimates did not differ between watersheds in the early years, a one-way analysis of variance (ANOVA) was used to test for watershed differences in wood N stocks in recent years. To control for initial conditions and to account for repeated measures, watershed differences in C production in woody biomass and aboveground NPP were assessed with a repeated measures mixed effects ANOVA where WS, Year, and WS*Year were fixed effects, 1991 basal area was a covariate, and plot was a random effect. Foliar N pools and N retranslocation were compared between watersheds using a mixed-effects ANOVA with watershed as the main effect and year as a random effect. A one-way ANOVA also tested watershed differences in soil C and N pools, which had only one observation per plot (n = 15), and reported error represents plot-to-plot spatial variability. Watershed differences in litterfall C

and N production (2015-2017) were tested using a nested ANOVA, with watershed as a fixed effect, year as a random nested effect within watershed. Similarly, watershed differences in fine root biomass and soil respiration were tested using a nested ANOVA, with watershed as a fixed effect, year as a random nested effect within watershed, and plot as a random nested effect within watershed.

As is common in watershed-scale and other large ecosystem experiments, this study is an example of simple pseudoreplication, as each watershed represents an experimental treatment with a sample size of one (Hurlbert, 1984). Results should be interpreted with this in mind, but given the duration and extent of the treatment, differences found are most likely treatment effects rather than characteristic differences between watersheds.

Residuals of all ANOVA models were tested for normality (Shapiro-Wilks test), and where this assumption was not met, observations were transformed to meet ANOVA assumptions. When reported, back-transformed means +/- standard errors are identified in figures and tables. Most statistical analyses were executed in R version 3.6.1 (R Core Team, 2019) using the 'lme4' package for mixed-effects ANOVAs (Bates *et al.*, 2015), and least square means were calculated using the 'lsmeans' package (Lenth, R. 2016). Nested ANOVA models were performed in SAS JMP (JMP, Version 14.0).

2.4 Results

Aboveground biomass and productivity

As expected for an aggrading forest, aboveground woody biomass increased during the experiment in both the fertilized and unfertilized watersheds, though at a faster rate in +N WS3 (Fig. 2-2**a**; F=8.607, P=0.005, n=25). Autumnal leaf litterfall mass did not differ between watersheds and increased at the same rate in both watersheds since 1991 (~12 g y^{-1}; P_{year}<0.001; Fig. 2-2**b**). From nutrient analyses of 2015 and 2016 leaf litter (Table S2-2), we estimated a slightly greater return of litter C and N and lower C:N ratio for leaf litter in +N WS3 (Table 2-2; F=32.37, P<0.001, n=10). Controlling

for the greater basal area in +N WS3 at the beginning of the study, repeated measures ANOVA found ANPP (g C m^{-2} y^{-1}) was ~ 25% greater in +N WS3 over the course of the study (Fig. 2-2**c**; Table 2-2; F=13.63, P<0.001, n=25). Furthermore, the C:N ratio of woody biomass in the +N WS3 was ~ 35% greater (Table 2-2; F=103, P<0.001, n=25).

Belowground biomass and productivity

Fine root biomass varied among years: organic horizon fine root C stocks were greater in +N WS3 in two of the three years measured and lower in one (Fig. S2--3), and mineral fine root C stocks trended lower in +N WS3 in 1991, 2013, and 2015 but trended greater when measured to 10-cm depth in 2016 (Fig. S2-3). Fine root N stocks followed the same pattern as the C stocks, and the C:N ratios of fine root pools did not differ between watersheds (Table 2-2). However, when patterns in biomass were considered collectively with their tissue concentrations, fine root C and N stocks from 2012-2016 were smaller in the organic horizon of +N WS3 (P_C=0.011, P_N=0.002, n=18), and not detectably different in the upper mineral horizon (0-15 cm; Table 2-2). Fine root pools of C and N in the upper mineral soil did not change significantly over time. Furthermore, fine root production and turnover (0-10 cm depth) did not differ between watersheds (Table 2-2).

Annual N uptake and foliar N resorption

N pools of green canopy leaves were unexpectedly lower in +N WS3 (Table 2-2; F=4.57, P=0.037, n=10). Because foliar N concentrations did not differ between watersheds when comparing single species (Table S2-4), this distinction in foliar N pools is likely driven by slight differences in species composition, where low foliar N species (*A. rubrum and Q. rubra*) are more abundant in +N WS3 and one particularly high foliar N species (*L. tulipifera*) is more abundant in Ref WS7 (Fig. S2-1, Table S2-4). This distinction may be conservative since it does not account for the greater abundance of *R. pseudoacacia* (a high N-content, N-fixing species) in Ref WS7 (Fig. S2-1). Alternatively, leaf litter mass

in the 10 litter chemistry plots (Fig. 2-1a) was slightly lower in +N WS3 for the three years used to estimate foliar mass (2015-2017), despite the lack of long-term differences in litter mass. Even so, foliar N retranslocation was 22% less, by mass, in the +N WS3 (Table 2-2; F=14.46, P=0.001, n=10), and the N resorption efficiency was also lower in +N WS3 (Table 2-2; F=24.93, P<0.001, n=10). Despite less N retranslocation in +N WS3, soil N uptake was similar in both watersheds (Table 2-2).

Soil C and N stocks

No differences in organic horizon C pools, N pools, nor C:N ratios were detected between watersheds (Fig. 2-3). Despite measuring mineral soil C and N at 15 locations per watershed, statistical comparisons between watersheds were strongly affected by the high spatial variability of mineral soil C (CV=15-67%) and N (CV=48-76%), and no differences between watersheds were found between total soil C or N pools to a depth of 45 cm. However, we did find that C pools were 1,328 g C m^{-2} larger and N pools were 84 g N m^{-2} larger in the surface (0-10 cm) mineral soil of the +N WS3 at $\alpha = 0.1$ (Fig. 2-3; F_C=3.588, P_C=0.069; F_N=4.206, P_N=0.050; n=15), consistent with more numerous observations of the 0-5 cm soil increment (n=100, P<0.05; Gilliam *et al.* 2018). The C:N ratio of soil was significantly higher for all depth increments in +N WS3, with the exception of the 0-10 cm increment (Fig. 2-3; $F_{10\text{-}10cm}$=5.353, $P_{10\text{-}20cm}$=0.028; $F_{20\text{-}30cm}$=4.81, $P_{20\text{-}30cm}$=0.037; $F_{30\text{-}45cm}$=4.688, $P_{30\text{-}45cm}$=0.039; n=15). However, the C:N ratio of the 0-5 cm of mineral soil, when measured at 100 locations per watershed, exhibited a greater C:N ratio (17.6 in +N WS3 vs. 14.6 in Ref WS7; see Gilliam *et al.* 2018; F= 4.04, P<0.001, n=100), underscoring the benefits of a larger sample size when characterizing highly heterogeneous ecosystem stocks.

Soil and stream C and N fluxes

Measured rates of soil respiration and estimated values for the annual soil CO_2-C efflux were ~14% lower in +N WS3 from June 2016-May 2018, despite similar soil temperatures in both watersheds and greater soil moisture in the +N WS3 (Fig. S2-4; B.A. Eastman & W.T. Peterjohn, unpublished data). Because aboveground litter inputs and fine root production were both similar between the watersheds, this reduced output (soil respiration) in +N WS3 drove the ~12% lower TBCF (Table 2-2).

Based on infrequent measurements of streamwater dissolved organic C (DOC) in 2007, we estimated that +N WS3 had 12% lower C loss in streamwater DOC than Ref WS7 (Table 2-2). While quite uncertain, these estimates suggest that the export of DOC in streamflow may account for over 10% of total C losses from the ecosystem, and better measurements would be useful for a more complete picture of TBCF and biogeochemistry at this site.

As expected, stream-water inorganic N losses were much greater in +N WS3, representing more than one-third of total N inputs to that watershed. Cumulative N inputs (ambient + experimental) in +N WS3 were five times greater than N inputs to Ref WS7, or ~100 g N m^{-2} greater (Table 2-1). However, cumulative N exports from 1989-2018 in +N WS3 exceeded Ref WS7 exports by only 12 g N m^{-2} (Fig. 2-4). Over a 29-year period during this study (1989-2018), the total apparent N retained in +N WS3 was 98 g N m^{-2}, leading to annual increases in the ecosystem N stock in the absence of significant gaseous N losses. From the N mass balance budgets, there was a large missing N sink in +N WS3 and a comparatively small but substantial (13 g N m^{-2}) missing N source in Ref WS7 (Figs. 2-4, S2-5).

C partitioning and C cost of N acquisition

N fertilization resulted in a shift in N acquisition strategy and C partitioning (Fig. 2-5**a**). In response to N additions, +N WS3 retranslocated less foliar N prior to senescence, acquiring a greater proportion of total N flux from the soil compared to Ref WS7 (Fig. 2-5**b**). Assuming TBCF represents the maximum C cost of N acquisition (Fisher *et al.*, 2010; Gill & Finzi, 2016; Terrer *et al.*, 2016), and considering TBCF was ~14% less in +N WS3, we estimated that the maximum C cost of N uptake in +N WS3 (83.2 g C g N^{-1}) was ~27 g C g N^{-1} lower than in Ref WS7 (110 g C g N^{-1}; Fig. 2-5**c**). Thus, partitioning of photosynthate shifted away from belowground components and towards aboveground woody biomass production with N additions (Fig. 2-5).

2.5 Discussion

We synthesized a unique and diverse set of site-specific information to assess how 25+ years of $(NH_4)_2SO_4$ additions altered C and N storage and partitioning at the Fernow Experimental Forest. Our

findings indicate that generalizations from optimal allocation theory (Bloom *et al.*, 1985) can scale to an entire ecosystem through a shift in N acquisition strategy under enhanced N inputs. Specifically, we observed greater ecosystem C storage in aboveground woody biomass (Fig. 2-2**a**), less C transferred belowground (Fig 2-5**d**), and increased soil C storage and soil C:N ratios in the +N WS3 (Fig. 2-3). The shift in soil stoichiometry (greater C:N), as well as the increased proportion of plant biomass with high residence times (wood vs. leaves and roots), may have long-term impacts on forest recovery in this ecosystem and other forests in the NE USA by potentially slowing N cycling (Craine *et al.*, 2018; Groffman *et al.*, 2018).

Increases in aboveground C storage dominated the ecosystem response to long-term N additions, as most of the ~24% greater ecosystem C stock in +N WS3 was due to greater C flux to woody C (Table 2-2). This enhanced aboveground C accumulation was noted in several meta-analyses of N addition experiments on seedlings and younger trees (Xia & Wan, 2008; Janssens *et al.*, 2010; Schulte-Uebbing & de Vries, 2017a), but this study demonstrates that this pattern can persist in more mature forests (see also Pregitzer *et al.* 2008). Furthermore, we may have underestimated the N effect on biomass accumulation because Ibañez *et al.* (2016) found that N fertilization widens the height:DBH ratio of some trees, This could create a potential bias when using standard allometric equations that do not include height (such as those used in this study) in fertilization experiments. Indeed, terrestrial LiDAR analysis conducted in 2016 found that trees in the +N WS3 were 2.4 m taller, on average, than those measured in WS7 (Atkins *et al.*, 2020). Although stand-level data (including in-growth and mortality) used in this study found a greater overall rate of biomass production with N additions (Fig. 2-2), this effect may diminish in the future. Recent tree-ring data for mature trees of several species document slower growth in the +N WS3 relative to Ref WS7 (Fig. S2-6; Malcomb *et al.*, 2020). Thus, the enhanced cumulative ANPP detected in +N WS3 may represent an initial positive response by fast-growing and acid-tolerant *P. serotina*, but this response may not persist due to a relative decline in tree growth among several dominant species (Fig. S2-6).

Under N limitation, a large proportion of assimilated plant C can be expended on N acquisition via mycorrhizae and foliar N resorption (Fahey *et al*., 2005; Högberg *et al.*, 2010; Gill & Finzi, 2016). However, following N additions, more N can be acquired directly by roots through passive uptake, reducing the partitioning of C for N retranslocation, active transport, or mycorrhizal symbioses (Fig. 2-5**a**; Vitousek, 1982; Rastetter *et al.*, 2001; Fisher *et al.*, 2010; Brzostek *et al.*, 2014). Given similar foliar N pools and, thus, likely similar rates of GPP in these watersheds, our observation of less foliar N retranslocation (Table 2-2) and less mycorrhizal colonization (Carrara *et al.*, 2018) in +N WS3 suggest greater N uptake directly by roots. This 'cheaper' (in terms of C expenditure) strategy for N-acquisition could free up C for woody biomass production (Fig. 2-5**a**; Holopainen & Peltonen, 2002; Wright & Westoby, 2003). While lower rates of N resorption from leaves in the +N WS3 suggest a lower N use efficiency (Fig. 2-5, Table 2-2), we still estimated a stimulation in C storage at the ecosystem scale (roots + soil + woody biomass) of ~46 g C per g N experimentally added over the course of the experiment, which is in the range of values typically reported in other studies (30-75 g C g^{-1} N; Hyvönen *et al.*, 2008; Pregitzer *et al.*, 2008; Sutton *et al.*, 2008). Given that the C cost of N acquisition in this study was ~24% 'cheaper' in the fertilized watershed, the reduction in C flux belowground for N uptake in +N WS3 could account for over half of the enhanced ANPP (Table 2-2). This shift in C partitioning under N additions is consistent with theories and reviews of photosynthate allocation in plants (Litton *et al.* 2007).

In addition to the greater woody C accumulation in the +N WS3, we detected a slightly greater C pool in the surface mineral soil of +N WS3 (0-10 cm; a=0.10), despite similar inputs of fine plant litter. Interestingly, although N additions lowered the C:N ratio of leaf litter inputs (Tables 2-2, S2-2), the C:N ratio of SOM is greater in +N WS3, suggesting that an important disconnect occurred in the soil environment between the stoichiometry of substrates (leaf litter) and products (SOM). This alteration of organic matter stoichiometry was found by other studies in temperate forests (Nave *et al.*, 2009; Yanai *et al.*, 2013; Forstner *et al.*, 2019). A possible explanation for this pattern is that reduced TBCF slowed the priming of organic matter decomposition by depriving soil microbes of labile C inputs from plants, allowing the accumulation of recalcitrant plant material with high C:N ratios in the surface soil

(Kuzyakov, 2010; Cotrufo *et al.*, 2015; Sulman *et al.*, 2017). Though speculative, this proposed mechanism is supported by the reductions in soil respiration (Fig. S2-4) and mycorrhizal colonization (Carrara *et al.*, 2018) in the +N WS3. Furthermore, previous studies at this site measured slower leaf litter decomposition rates (Adams & Angradi, 1996) and lower ligninolytic enzyme activity in the +N WS3—beyond what is expected from the reduced pH in +N WS3 (Carrara *et al.*, 2018; SanClements *et al.*, 2018). However, if the decay of any enhanced soil C stock in +N WS3 is inhibited by N additions, this C pool could become susceptible to decomposition and promote greater N availability once experimental N inputs subside. Alternatively, more N-limited trees in Ref WS7 may promote priming through increased TBCF to gain access to microbially mineralized N, and C losses associated with this priming could be greater than any reduced potential for SOC formation through TBCF in the +N WS3.

Given the potential for ecosystem-scale interactions that operate over decades to influence forest ecosystem responses to N additions, this study highlights the value of long-term, watershed-scale experiments in gaining insight into how above- and below-ground components interact and respond to environmental change. However, there are also limitations to the approach used in this—and other—watershed-scale studies due to a lack of replicated treatments. In the case of our study sites, causal attribution is confounded by differences in species composition (S1) and land use history (Table 2-1) that must be carefully considered when interpreting the results. However, the large dose of added N and subsequent changes in streamwater nutrient export and soil chemistry support our view that the +N WS3 is primarily responding to the treatment (Adams *et al.*, 2006). Furthermore, there is a nearby (< 2 km from our study sties), fully replicated, N-fertilization experiment with the same annual N additions as +N WS3 (Adams *et al.*, 2004). This replicated study has been used to test observations from the watershed experiment and confirm many of these responses—including enhanced tree productivity (Fowler *et al.*, 2015), reduced soil respiration (B.A. Eastman & W.T. Peterjohn, unpublished data), and lower mycorrhizal colonization and soil enzyme activity (Carrara *et al.*, 2018).

One invaluable feature of watershed-scale studies is the ability to create mass balance budgets at a broad spatial scale. From the watershed N budgets we constructed, over our 29-year study period (1989-2018), the total apparent N retained in +N WS3 was 98 g N m^{-2}. The accumulation of N in vegetation N pools in both watersheds was slight (20 g N m^{-2}), explaining only 20% of the N retention in +N WS3. Changes in soil stocks are very difficult to measure, even at decadal time scales, and the lack of good pretreatment measurements and robust bulk density measurements in these watersheds prevents us from confidently estimating the change in the soil N stock over the experimental period. However, if the watershed differences in mean soil N stocks of the top 10 cm of mineral soil (84 g N m^{-2}) indicates a fertilization effect in the +N WS, this difference could account for the missing N sink in +N WS3 (Fig. 2-4). This would be consistent other N fertilization studies that detected greater soil C and N stocks in the surface soil layers (Zak *et al*., 2008; Pregitzer *et al.*, 2008; Frey *et al.*, 2014). Alternatively, unmeasured gaseous N losses and dissolved organic N outputs in streamwater could account for part of the imbalance (Enanga *et al.*, 2017). In Ref WS7, the missing source could be attributed to some combination of (i) N fixation by black locust (potentially ~1.89 g N m^{-2}; Fig. S2-7); (ii) free-living N fixation (2.9-14.5 g N m^{-2}; Schlessinger & Bernhardt, 2020); (iii) errors in estimates of wood N—based on only the outer 1 cm of bole wood; or (iv) errors in estimates of gaseous N deposition.

Globally, the positive response of aboveground productivity to N additions appears to be strongest in temperate forests (Fleischer *et al.*, 2015; Du & de Vries, 2018), where N limitation may be the historical norm. Given that the positive growth responses of forests to increasing atmospheric CO_2 and longer growing seasons are often constrained by N availability and N acquisition strategies (Norby *et al.*, 2010; Fernández-Martínez *et al.*, 2014; Feng *et al.*, 2015; Smith *et al.*, 2016; Terrer *et al.*, 2019), a mechanistic representation of plant controls on soil-microbe interactions—and their subsequent feedbacks on soil nutrient cycling and plant productivity—are necessary for global C models to accurately predict the potential for forests to mitigate climate change through C sequestration (Wieder *et al.*, 2015, 2019; Sulman *et al.*, 2018, 2019; Shi *et al.*, 2019). This study provides a unique perspective on ecosystem-scale C responses to altered N inputs, and the importance of studying both above- and below-ground responses

to environmental change. Future research focused on clarifying the mechanisms governing plant-soil interactions and quantifying the impact of N status on these processes may be critical, because it is uncertain whether this enhanced C storage will persist in the future—especially if ecosystem productivity becomes constrained over time due to changes in the patterns and processes of plant resource allocation that feedback on soil biogeochemistry.

2.6 Tables and Figures

Table 2-1. Site characteristics of a reference watershed (Ref WS7) and the adjacent N-fertilized watershed (+N WS3) in the Fernow Experimental Forest, WV.

Characteristic	Ref WS7	+ N WS3
Area (ha)	24	34
Aspect	East	South
Land use history	Upper 12 ha clearcut (1963); Maintained barren with herbicides (1964-1969); Lower 12 ha clearcut (1966); Entire WS maintained barren with herbicide (1967-1969); Natural recovery (1969-present)	Intensive selection cut (1958-1959, 1963); patch cuttings totaling 2.3 ha (1968); clearcut except 3-ha shade strip along stream (1970); stream shade strip cut & natural recovery (1972); experimental N additions (1989-2019)
Annual precipitation (mm)	1460	1460
Mean air temperature (°C)[a]	9.3	9.3
Cumulative N deposition,		
1989-2018 (g N m^{-2})		
Experimental	0	104
Ambient[b]	26	26
Total	26	131
Soil pH[c]	4.52	4.12
Top four dominant species (by % basal area)[d]	*Liriodendron tulipifera*, *Betula lenta, Prunus serotina*, *Acer rubrum*	*Prunus serotina*, *Acer rubrum*, *Betula lenta, Quercus rubra*

[a]From Young et al. 2019. [b]Data from CASTNET total wet + dry N deposition. [c]Means based on a 2011 soil sampling of 0-5 cm mineral soil at 100 points per watershed (Gilliam et al, 2018). [d]Data from 2016-2017 dendrometer plot census.

Table 2. Carbon and nitrogen budgets for reference watershed (Ref WS7) and the adjacent N-fertilized watershed (+N WS3). Means of pools and fluxes (standard error).

		Carbon		Nitrogen		C:N Ratio	
Ecosystem component	**Year**	**Ref WS7**	**+N WS 3**	**Ref WS7**	**+N WS3**	**Ref WS7**	**+N WS3**
Pools							
Woody biomass (g m^{-2})	*2018*	11,475 (634) *	15,364 (801)	28 (6)	29 (8)	416 (10) ***	560 (6.4)
Foliage (g m^{-2})	*2012-2016*	262 (49)	228 (42)	12.0 (1.7) *	10.0 (1.4)	21.9 (0.2)	22.3 (0.3)
Fine root biomass (g m^{-2})	*2012-2016*						
OH		31 (3.5) *	18 (2.5)	1.08 (0.09) **	0.65 (0.12)	29.4 (2.6)	28.0 (2.3)
Mineral (0-15 cm)		121 (32)	110 (30)	3.6 (0.8)	3.1 (0.7)	28.6 (1.0)	29.4 (0.8)
Soil (OH-45 cm; g m^{-2})	*2016*	8,838 (513)†	9,801 (1,055)†	638 (40)†	656 (59)†	13.8 (1.2)	14.9 (2.1)
Total ecosystem pool (g m^{-2})		20,465 (816)	25,293 (1,325)	671 (40)	689 (60)		
Fluxes							
Wood production (g m^{-2} y^{-1})	*2009-2018*	400 (24) ***	545 (42)	1.01 (0.06)	0.97 (0.07)	406 (8) ***	556 (13)
Wood mortality (g m^{-2} y^{-1})	*2009-2018*	98 (10)	69 (21)	0.14 (0.11)	0.18 (0.19)		
Leaf litter input (g m^{-2} y^{-1})	*2009-2018*	162 (2)	156 (3)	3.8 (0.05)	4.3 (0.08)	43 (1.7) ***	37 (1.8)
ANPP (g C m^{-2} y^{-1})	*2009-2018*	565 (25) ***	709 (43)	--	--	--	--
N uptake (g N m^{-2} y^{-1})[a]	*2009-2018*	--	--	7.6 (2.4)	8.7 (2.0)	--	--
Foliar N retranslocation (g m^{-2} y^{-1})	*2016*	--	--	8.2 (1.7) **	6.0 (1.4)	--	--
N resorption efficiency (%)	*2016*	--	--	67.8 (9.7) ***	60.5 (9.8)	--	--
Fine root production (0-10 cm; g m^{-2} y^{-1})[b]	*2016-2018*	89 (9)	122 (9)	2.8 (0.2)	3.4 (0.2)	41.0 (1.4)	42.8 (1.0)
Fine root turnover (0-10 cm; y^{-1})[c]	*2016-2018*	0.92 (0.1)	1.03 (0.1)	0.63 (0.07)	0.62 (0.06)	--	--
Respiration (g C m^{-2} y^{-1})[d]	*2016-2017*	982 (63) *	864 (28)	--	--	--	--
TBCF (g C m^{-2} y^{-1})[d]	*2016-2017*	838 (67) *	724 (29)	--	--	--	--
Stream export (g m^{-2} y^{-1})[e]	*2009-2018*	83	73	1.08 (0.06) **	1.68 (0.09)	--	--
C cost of N uptake (g C g^{-1} N)[f]		110 (12)	83.5 (6.7)				

Asterisks represent statistical significance at P=0.05 (*), P<0.01 (**), P<0.001 (***). † Denotes back-transformed means (max. se) of ln-transformed data. [a]N acquired from soil: N uptake = N wood increment + N leaf litter + N fine root production$_{(0\text{-}10\ cm)}$. [b]From B.A. Eastman, *et al*. (unpublished). [c]From B.A. Eastman, *et al*. (unpublished), estimated by dividing mean FRP (over two years) from initial biomass measured before inserting in-growth cores. [d]From B.A. Eastman, *et al*. (unpublished). TBCF=fine litterfall inputs minus soil CO_2-C efflux. [e]C leaching losses from 2007 are from intermittent streamwater DOC concentration measurements. [f]C cost of N uptake = TBCF/Nuptake from WS means, with standard errors propagated analytically.

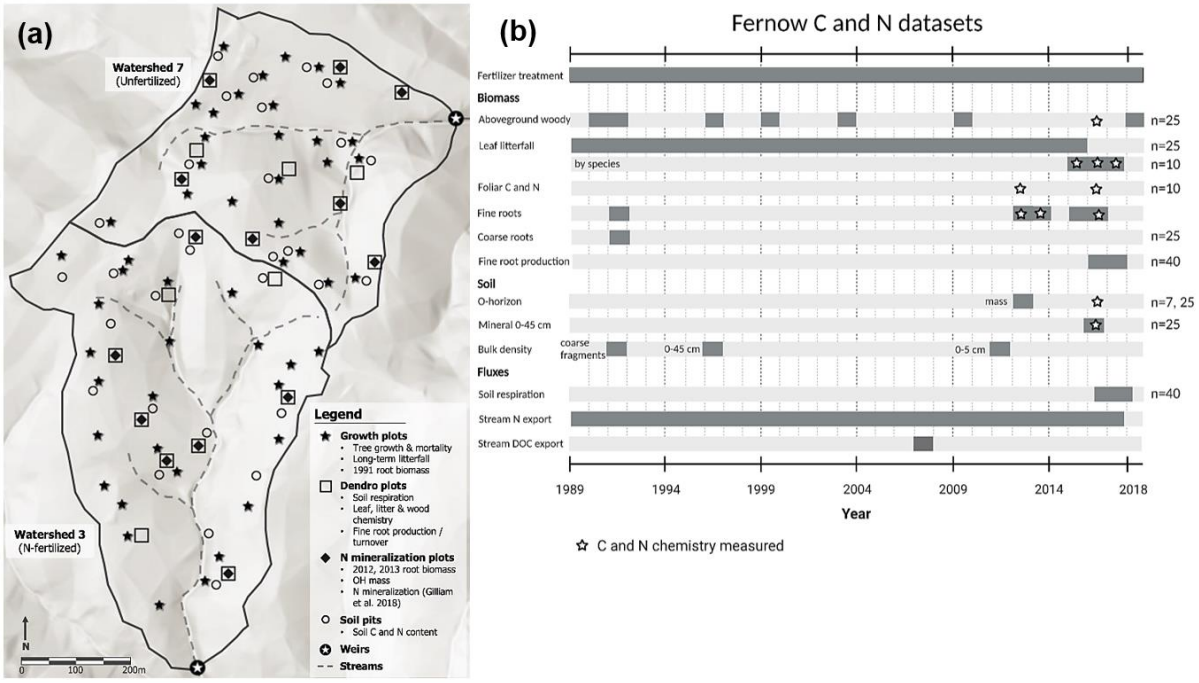

Figure 2-1. **(a) Map of the Fernow Experimental Forest and (b) data timeline of C and N datasets from the** whole-watershed fertilization experiment (1989-2018). **(a)** Map shows the locations of the principal study sites in the reference watershed (Ref WS7) and adjacent N-fertilized watershed (+N WS3). **(b)** Timeline indicates the years when data were collected (grey bars) and when C and N content were measured on ecosystem components (☆). Fig 2-1**b** created with BioRender.com.

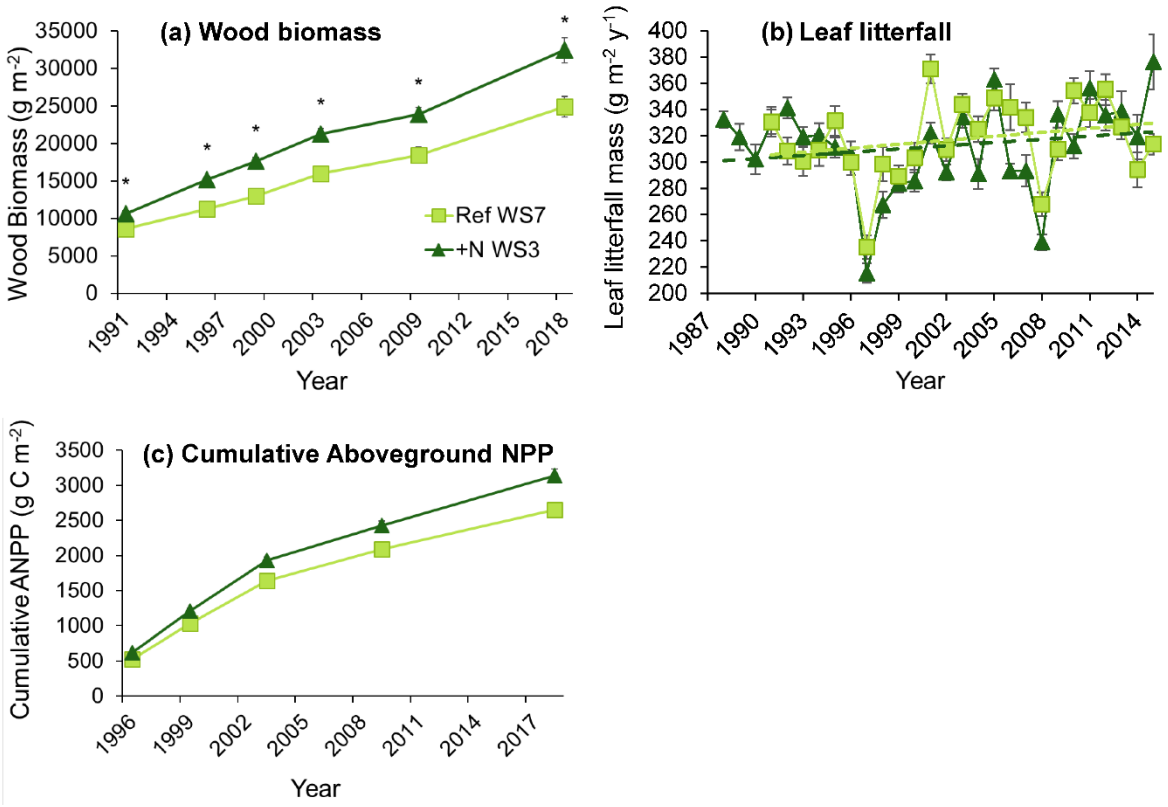

Figure 2-2. Long-term data on aboveground biomass productivity showed greater rates of **(a)** woody biomass stock increase (growth + ingrowth – mortality), **(b)** equal leaf litterfall production, and **(c)** greater cumulative aboveground net primary productivity (ANPP) C in the fertilized watershed. Points are means from 25 plots per watershed in the fertilized watershed (+N WS3, dark green triangles) and the reference watershed (Ref WS7, light green squares). Error bars represent +/- one standard error. Trend lines in **(b)** litterfall production fit by linear regression and slopes do not differ between watersheds.

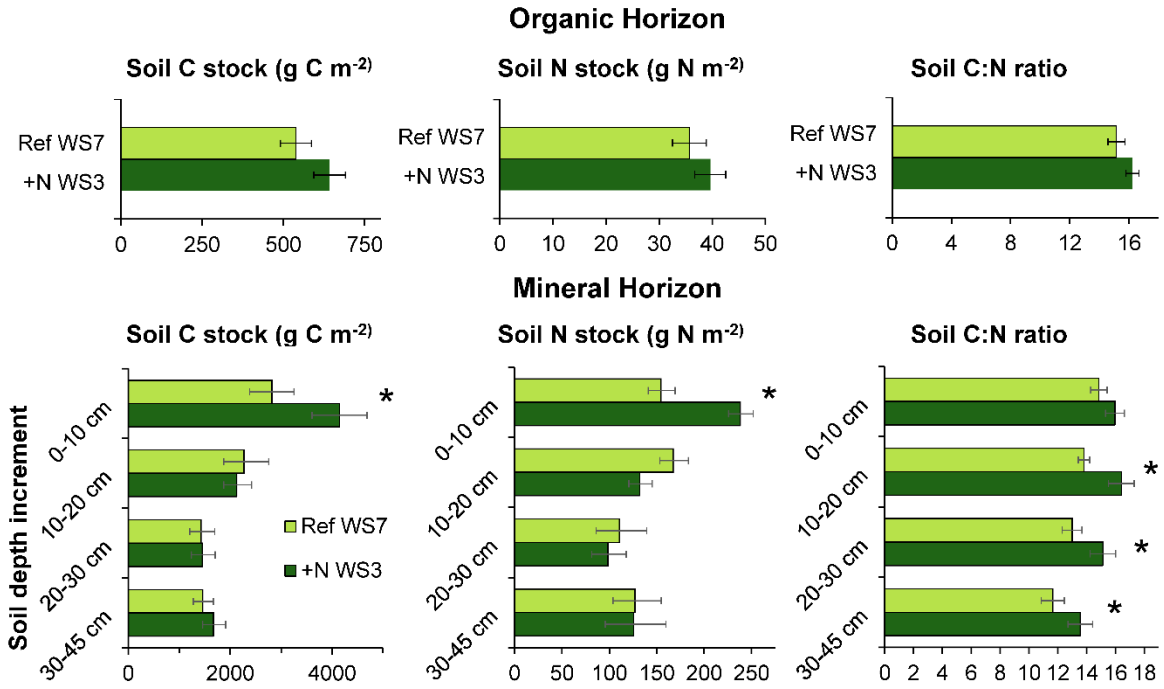

Figure 2-3. C stocks (left), N stocks (center), and C:N ratios (right) in the organic horizon (top) and surface mineral soil (bottom) of reference watershed 7 (light green) and fertilized watershed 3 (dark green). Results showed greater C and N stocks in surface mineral soil of +N WS3, and a greater C:N ratio of deeper mineral soil in +N WS3. Means +/- 1 standard error (error bars). All mineral soil and N stocks present back-transformed means of ln-transformed data except for the soil C 0-10 cm stock. Given the high spatial variability, the threshold for significant differences was α=0.1. Asterisks represent significant differences between watersheds ($p<0.10$).

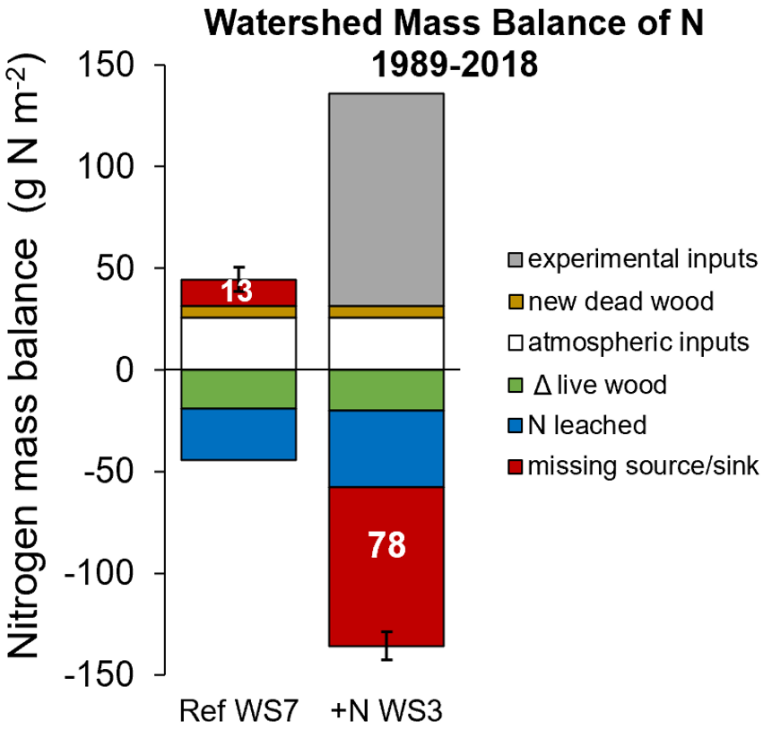

Figure 2-4. Cumulative watershed N budgets for reference watershed 7 (left) and fertilized watershed 3 (right) from 1989-2018. N inputs include experimental N additions (grey; 1989-2017 in +N WS3 only), atmospheric N deposition (white; 1989-2017), and wood N inputs from mortality (gold; 1990-2018). N outputs include live wood N accumulation (green; 1990-2018) and inorganic N losses in streamwater (blue; 1989-2017). Missing source/sink (red) is the difference between all N inputs and all N outputs. Error bars represent +/- one standard error, which was propagated analytically when summing the fluxes for which error terms existed (wood mortality and wood accumulation).

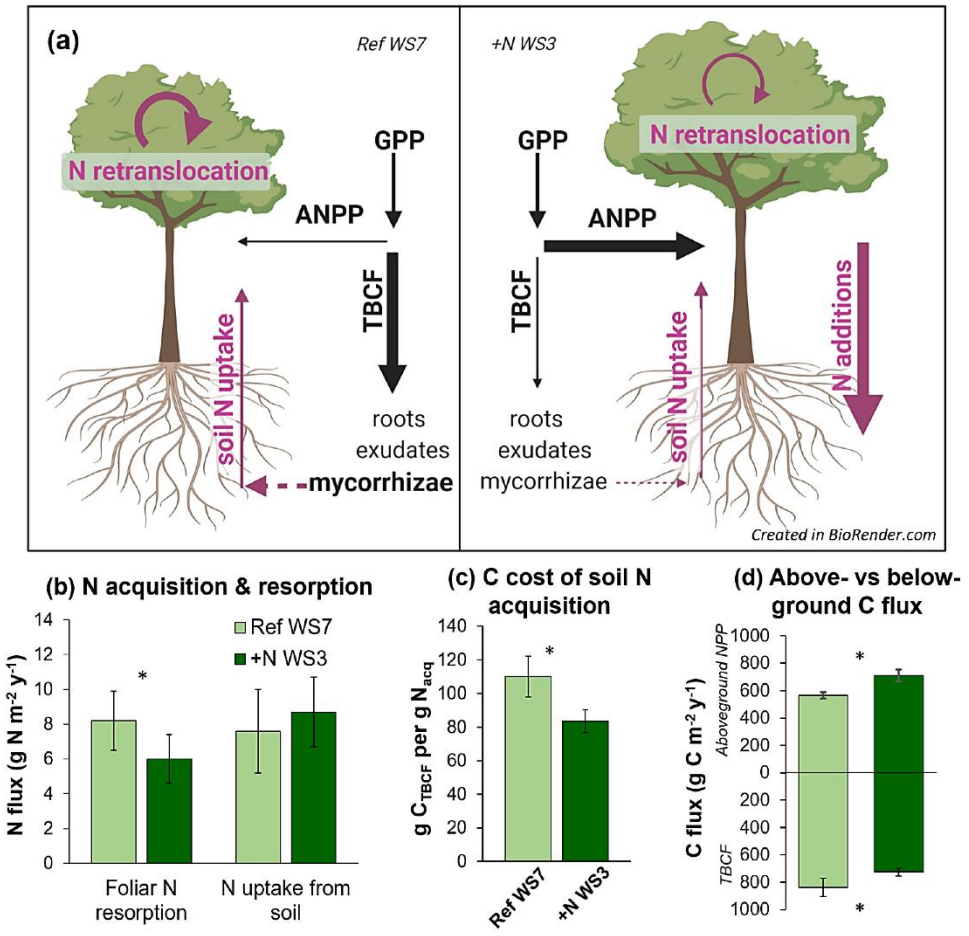

Figure 2-5. Conceptual diagram of interactions between N acquisition strategies and C partitioning and corresponding mean fluxes of C and N. (a) Conceptual diagram of the interactions between C partitioning of gross primary productivity (GPP) to aboveground net primary productivity (ANPP) and total belowground C flux (TBCF) and N acquisition strategies between Ref WS7 (left) and +N WS3 (right). With greater soil N availability in +N WS3, less N is retranslocated from foliage and less C is partitioned belowground, allowing for greater partitioning ANPP. **(b)** Mean (+/- s.e.) flux of N to meet N requirement from foliar N resorption and N uptake from soil in Ref WS7 (light green) and +N WS3 (dark green). **(c)** C cost of soil N acquisition (mean +/- se) in the reference (light green) and fertilized (dark green) watersheds. C cost of soil N acquisition estimated by dividing TBCF by soil N uptake. N uptake = woody N accumulation + fine root N production – litter N flux. **(d)** C flux to ANPP and TBCF (mean +/- se) for the reference (light green) and fertilized (dark green) watersheds. TBCF estimated with the mass balance equation: Total Soil Respiration – Leaf Litter-C. Asterisks represent significant difference between watersheds (P<0.05).

2.7 Literature cited

Adams, MB. 2008. Long-term litterfall mass from three watersheds on the Fernow Experimental Forest, West Virginia. *16th Central Hardwoods Forest Conference, USDA Forest Service* **304:** 179-186.

Adams MB. 2016. *Fernow Experimental Forest Watershed Acidification Root Data, 1991*. Parsons, WV, USA: Department of Agriculture, Forest Service, North Central Research Station.

Adams MB, Angradi TR. 1996. Decomposition and nutrient dynamics of hardwood leaf litter in the Fernow Whole-Watershed Acidification Experiment. *Forest Ecology and Management* **83**:61–69.

Adams MB, Burger J, Zelazny L, and Baumgras J. 2004. Description of the Fork Mountain Long-Term Soil Productivity Study: Site characterization. U.S. Forest Service Northern Research Station, Newtown Square, PA, USA.

Adams MB, DeWalle DR, Hom JL (Eds.). 2006. *The Fernow Watershed Acidification Study.* Springer Netherlands, Dordrecht.

Adams MB, Edwards PJ, Ford WM, Schuler TM, Thomas-Van Gundy M, Wood F. 2012. *Fernow Experimental Forest: Research History and Opportunities*. USDA Forest Service Washington, DC.

Atkins JW, Bond-Lamberty B, Fahey RT, Haber LT, Stuart-Haëntjens E, Hardman BS, LaRue E, McNeil BE, Orwig DA, Stovall AEL, *et al.* 2020. Application of multidimensional structural characterization to detect and describe moderate forest disturbance. *Ecosphere* **11**: e03156.

Averill C, Waring B. 2017. Nitrogen limitation of decomposition and decay: how can it occur? *Global Change Biology* **24**: 1417-1427.

Bates D, Mächler M, Bolker B, Walker S. 2015. Fitting linear mixed-effects models using "lme4." *Journal of Statistical Software* **67**: 1–48.

Bellassen V, Viovy N, Luyssaert S, le Maire G, Schelhaas M, Ciais P. 2011. Reconstruction and attribution of the carbon sink of European forests between 1950 and 2000. *Global Change Biology* **17**: 3274-3292.

Bloom AJ, Chapin FS, Mooney HA. 1985. Resource limitation in plants: An economic analogy. *Annual Review of Ecology and Systematics* **16**: 363–392.

Brenneman BB, Frederick DJ, Gardner WE, Schoenhofen LH, Marsh PL. 1978. Biomass of species and stands of West Virginia hardwoods. *In Proceedings of Central Hardwood Forest Conference II.* Pages 159–178. Purdue University, West Lafayette, IN, USA.

Brzostek ER, Fisher JB, Phillips RP. 2014. Modeling the carbon cost of plant nitrogen acquisition: Mycorrhizal trade-offs and multipath resistance uptake improve predictions of retranslocation. *Journal of Geophysical Research*: *Biogeosciences* **119**: 1684–1697.

Carrara JE, Walter CA, Hawkins JS, Peterjohn WT, Averill C, Brzostek ER. 2018. Interactions among plants, bacteria, and fungi reduce extracellular enzyme activities under long-term N fertilization. *Global Change Biology* **24**: 2721–2734.

Chapman SK, Langley JA, Hart SC, Koch GW. 2006. Plants actively control nitrogen cycling: uncorking the microbial bottleneck. *New Phytologist* **169:** 27-34.

Cotrufo MF, Soong JL, Horton AJ, Campbell EE, Haddix ML, Wall DH, Parton WJ. 2015. Formation of soil organic matter via biochemical and physical pathways of litter mass loss. *Nature Geoscience* **8**: 776-779.

Craine JM, Elmore AJ, Wang L, Aranibar J, Bauters M, Boeckx P, Crowley BE, Dawes MA, Delzon S, Fajardo A, *et al.* 2018. Isotopic evidence for oligotrophication of terrestrial ecosystems. *Nature Ecology and Evolution* **2**:1735–1744.

Davies-Barnard T, Meyerholt J, Zaehle S, Friedlingstein P, Brovkin V, Fan Y, Fisher R, Jones C, Lee H, Peano D, *et al.* 2020**.** Nitrogen cycling in CMIP6 land surface models: Progress and limitations. *Biogeosciences* **17**: 5129-5148.

Drake JE, Gallet-Budynek A, Hofmockel KS, Bernhardt ES, Billings SA, Jackson RB, Johnsen KS, Lichter J, Mccarthy HR, Mccormack ML, *et al.* 2011. Increases in the flux of carbon belowground stimulate nitrogen uptake and sustain the long-term enhancement of forest productivity under elevated CO_2. *Ecology Letters* **14**:349–357.

Du E, de Vries W. 2018. Nitrogen-induced new net primary production and carbon sequestration in global forests. *Environmental Pollution* **242**:1476–1487.

Enanga EM, Casson NJ, Fairweather TA, Creed IF. 2017. Nitrous oxide and dinitrogen: The missing flux in nitrogen budgets of forested catchments? *Environmental Science and Technology* **51**: 6036-6043.

Edwards PJ; Wood F. 2011. Fernow Experimental Forest daily streamflow. Newtown Square, PA: U.S. Department of Agriculture, Forest Service, Northern Research Station. Updated 09 January 2020. doi: 10.2737/RDS-2011-0015

Fahey TJ, Tierney GL, Fitzhugh RD, Wilson GF, Siccama TG. 2005. Soil respiration and soil carbon balance in a northern hardwood forest ecosystem. *Forestry* **35**: 244-253.

Feng Z, Rütting T, Pleijel H, Wallin G, Reich PB, Kammann CI, Newton PCD, Kobayashi K, Luo Y, Uddling J. 2015. Constraints to nitrogen acquisition of terrestrial plants under elevated CO_2. *Global Change Biology* **21**:3152–3168.

Fernández-Martínez M, Vicca S, Janssens IA, Sardans J, Luyssaert S, Campioli M, Chapin III FS, Ciais P, Malhi Y, Obersteiner M, *et al.* 2014. Nutrient availability as the key regulator of global forest carbon balance. *Nature Climate Change* **4**:471–476.

Fisher JB, Sitch S, Malhi Y, Fisher RA, Huntingford C, Tan S-Y. 2010. Carbon cost of plant nitrogen acquisition: A mechanistic, globally applicable model of plant nitrogen uptake, retranslocation, and fixation. *Global Biogeochemical Cycles* **24**: GB003621.

Fisher RA, Wieder WR, Sanderson BM, Koven CD, Oleson KW, Xu C, Fisher J, Shi M, Walker AP, Lawrence DM. 2019. Parametric controls on vegetation responses to biogeochemical forcing in the CLM5. *Journal of Advances in Modeling Earth Systems* **11**: 2879-2895.

Fleischer K, Wårlind D, Van Der Molen MK, Rebel KT, Arneth A, Erisman JW, Wassen MJ, Smith B, Gough CM, Margolis HA, *et al.* 2015. Low historical nitrogen deposition effect on carbon sequestration in the boreal zone. *Journal of Geophysical Research: Biogeosciences* **120**: 2542–2561.

Forstner SJ, Wechselberger V, Müller S, Keibinger KM, Díaz-Pinés E, Wanek W, Scheppi P, Hagedorn F, Gundersen P, Tatzber M, *et al.* 2019. Vertical redistribution of soil organic carbon pools after twenty years of nitrogen addition in two temperate coniferous forests. *Ecosystems* **22**: 379-400.

Fowler D, Coyle M, Skiba U, Sutton MA, Cape JN, Reis S, Sheppard LJ, Jenkins A, Grizzetti B, Galloway JN, *et al.* 2013. The global nitrogen cycle in the twenty-first century. *Philos Trans R Soc Lond B Biol Sci* **368**: 20130164

Fowler ZK, Adams MB, Peterjohn WT. 2015**.** Will more nitrogen enhance carbon storage in young forests stands in central Appalachia? *Forest Ecology and Management* **337:** 144-152.

Frey SD, Ollinger S, Nadelhoffer K, Bowden R, Brzostek E, Burton A, Caldwell BA, Crow S, Goodale CL, Grandy AS, *et al.* 2014. Chronic nitrogen additions suppress decomposition and sequester soil carbon in temperate forests. *Biogeochemistry* **121**:305–316.

Galloway JN, Trends R, Townsend AR, Erisman JW, Bekunda M, Cai Z, Freney JR, Martinelli LA, Seitzinger SP, Sutton MA. 2008. Transformation of the nitrogen cycle: potential solutions. *Science* **320**: 889–892.

Giardina CP, Ryan MG. 2002. Total belowground carbon allocation in a fast-growing eucalyptus plantation estimated using carbon balance approach. *Ecosystems* **5**: 487-499.

Gill AL, Finzi AC. 2016. Belowground carbon flux links biogeochemical cycles and resource-use efficiency at the global scale. *Ecology Letters* **19**:1419–1428.

Gilliam FS, Walter CA, Adams MB, Peterjohn WT. 2018. Nitrogen (N) dynamics in the mineral soil of a Central Appalachian hardwood forest during a quarter century of whole-watershed N additions. *Ecosystems* **21**: 1489-1504.

Groffman PM, Driscoll CT, Durán J, Campbell JL, Christenson LM, Fahey TJ, Fisk MC, Fuss C, Likens GE, Lovett G, *et al.* 2018. Nitrogen oligotrophication in northern hardwood forests. *Biogeochemistry* **141**: 523-539.

Van Heerwaarden LM, Toet S, Aerts R. 2003. Current measures of nutrient resorption efficiency lead to a substantial underestimation of real resorption efficiency: Facts and solutions. *Oikos* **101**: 664–669.

Helvey JD, Kunkle SH. 1986. Input-output budgets of selected nutrients on an experimental watershed near Parsons. *WV. Res. Pap. NE-584. USDA Forest Service. Northeastern Experiment Station. Broomall, PA.*

Hobbie, EA. 2006. Carbon allocation to ectomycorrhizal fungi correlates with belowground allocation in culture studies. *Ecology* **87**: 563-569.

Hobbie EA, Hobbie JE. 2008. Natural abundance of (15)N in nitrogen-limited forests and tundra can estimate nitrogen cycling through mycorrhizal fungi: a review. *Ecosystems* **11**: 815-830.

Högberg MN, Briones MJI, Keel SG, Metcalfe DB, Campbell C, Midwood AJ, Thornton B, Hurry V, Linder S, Näsholm T, *et al.* 2010. Quantification of effects of season and nitrogen supply on tree below-ground carbon transfer to ectomycorrhizal fungi and other soil organisms in a boreal pine forest. *New Phytologist* **187**:485–493.

Holopainen JK, Peltonen P, 2002. Bright autumn colours of deciduous trees attract aphids: nutrient retranslocation hypothesis. *Oikos* **99**:184-188.

Hurlbert SH. 1984. Pseudoreplication and the design of ecological field experiments. *Ecological Monographs* **54**: 187-211.

Hyvönen R, Persson T, Andersson S, Olsson B, Ågren GI, Linder S. 2008. Impact of long-term nitrogen addition on carbon stocks in trees and soils in northern Europe. *Biogeochemistry* **89**: 121-137.

Ibáñez I, Zak DR, Burton AJ, Pregitzer KS. 2016. Chronic nitrogen deposition alters tree allometric relationships: implications for biomass production and carbon storage. *Ecological Applications* **26**:913–925.

Ise T, Litton CM, Giardina CP, Ito A. 2010. Comparison of modeling approaches for carbon partitioning: Impact on estimates of global net primary production and equilibrium biomass of woody vegetation from MODIS GPP. *Journal of Geophysical Research: Biogeosciences* **115**:1–11.

Janssens IA a., Dieleman W, Luyssaert S, Subke J, Reichstein M, Ceulemans R, Ciais P, Dolman AJ, Grace J, Matteucci G, *et al.* 2010. Reduction of forest soil respiration in response to nitrogen deposition. *Nature Geoscience* **3**:315–322.

JMP®**,** Version 14.0. SAS Institute Inc., Cary, NC, 1989-2019.

Johnson NC, Graham JH, Smith FA. 1997. Functioning of mycorrhizal associations along the mutualism – parasitism continuum. *New Phytologist* **135:** 575–585.

Kochenderfer JN. 2006. Fernow and the Appalachian Hardwood Region. In: Adams MB, DeWalle DR, Hom JL, eds. *The Fernow Watershed Acidification Study*. Dordrecht, The Netherlands: Springer, 17-39.

Kochenderfer JN, Wendel GW. 1983**.** Plant succession and hydrologic recovery on a deforested and herbicided watershed. *Forest Science* **29**: 545-558.

Kuzyakov Y. 2010. Priming effects: Interactions between living and dead organic matter. *Soil Biology & Biochemistry* **42**: 1363-1371.

LeBauer DS, Treseder K. 2008. Nitrogen limitation of net primary productivity in terrestrial ecosystems is globally distributed. *Ecology* **89**: 371–379.

Lehrter JC, Cebrian J. 2010. Uncertainty propagation in an ecosystem nutrient budget. *Ecological Applications* **20**: 508–524.

Lenth RV. 2016**.** Least-Squares Means: The R package lsmeans. *Journal of Statistical Software* **69**: 1-33.

Litton CM, Raich JW, Ryan MG. 2007**.** Carbon allocation in forest ecosystems. *Global Change Biology* **13**: 2089-2109.

Liu L, Greaver TL. 2010. A global perspective on belowground carbon dynamics under nitrogen enrichment. *Ecology Letters* **13**:819–828.

Lloyd J, Taylor JA. 1994. On the temperature dependence of soil respiration. *Functional Ecology Functional Ecology* **8**: 315–323.

Lovett GM, Arthur MA, Weathers KC, Fitzhugh RD, Templer PH. 2013. Nitrogen addition increases carbon storage in soils, but not in trees, in an Eastern U.S. deciduous forest. *Ecosystems* **16**: 980–1001.

Malcomb JD, Scanlon TM, Epstein HE, Druckenbrod DL, Vadeboncoeur MA, Lanning M, Adams MB, Wang L. 2020. Assessing temperate forest growth and climate sensitivity in response to a long-term whole-watershed acidification experiment. *Journal of Geophysical Research: Biogeosciences* **125**: 1–16.

Meerts P. 2003. Mineral nutrient concentrations in sapwood and heartwood: a literature review. *Annals of Forest Science* **59**: 713–722.

Meyerholt J, Sickel K, Zaehle S. 2020. Ensemble projections elucidate effects of uncertainty in terrestrial nitrogen limitation on future carbon uptake. *Global Change Biology* **26**: 3978-3996.

Miles PD, Smith WB. 2009. Specific gravity and other properties of wood and bark for 156 tree species found in North America. *Res. Note NRS-38*. Newtown Square, PA: U.S. Department of Agriculture, Forest Service, Northern Research Station. 35 p.

Mohan JE, Cowden CC, Baas P, Dawadi A, Frankson PT, Helmick K, Hughes E, Khan S, Lang A, Machmuller M, *et al.* 2014. Mycorrhizal fungi mediation of terrestrial ecosystem responses to global change. *Fungal Ecology* **10**: 3–19.

Montané F, Fox AM, Arellano AF, MacBean N, Ross Alexander M, Dye A, Bishop DA, Trouet V, Babst F, Hessl AE, *et al.* 2017. Evaluating the effect of alternative carbon allocation schemes in a land surface model (CLM4.5) on carbon fluxes, pools, and turnover in temperate forests. *Geoscientific Model Development* **10**: 3499–3517.

Nave LE, Vance ED, Swanston CW, Curtis PS. 2009. Impacts of elevated N inputs on north temperate forest soil C storage, C/N, and net N-mineralization. *Geoderma* **153**: 231–240.

O'Sullivan M, Spracklen D V., Batterman SA, Arnold SR, Gloor M, Buermann W. 2019. Have synergies between nitrogen deposition and atmospheric CO_2 driven the recent enhancement of the terrestrial carbon sink? *Global Biogeochemical Cycles* **33**: 163–180.

Pan Y, Birdsey RA, Fang J, Houghton R, Kauppi PE, Kurz WA, Phillips OL, Shvidenko A, Lewis SL, Canadell JG, *et al.* 2011. A large and persistent carbon sink in the world's forests. *Science* **333**: 988-993.

Peterjohn WT, Adams MB, Gilliam FS. 1996. Symptoms of nitrogen saturation in two Central Appalachian hardwood forest ecosystems. *Biogeochemistry* **35**: 507–522.

Phillips RP, Brzostek E, Midgley MG. 2013. The mycorrhizal-associated nutrient economy: A new framework for predicting carbon-nutrient couplings in temperate forests. *New Phytologist* **199:** 41-51.

Pregitzer KS, Burton AJ, Zak DR, Talhelm AF. 2008. Simulated chronic nitrogen deposition increases carbon storage in Northern Temperate forests. *Global Change Biology* **14**:142–153.

Raich JW, Nadelhoffer KJ. 1989. Belowground carbon allocation in forest ecosystems: global trends. *Ecology* **70**: 1346-1354.

Rastetter EB, Vitousek PM, Field CB, Shaver GR, Herbert D, Agren GI. 2001. Resource optimization and symbiotic nitrogen fixation. *Ecosystems* **4:** 369-388.

SanClements MD, Fernandez IJ, Lee RH, Roberti JA, Adams MB, Rue GA, McKnight DM. 2018. Long-term experimental acidification drives watershed scale shift in dissolved organic matter composition and flux. *Environmental Science and Technology* **52**: 2649-2657.

Schlesinger W, Burnhardt. 2020. Biogeochemical Cycling on Land. In: *Biogeochemistry: An analysis of global change. 4th Ed.* San Diega, CA, USA: Academic press 198.

Schmidt MWI, Torn MS, Abiven S, Dittmar T, Guggenberger G, Janssens I a., Kleber M, Kögel-Knabner I, Lehmann J, Manning D a. C, *et al.* 2011. Persistence of soil organic matter as an ecosystem property. *Nature* **478**:49–56.

Schulte-Uebbing L, de Vries W. 2017. Global-scale impacts of nitrogen deposition on tree carbon sequestration in tropical, temperate, and boreal forests: A meta-analysis. *Global Change Biology* **24**: e416-e431.

Shi M, Fisher JB, Brzostek ER, Phillips RP. 2016**.** Carbon cost of plant nitrogen acquisition: Global carbon cycle impact from an improved plant nitrogen cycle in the Community Land Model. *Global Change Biology* **22:** 1299–1314**.**

Shi M, Fisher JB, Phillips RP, Brzostek ER. 2019. Neglecting plant-microbe symbioses leads to underestimation of modeled climate impacts. *Biogeosciences* **16**:457–465.

Smith P, Davis SJ, Creutzig F, Fuss S, Minx J, Gabrielle B, Kato E, Jackson RB, Cowie A, Kriegler E, *et al.* 2016. Biophysical and economic limits to negative CO_2 emissions. *Nature Climate Change* **6**: 42–50.

Sulman BN, Brzostek ER, Medici C, Shevliakova E, Menge DNL, Phillips RP. 2017**.** Feedbacks between plant N demand and rhizosphere priming depend on type of mycorrhizal association. *Ecology Letters* **20**: 1043–1053.

Sulman BN, Moore J, Abramoff R, Averill C, Kivlin S, Georgiou K, Sridhar B, Hartman M, Wang G, Wieder W, *et al.* 2018. Multiple models and experiments underscore large uncertainty in soil carbon dynamics. *Biogeochemistry* **141**:109–123.

Sulman BN, Shevliakova E, Brzostek ER, Kivlin SN, Malyshev S, Menge DNL, Zhang X. 2019. Diverse mycorrhizal associations enhance terrestrial C storage in a global model. *Global Biogeochemical Cycles* **33**: 501–523.

Sutton MA, Simpson D, Levy PE, Smith RI, Reis S, Van Oijen M, De Vries WIM. 2008. Uncertainties in the relationship between atmospheric nitrogen deposition and forest carbon sequestration. *Global Change Biology* **14**: 2057-2063.

Terrer C, Vicca S, Hungate BA, Phillips RP, Prentice IC. 2016. Mycorrhizal association as a primary control of the CO_2 fertilization effect. *Science* **353**: 72–74.

Terrer C, Jackson RB, Prentice IC, Keenan TF, Kaiser C, Vicca S, Fisher JB, Reich PB, Stocker BD, Hungate BA, *et al.* 2019. Nitrogen and phosphorus constrain the CO_2 fertilization of global plant biomass. *Nature Climate Change* **9**: 684–689.

Thornton PE, Lamarque JF, Rosenbloom NA, Mahowald NM. 2007. Influence of carbon-nitrogen cycle coupling on land model response to CO_2 fertilization and climate variability. *Global Biogeochemical Cycles* **21**: 1–15.

Todd-Brown KEO, Randerson JT, Post WM, Hoffman FM, Tarnocai C, Schuur EAG, Allison SD. 2013. Causes of variation in soil carbon simulations from CMIP5 Earth system models and comparison with observations. *Biogeosciences* **10**:1717–1736.

van't Hoff JH. 1898. Lectures on theoretical and physical chemistry. *Chemical Dynamics Part I.* 224-229. Edward Arnold, London.

Venterea RT, Groffman PM, Castro MS, Verchot LV, Fernandez IJ, Adams MB. 2004. Soil emissions of nitric oxide in two forest watersheds subject to elevated N inputs. *Forest Ecology and Management* **196**: 335-349.

Vitousek PM. 1982. Nutrient cycling and nutrient use efficiency. *American Naturalist* **119**: 553–572.

de Vries W, Du E, Butterbach-Bahl K. 2014. Short and long-term impacts of nitrogen deposition on carbon sequestration by forest ecosystems. *Current Opinion in Environmental Sustainability* **9**: 90–104.

Wieder WR, Cleveland CC, Smith WK, Todd-Brown K. 2015. Future productivity and carbon storage limited by terrestrial nutrient availability. *Nature Geoscience* **8**: 441–444.

Wieder WR, Lawrence DM, Fisher RA, Bonan GB, Cheng SJ, Goodale CL, Grandy AS, Koven CD, Lombardozzi DL, Oleson KW, *et al.* 2019. Beyond static benchmarking: Using experimental manipulations to evaluate land model assumptions. *Global Biogeochemical Cycles* **33**: 1289-1309.

Wright IJ, and Westoby M, 2003. Nutrient concentration, resorption and lifespan: leaf traits of Australian sclerophyll species. *Functional Ecology* **17**: 10-19.

Xia J, Wan S. 2008. Global response patterns of terrestrial plant species to nitrogen addition. *The New Phytologist* **179**: 428–439.

Yanai RD, Vadeboncoeur MA, Hamburg SP, Arthur MA, Fuss CB, Groffman PM, Siccama TG, Driscoll CT. 2013. From missing source to missing sink: Long-term changes in the nitrogen budget of a northern hardwood forest. *Environmental Science and Technology* **47**: 11440–11448.

Young D, Zégre N, Edwards P, Fernandez R. 2019. Assessing streamflow sensitivity of forested headwater catchments to disturbance and climate change in the central Appalachian Mountains region, USA. *Science of the Total Environment* **694**: 133382.

Zak DR, Holmes WE, Burton AJ, Pregitzer KS, Talhelm AF. 2008. Simulated atmospheric NO_3^- deposition increases soil organic matter by slowing decomposition. *Ecological Applications* **18**: 2016-2027.

Zak DR, Freedman ZB, Upchurch R, Steffens M, Kögel-Knabner I. 2017. Anthropogenic N deposition increases soil organic matter accumulation without altering its biochemical composition. *Global Change Biology* **23**: 933–944.

Chapter 3. The path less taken: Long-term nitrogen additions slow leaf decomposition and favor the physical transfer pathway of soil organic matter formation

"The soil is the great connector of lives, the source and destination of all. It is the healer and restorer and resurrector, by which disease passes into health, age into youth, death into life. Without proper care for it we can have no community, because without proper care for it we can have no life."

- **Wendell Berry**

Reprinted from

Eastman, B.A., Adams, M.B., Peterjohn, W.T., 2022. The path less taken: Long-term N additions slow leaf litter decomposition and favor the physical transfer pathway of soil organic matter formation. *Soil Biology & Biochemistry* **166:** 108567.

3.1 Abstract

Understanding soil organic matter (SOM) formation as a balance between soil microbial access to organic plant inputs and protection by chemical recalcitrance and mineral associations can greatly improve our projections of this important terrestrial carbon pool. However, gaps remain in our understanding of the processes controlling the formation and destabilization of SOM and how these processes are affected by persistent global changes, such as nitrogen (N) deposition. To assess how elevated N deposition influences decomposition dynamics and the fate of plant inputs in a temperate deciduous forest, we coupled a reciprocal transplant leaf litter decomposition study with an analysis of the distribution of SOM in mineral associated and particulate organic matter fractions at a long-term, whole-watershed, N fertilization experiment. Nearly 30 years of N additions slowed leaf litter decomposition rates by about 11% in the fertilized watershed, regardless of the watershed from which the initial litter was collected. An apparent consequence of the altered rates of decomposition was that the proportion of SOM in light particulate organic matter in soil from the fertilized watershed was about 40% greater than that of the reference watershed, and was positively correlated with the bulk soil carbon to nitrogen ratio. Collectively, our results suggest that N saturation in a temperate forest alters SOM formation by slowing decomposition and favoring the accumulation of particulate organic matter as opposed to microbially processed mineral associated organic matter.

3.2 Introduction

Forest soils represent one of the largest terrestrial pools of carbon (C) (Pan *et al.*, 2011; Ciais *et al.*, 2013), and one whose rates of formation and loss may be significantly altered by prolonged changes in the global environment (e.g., soil warming; Melillo *et al.*, 2017; Nottingham *et al.*, 2020; Ofiti *et al.*, 2021). While many recent studies have focused on the processes of soil C formation, we still lack a robust understanding of how the complex and interacting mechanisms responsible for soil C stabilization and destabilization will impact overall soil C stocks under future environmental and land management conditions (Friedlingstein *et al.*, 2014; Bradford *et al.*, 2016; Griscom *et al.*, 2017; Bailey *et al.*, 2019). An important factor controlling soil organic matter (SOM) dynamics is the nitrogen (N) status of an ecosystem. Numerous N addition studies in forest ecosystems suggest that elevated N inputs can slow the decomposition of plant inputs (especially lignin), reduce rates of soil CO_2 efflux, and may allow the accumulation of soil C with potentially greater C:N ratios (Pregitzer *et al.*, 2008; Nave *et al.*, 2009; Janssens *et al.*, 2010; Frey *et al.*, 2014). However, plant residue decomposition and SOM properties are typically studied separately, hindering our understanding of how reductions in decomposition with N additions may translate to changes in overall C stocks and shifts in the nature of SOM.

The effects of N additions on SOM formation can be expressed through their influence on both the quality of organic inputs and the composition and function of the soil microbial community. Plant materials with lower C:N ratios and less molecular complexity (less lignin) are decomposed by microbes more efficiently, promoting mineral-associated organic matter (MAOM) through the sorption of microbial necromass and byproducts to soil mineral surfaces (Melillo *et al.*, 1989; Kölbl and Kögel-Knabner, 2004; Talbot *et al.*, 2012; Bradford *et al.*, 2016; Winsome *et al.*, 2017; Córdova *et al.*, 2018). In contrast, plant inputs with greater recalcitrance

to decomposition may form particulate organic matter (POM) simply through a lower tendency of microbes to decompose these components and their physical transfer through the soil profile (Von Lützow *et al.*, 2008; Cotrufo *et al.*, 2013, 2015).

In general, the POM fractions are more plant-like in chemistry, more vulnerable to disturbance, and are thought to have a faster turnover time than MAOM (Gregorich *et al.*, 2006). Also within this view of SOM formation/destabilization, microbial activity and physical access to SOM regulates persistence and/or vulnerability of SOM pools. Consistent with these ideas, results from N addition experiments have shown decreased oxidative enzyme activity, as well as reductions in the relative abundance of fungal decomposers in the soil, which slow the degradation of lignin-containing plant inputs and can shift the pathway of SOM formation to favor POM accumulation (Frey *et al.*, 2014; Averill *et al.*, 2018; Carrara *et al.*, 2018; Zak *et al.*, 2019a). Because different SOM pools may form through different processes and have different sensitivities to environmental controls, it is important to study how they individually respond to environmental changes such as N additions (Lavallee *et al.*, 2020).

Long-term N addition experiments to forest ecosystems provide a unique opportunity to assess the linkages between litter quality, soil microbial processes, and SOM formation. For example, a recent synthesis of a 30-year, whole-watershed, N-addition study in a temperate forest found reduced belowground C allocation by plants, an accumulation of surface mineral soil C, and an increase in the C:N of SOM of surface mineral soil (Eastman *et al.*, 2021). Collectively, the pattern of observed changes from this synthesis suggests that the shift in C allocation with N fertilization influenced the soil microbial community and activity in ways that allowed an accumulation of high C:N SOM. This interpretation is supported by previous studies at this site and elsewhere that found reduced leaf litter decomposition (Adams and Angradi, 1996; Pregitzer *et al.*, 2008; Frey *et al.*, 2014; Argiroff *et al.*, 2019; Wang *et al.*, 2019), and

reduced mycorrhizal colonization and ligninolytic enzyme activity with experimental N additions (Treseder, 2004; Carrara *et al.*, 2018). These responses can reduce mid- to late-stage decomposition rates and favor POM formation through the physical transfer and accumulation of plant litter inputs that bypass microbial decomposition. Past studies suggest N addition alter POM accumulation in temperate forests (Von Lützow *et al.*, 2008) but long term studies on how chronic N additions influence litter decomposition and the distribution of soil organic matter are rare. This is particularly important because soil C stabilization responses to environmental change may take decades to be fully expressed.

To examine how shifts in leaf litter quality and soil microbial activity due to experimental N additions influences rates of leaf litter decomposition and the distribution of SOM among distinct fractions, we paired a leaf litter decomposition study with a soil density fractionation analysis of the SOM at the Fernow Experimental Forest long-term N fertilization experiment (West Virginia, USA). Considering existing evidence for both a shift in leaf litter quality (lower C:N ratio) and soil microbial biochemistry (lower mycorrhizal colonization rates and reduced ligninolytic enzyme activity) in response to chronic N additions (Carrara *et al.*, 2018; Eastman *et al.*, 2021), this site serves as a model system for understanding SOM formation and destabilization under conditions of elevated N inputs. We focused on testing three specific hypotheses: 1) Decomposition will be slower for leaf litter transplanted into N amended soil, especially for litter with high lignin and/or low N content; 2) There will be a greater proportion of POM in the surface mineral soils of the N addition watershed due to greater plant particulate litter that bypasses microbial decomposition; and 3) There will be a greater proportion of MAOM in the surface mineral soils of the N addition watershed due to greater microbial CUE with N amendments.

3.3 Material and methods

Site description

Both the litter decomposition and soil density fractionation studies were conducted at the Fernow Experimental Forest, WV, USA (39º1'48''N, 79º40'12''W), in two temperate deciduous forested watersheds that compose a long-term, whole-watershed fertilization experiment (Adams *et al.*, 2012). One watershed, +N WS3 (34 ha), received 35 kg N ha^{-1} yr^{-1} from 1989-2019 in the form of ammonium sulfate ($(NH_4)_2SO_4$). These N additions were about double the rate of ambient N in throughfall at the start of the experiment in 1989 (Helvey and Kunkle, 1986) and about quadruple the ambient rate towards the end of the experiment in 2019 (NADP https://nadp.slh.wisc.edu/; CASTNET https://www.epa.gov/castnet). An adjacent, similarly aged watershed, Ref WS7 (24 ha), serves as a reference to +N WS3. Land-use history for these watersheds has been previously described (see Kochenderfer and Wendel, 1983; Kochenderfer, 2006). A major difference between these watersheds was that Ref WS7 was cut in two phases and subsequently treated with herbicide for 3 or 6 years before recovery began in 1969, whereas +N WS3 was clear cut without herbicide treatment in 1970.

The study site is located in the Allegheny Mountain region of the Central Appalachian Mountains, with elevations ranging from 530-1115 m, and slopes from 20-50% (Adams *et al.*, 2012). Mean annual precipitation is relatively evenly distributed throughout the year, averaging 146 cm annually, and mean annual temperature is 9.3 ºC with the growing season lasting from May through October (Adams *et al.*, 2012; Young *et al.*, 2019). Soils are a shallow (typically < 1 m), well-drained, silty loam, Typic Drystocrepts, derived from sandstone and shale parent material (Adams *et al.*, 2012).

We conducted both studies at 10 circular, 0.04-ha plots per watershed, which were previously established to encompass the full range of elevation and slope aspect (Gilliam *et al.*,

1994). Dominant tree species were similar in the selected plots in both watersheds and included sugar maple (*Acer saccharum* L.), tulip poplar (*Liriodendron tulipifera* L.), black cherry (*Prunus serotina* Ehrh.), and sweet birch (*Betula lenta* L.). However, the relative abundance of these dominant species differed between watersheds, as the +N WS3 had a greater abundance of black cherry and less tulip poplar by basal area than the Ref WS7 (see Eastman *et al.*, 2021).

Reciprocal litter decomposition experiment

We collected freshly fallen leaf litter of the four dominant species in October of 2017 from a single site in each watershed prior to any rain event. Leaf litter from each watershed was thoroughly mixed, sorted by species, then dried at 65 °C for > 48 hours. For two species (black cherry and sweet birch) sourced from Ref WS7, insufficient litter mass was collected, so we used dried and archived leaf litter collected in 2015 (<8% of total leaf litter used in this study) to supplement the 2017 freshly fallen leaf litter.

We measured rates of leaf litter decomposition using 1-mm mesh fiberglass litterbags (~ 20 cm x 10 cm) filled with 2 g (+/- 0.25 g) of dried leaf litter of a single species and from a single source watershed. In March 2018, five replicate litterbags for each combination of tree species and source watershed were randomly assigned to each plot and placed flat on the surface of the mineral soil horizon after removing the litter layer. All litterbags in a plot were arranged in a 1-m x 1-m square, covered with coarse plastic mesh to prevent disturbance, and the litter layer was replaced. Litterbags were collected four times between deployment (March 2018) and the end of the study (March 2020). One litterbag of each species and watershed of origin was collected from each plot after 3, 6, and 12 months (10 replicates). After 24 months, two litterbags of each species and watershed of origin were collected from each plot for the final collection (20 replicates). Following collection, litter in each bag was gently brushed to remove

soil, and roots and invertebrates were removed as best as possible without losing leaf litter material. Litter was then dried at 65 °C for > 48 hours and weighed.

Overall, the experimental design consisted of 2 watersheds of origin x 2 watersheds of transplant x 10 plots per watershed x 4 species x 5 time points for a total of 40 litterbags per plot and 800 litterbags in total. The reciprocal design of this experiment allowed us to assess whether any detectable differences in decomposition rates between the watersheds were due to differences in litter chemistry between source watersheds or differences in the soil environment into which litter bags were transplanted.

Litter quality

To determine initial litter quality, three subsamples of freshly fallen litter collected for each species and watershed of origin were dried, ground, and analyzed for C and N content using Dumas combustion in an elemental analyzer (NA 1500 Series 2, Carlo Erba Instruments, Milan, Italy). Dried, partially decomposed leaf litter from all 800 litterbags collected during the two-year experiment were similarly ground and analyzed for C and N content.

Initial lignin and cellulose content of leaf litter from each species and watershed of origin were determined using an acid detergent digest method (Van Soest, 1963; as described by Holtzapple, 2003). In summary, 4-5 subsamples of dried, ground leaf litter were digested in an acid-detergent fiber digest solution to isolate cellulose, lignin, and ash. This residue was dried at 65 °C for > 48 hours and weighed. To remove and estimate cellulose in the residue, the samples were then soaked in 75% sulfuric acid, rinsed with deionized (DI) water, dried at 65 °C for > 48 hours, then weighed. Final residue was then heated in a muffle furnace at 525 °C for 2 hours to determine ash-free dry weight. For the purposes of this study, we consider the ash-free mass remaining after the acid detergent and strong acid digests to be "lignin." We similarly assessed

lignin and cellulose content of final decomposed litter (after 24 months) by randomly selecting a subset of three litter samples for each species, source watershed, and watershed of transplant category (48 total).

We estimated the lignocellulose index (LCI) as lignin content/(lignin content + cellulose content) (Melillo *et al.*, 1989). We also calculated the lignin:N ratio of initial and final leaf litter. Final leaf litter lignin:N was calculated for the subset of samples that were analyzed for lignin and % N (48 samples total). Because our initial litter chemistry analysis used a different number of subsample replicates for determination of % N (n=3) and % lignin (n=4 or 5), we paired every % N measurement with every % lignin measurement for a given species and source watershed category to determine the range and statistics of initial leaf litter lignin:N values.

Soil chemistry

The total C and N content of the 0-5 cm of mineral soil in each of the litter decomposition plots were measured on three 2.5-cm diameter soil cores collected in October 2018. The three soil cores per plot were combined, sieved (to pass a 2-mm mesh), dried at 65 °C for > 48 hours, and ground prior to analysis of C and N content by Dumas combustion.

Calculations

Percent mass remaining was calculated for each litterbag. Despite our efforts to clean the decomposed litter of soil, some soil could not be removed without potentially losing leaf tissue. To correct for soil contamination, we assumed that the C concentration of the leaf litter remains constant over decomposition. Thus, any decomposed leaf litter with a C concentration lower than the initial value was considered to be contaminated with mineral soil (Blair & Crossley, 1988; Janzen *et al.*, 2002; Midgley *et al.*, 2015). The following mixing model was used to determine the fraction of final mass that was litter:

$$fLitter = (Cd - Cs)/(Ci - Cs)$$

where *fLitter* = the fraction of the total litterbag sample mass that is actually litter; *Cd* = the decomposed litter C concentration; *Cs* = the mineral soil (0-5 cm) C concentration, previously obtained (see 2.2.2); *Ci* = the initial leaf litter C concentration. The mass of the decomposed litter sample was then multiplied by *fLitter* to correct for soil contamination.

We calculated the decomposition rates of leaf litter using a single-pool negative exponential model,

$$M_t = exp^{-kt}$$

where M_t is the proportion of initial mass remaining at a given timepoint, *k* is the decomposition rate (year^{-1}) and *t* is the decomposition time (years) (Jenny *et al.*, 1949; Olsen, 1963). To estimate the decomposition rate (*k*), an exponential model was fit to the proportion of mass remaining over time (years) for each combination of species, source watershed, and watershed of transplant. In this analysis, plots were the replicates (n=10), and 160 models were fit to 160 sets of litterbags (4 species x 2 watersheds of origin x 2 watersheds of transplant x 10 plots). We also used a model structure with the intercept set to zero to avoid bias in single-pool decomposition models (Adair *et al.*, 2010). R^2 values were > 0.80 for > 80% of model fits, and given the relatively short duration of this study, the single-pool exponential model is thought to best capture early-stage decomposition dynamics (Harmon *et al.*, 2009).

Soil density fractionation study

Soil sampling

To assess how elevated N inputs may influence the fate of plant inputs, we separated SOM into three fractions: light POM, heavy POM, and MAOM. Soil was collected from four 5-

cm diameter soil cores of the 0-15 cm of mineral soil in each plot in October 2018, for a total of 80 soil samples (2 watersheds x 10 plots x 4 soil cores). Soils were stored less than six weeks at 4 °C before being sieved (2 mm) to remove plant and rock material, homogenized, and dried at 65 °C for > 48 hours.

Fractionation procedure

We evaluated the nature of organic matter in the mineral soil in each plot using a three-pool soil density fractionation framework described by Lavallee *et al.* (2020). Briefly, SOM was separated into three pools based on their densities and sizes, which is thought to represent the degree of organic matter stabilization (Gregorich *et al.*, 2006). Two steps were used to isolate the light POM fraction, which we define as plant-like residue with a density < 1.85 g cm^{-3} because it is minimally bound to soil minerals. First, 5.5-6.0 g of dry soil subsamples were shaken for 15 minutes in DI water at ~100 oscillations per minute, centrifuged at 1874 *g* for 15 minutes, and then the supernatant was filtered through a 20 µm nylon filter to catch the light POM. Second, we isolated the rest of the light POM by shaking soils in a liquid of density 1.85 g cm^{-3} (sodium polytungstate, SPT) for 18 hours to disperse soil macroaggregates. Samples were centrifuged at 1874 *g* for 30 minutes, the light POM that floated out of the dense liquid was aspirated onto a 20 µm nylon filter and rinsed thoroughly.

The heavy POM is defined as plant-like, chemically, but has some mineral association or microbial biproducts that increases its density and may protect the SOM in soil aggregates. Thus, the centrifuged soil pellets containing the heavy fractions (>1.85 g cm^{-3} density) were thoroughly rinsed and centrifuged with DI water at least three times to remove excess SPT. The heavy POM and MAOM that remained in the soil pellet were separated by size, suspending the pellet in DI water and sieving through a 53 µm sieve. The material remaining on the sieve was

considered the heavy POM and sand (>1.85 g cm^{-3} density and > 53 μm in size), while the matter that passed through the sieve was considered the MAOM, silt and clay fraction (< 53 μm).

All soil fractions were dried at 65 °C, and ground for C and N analysis. If 100% (+/- 5%) of initial soil sample mass was not recovered in all fractions, then the fractionation procedure was repeated for that sample; this occurred for 7 of the 80 samples that were fractionated. Additionally, subsamples of the dried soil prior to fractionation, hereafter referred to as bulk soil, was analyzed for C and N.

Statistical analysis

For the leaf litter decomposition study, we tested for differences in initial litter chemistry with a two-way ANOVA with species and source watershed as fixed effects and litter chemical properties as dependent variables (%C, %N, C:N ratio, %cellulose, %lignin, LCI, lignin:N ratio). To test for differences in final litter chemistry and decomposition rate, we conducted a 3-way ANOVA with litter species, source watershed, and watershed of transplant as fixed effects; and final litter chemical properties and decomposition rate as dependent variables (%N, C:N ratio, %cellulose, %lignin, LCI, lignin:N ratio, *k*). Robust two- and three-way ANOVAs (using the R package "rfit"; Hocking, 1985; as described in Kloke and McKean, 2012, 2014) were performed to compare initial % lignin, lignin:N ratio and LCI, and final % N and C:N ratio, respectively, as the assumption of a normal distribution of residuals were not met by these dependent variables.

For the soil density fractionation study, we tested for differences in the chemistry of bulk soil between the watersheds with a one-way, nested ANOVA with watershed as a fixed effect, plot as a random nested effect (within WS), and bulk soil chemical properties as dependent variables (%C, %N, and C:N ratio). To test for differences in fraction of bulk soil in each density fraction and chemistry of individual fractions between watersheds, we conducted a one-

way, nested ANOVA with watershed as the fixed effect, plot as the random nested effect (within WS), and fraction of total mass, total C, and total N, and chemical properties (%C, %N, C:N ratio) of each fraction as dependent variables. To test our hypothesis that a greater proportion of light POM may contribute to a greater C:N ratio in the bulk soil, we regressed the bulk soil C:N ratio against the fraction of total mass in the light POM.

For all parametric ANOVAs, comparisons among means were analyzed with Tukey-Kramer HSD *post hoc* tests, the normal distribution of residuals was tested using the Shapiro-Wilks test, and homogeneity of variance was tested using Levene's test. Variables that did not meet these assumptions were transformed using the natural logarithm prior to statistical analysis.

Replication of whole-watershed experiments is often logistically and financially challenging or impossible, and experimental treatments are commonly pseudoreplicated, as they are in this study (Hurlbert, 1984). Results should be interpreted with this in mind, but—given the duration and extent of the fertilization treatment—we consider the differences observed in leaf litter decomposition and soil density fractionation results to be primarily the result of the fertilization treatment. Furthermore, extensive differences have been previously observed between biogeochemical processes in these watershed, many of which were also observed in a nearby, fully-replicated field experiment (Adams *et al.*, 2004; Fowler *et al.*, 2015; Burnham *et al.*, 2017; Carrara *et al.*, 2018; Eastman *et al.*, 2021).

3.4 Results

Reciprocal litter decomposition experiment

Initial litter chemistry

The four species and two source watersheds of litter used in this experiment provided a sufficiently diverse array of tissue characteristics to examine the potential interaction between N additions and litter chemistry on decomposition rates. Initial litter chemistry varied among

species for all chemical properties, and differences between source watersheds typically depended on the species (Table S3-1). Most notably, the % N of the initial litter ranged from 0.69 % to 1.29 %, the C:N ratio ranged from 37.7 to 70.9, and the lignin:N ratio ranged from 13.6 to 26.6 (Table 3-1). Specifically, red maple and tulip poplar leaf litter sourced from +N WS3 had greater % N and a lower C:N ratio, whereas black cherry litter from +N WS3 had lower % N and greater C:N than litter sourced from Ref WS7 (Table 3-1). All leaf litter sourced from +N WS3 had a lower lignin:N ratio than litter sourced from Ref WS7 (Table 1). In general, red maple and sweet birch had lower quality litter, as red maple litter had the lowest % N and greatest C:N and lignin:N ratios, while sweet birch litter had the greatest % lignin (Table 3-1; Tukey-Kramer HSD). In contrast, black cherry and tulip poplar had relatively high-quality litter, both with greater % N and lower % lignin than the other two species (Table 3-1; Tukey-Kramer HSD). The LCI only differed between tulip poplar and sweet birch litter, as tulip poplar had the lowest, sweet birch had the greatest, and red maple and black cherry had intermediate LCI (Table 3-1).

Final litter chemistry

After two years of decomposition in the field, we observed differences in final litter chemistry between watersheds of transplant (Table S3-2). Specifically, final leaf litter transplanted into +N WS3 had greater % N, % cellulose, and % lignin, and a lower C:N ratio than leaves transplanted into Ref WS7 (Table 3-2). These patterns were consistent for all species regardless of the watershed from which they originated (Table S3-2).

Additionally, we observed some differences in final litter % N, C:N ratios, and LCI between litter sourced from +N WS3 and Ref WS7, regardless of the watershed into which they were transplanted (Table S3-2). Specifically, final litter material that was sourced from +N WS3

had greater % N and a lower C:N ratio for all species (Table S3-3). Also, final litter material sourced from +N WS3 had a greater LCI after decomposition, meaning more lignin relative to cellulose remained at the end of the decomposition experiment for these litter bags (Table S3-3). The initial difference in the lignin:N ratio between source watersheds did not persist in the decomposed leaves, despite the greater final % N of litter sourced from +N WS3.

Comparing final litter chemistry among species, all litter chemical properties differed among species regardless of source watershed or watershed of transplant (Table S3-2). Similar to initial chemistry, final red maple litter had the lowest % N and LCI and the greatest C:N ratio of all species (Table 3-3). Interestingly, final black cherry litter had the highest % N yet also the greatest % lignin, lignin:N ratio, and LCI (Table 3-3). Final sweet birch litter also had high % N and LCI, but a low C:N ratio (Table 3-3). Final tulip poplar litter generally had an intermediate chemical composition in comparison with the other species (Table 3-3). Relative to the initial litter chemistry, final litter chemistry of all species had much greater % N (more than 2x), a much lower C:N ratio (about half) that was less variable among species, and generally greater % lignin and LCI (Table 3-3). The % lignin and LCI for sweet birch litter—the species with the greatest initial % lignin and LCI—did not change as much between initial and final litter chemistry compared to the other three species (Table 3-1; Table 3-3).

Soil chemistry

Mineral soil that was sampled at each litter decomposition plot (n=10) had similar % C in both watersheds (~7%), while the % N was greater in the Ref WS7 (Table 3-4). The C:N ratio of the top 5 cm of mineral soil was significantly greater in +N WS3, 18.8, compared to a C:N ratio of 14.9 in Ref WS7 (Table 3-4). Similar results were found for the 0-15 cm soil sampled in the soil density fractionations sampling (Table 3-4). Likely due to the difference in soil sampling

depth between the soil density fractionation samples and the litter decomposition soil samples (0-15 cm and 0-5 cm, respectively), we detected greater % C and % N in the litter decomposition soil samples, but similar C:N ratios from both samplings (Table 3-4; Fig. S3-1).

Decomposition rates

Decomposition rates did not differ between source watershed despite differences in initial litter chemistry between the source watersheds (Fig. S3-2, Table 3-1, S3-4). However, differences in decomposition rates were detected between watersheds of transplant and among species (Fig. 3-1; Tables 3-2, 3-3, S3-4). As we expected, the annual rate of decomposition was ~20 % lower for leaf litter transplanted to +N WS3 (Table 3-2). Decomposition rates also varied among species regardless of the watershed into which they were transplanted, and were faster for higher quality litters (black cherry and tulip poplar) and slower for lower quality litters (red maple and sweet birch; Fig. 3-1, Table 3-3). The greatest difference in average decomposition rates was between black cherry and sweet birch, with black cherry mass loss per year about twice that of sweet birch litter (Table 3-3).

Soil density fractionation

When comparing across soil density fractions, the light fractions in both watersheds had similar % C, % N, and C:N ratios (Fig. 3-2**A-C**). The % C and % N were lower in heavy POM from +N WS3, while the C:N ratio was greater compared to Ref WS7 (Fig. 3-2**A-C**). MAOM from +N WS3 also had a greater C:N ratio than MAOM from Ref WS7 (Fig. 3-2**A-C**).

We did not detect any watershed differences in the fraction of total mass attributed to the three soil fractions (Fig. 3-2**D**), but we did detect watershed differences in the fraction of total soil C and N in the light and heavy POM fractions. Specifically, the light fraction contributed a greater fraction of the total soil C and N in the +N WS3 compared to Ref WS7, consistent with

our Hypothesis 2 (Fig. 3-2**E**,**F**). Heavy POM contributed less to the total soil C and N stocks in +N WS3 (Fig. 3-2**E**,**F**). In contrast to POM pools, there was no detectable difference in the contribution of MAOM to total soil C and N stocks between watersheds (Fig. 3-2**E,F**).

When considered the role of SOM distribution among fractions in the total bulk soil chemistry. We found a strong positive relationship between the C:N ratio of bulk soil and the proportion of total soil C in the light POM fraction for both watersheds (Fig. 3-3; $P < 0.001$, $R^2 = 0.55$), but no relationship for heavy POM nor MAOM fractions. We also found a weak positive relationship between the % N of bulk soil and the proportion of total soil C in the heavy POM fraction, but it explained little variance in bulk soil % N ($P < 0.001$, $R^2 = 0.38$).

3.5 Discussion

We paired a two-year leaf litter decomposition study with a density fractionation of the SOM in the top 15 cm of mineral soil to evaluate how long-term N additions impact pathways of SOM formation. From these studies, we found support for two of our three hypotheses, as chronic N additions led to reduced leaf litter decomposition rates (~11%) over a two-year period (Fig. 3-1) and a greater contribution of light POM to total SOM (~40%; Fig. 3-2). Together, these results suggest that the commonly observed reduction in decomposition with N fertilization can lead to differences in the composition and distribution of SOM fractions. Specifically, the physical transfer pathway of SOM formation (undecomposed plant inputs remaining in the soil) was favored over the microbial decomposition pathway with subsequent stabilization of microbial biproducts (Cotrufo *et al.*, 2019). Additionally, the greater proportion of lignin remaining in the litter bags transplanted to +N WS3 (Table 3-2) was consistent with previous findings at this site of reduced ligninolytic enzyme activity with N additions (Carrara *et al.*, 2018), a direct effect of N additions often observed elsewhere (Berg, 1986; Carreiro *et al.*, 2000; DeForest *et al.*, 2004). With N additions, lignin from aboveground litter may be a primary source of POM via physical

transfer through the soil profile. Indeed, a meta-analysis by Chen *et al.* (2018) found a negative correlation between lignin-modifying enzymes and both the soil C stocks and the proportion of organic matter in the POM fraction across 40 N addition experiments.

Decomposition rates and leaf litter lignin accumulation

When N is scarce, microbes produce lignin degrading enzymes to access N-containing molecules shielded by lignin; however, under N additions microbial C limitation may occur and, thus, enzyme production and activity may shift to favor cellulose degradation (Hobbie *et al.*, 2012). Alternatively, as lignin accumulates during mid- to late-stage decomposition, non-ligninolytic enzyme activity can also slow because of the higher activation energy associated with accessing compounds shielded by lignin (Talbot & Treseder, 2012; Tan *et al.*, 2020). These soil biogeochemical responses to elevated N could help explain the reduced decomposition rates of leaf litter transplanted to +N WS3 (Fig. 3-1) and are consistent with the reduced rates of soil respiration observed at this site (Eastman *et al.*, 2021). This reasoning also follows soil biogeochemical theory that increased N availability enhances microbial biomass growth relative to substrate mineralization (Schimel & Weintraub, 2003).

Furthermore, the reduced decomposition rate in +N WS3 was observed despite similar soil temperatures, greater % soil moisture (Eastman *et al.*, 2021), and lower C:N ratios of two dominant litter types (Table 3-1). Our results (data not shown) provide little indication that surface soil properties (i.e., % C, % N, C:N) contribute to the variability in decomposition rates at our sites. This suggests that the microbial response to N additions, rather than the environment of the soils or the quality of litter, was responsible for the differences between watersheds. Indeed, N additions are known to alter the composition of soil microbial communities, decrease microbial biomass, increase the bacteria:fungi ratio, and reduce the

abundance of soil microbes that typically degrade more chemically recalcitrant organic matter (DeForest *et al.*, 2004; Ramirez *et al.*, 2012; Moore *et al.*, 2021). Apparently, any potential influence of litter quality differences between the watershed of origin on decomposition dynamics was overwhelmed by these shifts in soil microbial ecology. Although slight changes in litter quality with N fertilization did not affect decomposition rates (Fig. S3-2), the species of leaf litter had a strong influence on decomposition rates (range from *k* of 0.39-0.81). This highlights the importance of tree species composition—and any changes in species composition that may occur with chronic N additions—for decomposition dynamics, as opposed to the slight intraspecific changes in leaf litter chemistry (%N and C:N) that may result from N additions.

Fertilization effects on soil density fractions

Our observations of decreased decomposition rates of leaf litter in response to long-term N fertilization likely influenced the distribution of organic matter among surface soil density fractions. Specifically, N additions increased the light POM fraction, reduced the heavy POM fraction, and had little or no effect on the MAOM fraction. The greater fraction of organic matter in the light POM in the +N WS3 aligns with the greater C:N ratio of bulk soil in the +N WS3 (Figs. 3-2, 3-3). This greater C:N ratio persists despite higher N concentrations of some leaf litter (Table 3-1), greater inputs of inorganic N to the soil through experimental fertilization, and lower C:N ratio of final leaf litter in after two years of decomposition (Table 3-2). Eastman *et al.* (2021) proposed that reduced total belowground carbon flux by vegetation in the +N WS3 may have deprived mycorrhizae and soil microbes of labile carbon needed to decompose SOM and indirectly caused the observed increases in soil C stocks, increases in the C:N ratio of surface mineral soil, and reductions in soil CO_2 efflux. Similar patterns were also observed at other sites and at the global scale (Phillips *et al.*, 2012; Gill and Finzi, 2016; Sulman *et al.*, 2017).

The light POM in +N WS3 was likely protected from decomposition; previous studies have found that experimental N additions can directly alter soil microbial communities and reduce oxidative enzyme activity in the soil (Frey *et al.*, 2014; Morrison *et al.*, 2016; Zak *et al.*, 2019b). However, as forests recover from chronic N deposition—and as demand for N increases with increasing atmospheric CO_2—nutrient acquisition strategies for plants may shift to promote the decomposition of the light POM fraction, possibly contributing to a loss in total soil C storage (Phillips *et al.*, 2012; Terrer *et al.*, 2017; Craine *et al.*, 2018; Groffman *et al.*, 2018). Thus, despite the current emphasis on more stable MAOM fractions as globally important C stocks, the sensitivity of light POM to environmental change can significantly impact the land-atmosphere exchange of C in the short term.

Less belowground C flux and, subsequently, lower mycorrhizal colonization rates in +N WS3 (Carrara *et al.*, 2018; Eastman *et al.*, 2021) could also drive the 33% smaller proportion of SOM in the heavy POM fraction (Fig. 3-2). Root-derived and fungal byproducts can increase aggregation in soils (Six *et al.*, 2004; Wilson *et al.*, 2009), and thus the oft-observed reduction in fungal biomass and productivity under elevated N additions can cause less macro aggregation and greater heavy POM formation (Wallenstein *et al.*, 2006; Morrison *et al.*, 2016; Kemner *et al.*, 2021). Thus, our results indicate a tradeoff may exist between heavy and light POM formation where more POM ends up in the light fraction relative to the heavy with N additions, which we observed as a negative correlation between heavy and light POM in this study ($r = -0.47$; Fig. S3-3).

On the other hand, the MAOM and heavy POM fractions in +N WS3 also had greater C:N ratios than those from Ref WS7, likely contributing to the greater bulk soil C:N (Fig. 3-3). Though MAOM is often considered a relatively stable form of SOM derived from microbial byproducts (Cotrufo *et al.*, 2013; Blankinship *et al.*, 2018), recent studies suggest that MAOM

may be equally or even more preferentially formed from plant-derived compounds that bypass microbial assimilation, especially in forest ecosystems (Mikutta *et al.*, 2019; Angst *et al.*, 2021). Alternatively, a greater C:N ratio of the MAOM and heavy POM fractions could indicate a shift in the microbial community (i.e., greater bacteria:fungi ratio; Fanin *et al.*, 2013; Mooshammer *et al.*, 2014; Midgley and Phillips, 2016) or a less active fungal community with a greater biomass C:N ratio biomass than their active counterparts (Camenzind *et al.*, 2020). A closer look at the chemical composition of SOM (e.g., biomarkers) in each of the soil density fractions would help clarify the mechanisms and microbial controls of SOM stabilization in these watersheds (Angst *et al.*, 2021).

An unexpected result from the soil density fractionation study was the similar proportion of MAOM to total SOM in both watersheds (Fig. 3-2), which contributed over 50% of C and over 60% of N in the top 15 cm of mineral soil from this study (Fig. 3-2). We hypothesized that MAOM pools would be greater in the +N WS3, based on theoretical predictions of greater microbial carbon use efficiency with greater N availability (Manzoni *et al.*, 2012; Mooshammer *et al.*, 2014). Nevertheless, there are some circumstances where we might expect the contribution of MAOM to be similar in these watersheds. First, levels of MAOM may saturate because of the limited surface area and binding sites of soil minerals (Castellano *et al.*, 2015; Lavallee *et al.*, 2020), further emphasizing the importance of POM that can theoretically grow infinitely in forest soils (Cotrufo *et al.*, 2019). Additionally, because of the relatively shallow sampling depth (0-15 cm) in this study, any potential differences in MAOM fractions may become more evident if sampled to a greater depth with potentially more weatherable minerals. Alternatively, reduced root-derived C in +N WS3 (Eastman *et al.* 2021) may limit MAOM formation in that watershed, consistent with the view that MAOM is most likely formed from belowground inputs that are closer in proximity to soil minerals and microbes (Sokol and

Bradford, 2019; Sokol *et al.*, 2019; Villarino *et al.*, 2021). Finally, depleted concentrations of extractable Ca^{2+} and other soil cations in the +N WS3 (Gilliam *et al.*, 2001; Adams *et al.*, 2006) may decrease adsorption of organic matter to mineral surfaces (Chen *et al.*, 2020).

Conclusions

This long-term N addition experiment at the Fernow Experimental Forest enhances our understanding of the processes driving SOM formation and destabilization by serving as a model system to consider the impacts of N deposition on plant input decomposition dynamics and different SOM formation pathways. Our results highlight significant effects of N fertilization through reduced rates of leaf litter decomposition and differences in the fate of plant inputs in different SOM fractions. Specifically, the greater light POM fraction present in +N WS3 suggests that N additions may increase the turnover time and stock of a C pool that can potentially accumulate indefinitely (Gregorich *et al.*, 2006; Cotrufo *et al.*, 2019), and emphasizes the need for a more process-oriented conceptualization of soil C cycling (Waring *et al.*, 2020). The response of SOM stocks and associated soil biogeochemical processes to N additions are essential to predicting how global soil C stocks may respond to a changing environment. For example, if the pattern of increased light POM is widespread in regions of historically high N deposition, then the oft observed increases in forest soil C stocks with N addition may not persist under future conditions. If soil bacteria and fungi recover in ways that increases decomposition of light POM in order to access soil N, this soil C sink could become a C source. Thus, the complex response of plant-microbe interactions that link decomposition and the stabilization of SOM to N deposition and availability is likely a key component of predicting the future terrestrial C stocks and making forest management decisions for C sequestration.

3.6 Tables and Figures

Table 3-1. Chemical composition of original freshly fallen leaf litter from four dominant tree species and two watersheds of origin. Mean (SE) values are reported; bold values indicate difference between watershed means; values with the same lowercase letters (a-d) are not different according to Tukey HSD test on WS * Species interaction; values with the same uppercase letters (A-D) are not different according to Tukey HSD test on Species differences.

Species	Watershed of origin	% N *n = 6*	% C *n = 6*	C:N *n = 6*	*n*	% cellulose	% lignin	LCI	lignin:N[1]
Red maple	Ref WS7	**0.69 (0.03)**a	48.6 (0.38)bc	**70.9 (2.7)d**	*5*	19.9(0.5) A	18.3(2.4) AB	0.47(0.04) AB	**26.6(1.4)**
	+N WS3	**0.85 (0.02)**b	47.5 (0.16)ab	**56.3 (1.1)c**	*5*	18.3(1.9)	19.8(2.6)	0.52(0.06)	**23.4(1.2)**
Sweet birch	Ref WS7	1.30 (0.02)d	49.1 (0.14)c	37.7 (0.6)a	*4*	19.3(2.3) A	30.4(2.9) B	0.61(0.06) B	**23.3(0.8)**
	+N WS3	1.29 (0.05)d	48.4 (0.31)bc	37.8 (1.7)a	*5*	20.2(1.5)	25.3(2.7)	0.55(0.04)	**19.8(0.9)**
Tulip Poplar	Ref WS7	**0.92 (0.04)**cd	**46.6 (0.33)a**	**51.0 (2.1)bc**	*5*	25.8(1.1) B	18.8(1.9) A	0.42(0.03) A	**20.6(0.9)**
	+N WS3	**1.14 (0.04)**b	**48.2 (0.46)bc**	**42.6 (1.6)a**	*4*	24.4(0.5)	16.8(1.9)	0.40(0.03)	**14.9(0.7)**
Black cherry	Ref WS7	**1.26 (0.02)**d	49.0 (0.25)c	38.8 (0.5)ab	*5*	18.6(1.4) A	19.8(2.5) A	0.51(0.05) AB	**15.7(0.7)**
	+N WS3	**1.10 (0.04)**c	48.9 (0.16)bc	44.5 (1.3)a	*5*	18.7(1.3)	14.9(1.2)	0.44(0.03)	**13.6(0.4)**

[1]Lignin:N ratio calculated by combining all possible %lignin values with all possible %N values for each given species x watershed category.

Table 3-2. Chemical composition and decay rates (*k*) of final leaf litter (decomposed for two years in field) summarized by watershed into which leaves were transplanted. Mean (SE) values are reported and bold values indicate difference between watershed of transplant means (P<0.05).

Watershed of transplant	% N	C:N ratio	% cellulose	% lignin	lignocellulose index	lignin:N ratio	*k* (year^{-1})
	n = 393-399	*n = 393-399*	*n=24*	*n=24*	*n=24*	*n=24*	n_{ws7}=73, n_{ws3}=*80*
Ref WS7	**2.19(0.1)**	**23.8(0.02)**	**15.5(0.13)**	**33.0(0.27)**	68.0(0.002)	13.4(0.13)	**0.67(0.02)**
+N WS3	**2.32(0.1)**	**21.7(0.01)**	**16.9(0.12)**	**36.4(0.23)**	68.2(0.002)	13.7(0.08)	**0.53(0.02)**

Table 3-3. Chemical composition and decomposition rates (*k*) of final leaf litter (decomposed for two years in field) from four dominant tree species. Mean (SE) are reported and values with the same letter are not different among species (Tukey-Kramer HSD, P<0.05).

Species	% N	C:N ratio	% cellulose	% lignin	lignocellulose index	lignin:N ratio	*k* (year^{-1})
	n=197-200	*n=197-200*	*n=12*	*n=12*	*n=12*	*n=12*	*n*=40
Red Maple	2.05(0.24)a	25.1(0.04)c	18.4(0.2)b	34.5(0.3)a	0.65(0.003)a	14.6(0.2)bc	0.53(0.03)b
Sweet Birch	2.41(0.20)b	20.9(0.02)a	14.1(0.2)a	31.2(0.4)a	0.69(0.002)bc	11.4(0.2)a	0.39(0.02)a
Tulip Poplar	2.12(0.21)a	23.3(0.03)b	15.9(0.3)ab	31.2(0.4)a	0.66(0.004)ab	12.8(0.2)ab	0.67(0.02)c
Black Cherry	2.44(0.18)b	20.5(0.02)a	16.4(0.1)a	41.9(0.3)b	0.71(0.019)c	15.5(0.1)c	0.81(0.03)d

Table 3-4. Soil chemistry of litter decomposition plot samples and bulk soil density fractionation samples by watershed. Mean (SE) are reported and bold values indicate significant differences between watersheds.

Watershed	Soil sample depth (cm)	n	%C	%N	C:N
			Litter decomposition plot soil samples		
Ref WS7	0-5	10	7.07 (0.5)	**0.484 (0.04)**	**14.9 (0.6)**
+N WS3	0-5	10	6.82 (0.6)	**0.363 (0.03)**	**18.8 (0.8)**
			Soil density fractionation bulk soil		
Ref WS7	0-15	40	4.47 (0.04)	**0.312 (0.003)**	**15.3 (0.1)**
+N WS3	0-15	40	4.00 (0.03)	**0.224 (0.001)**	**17.9 (0.1)**

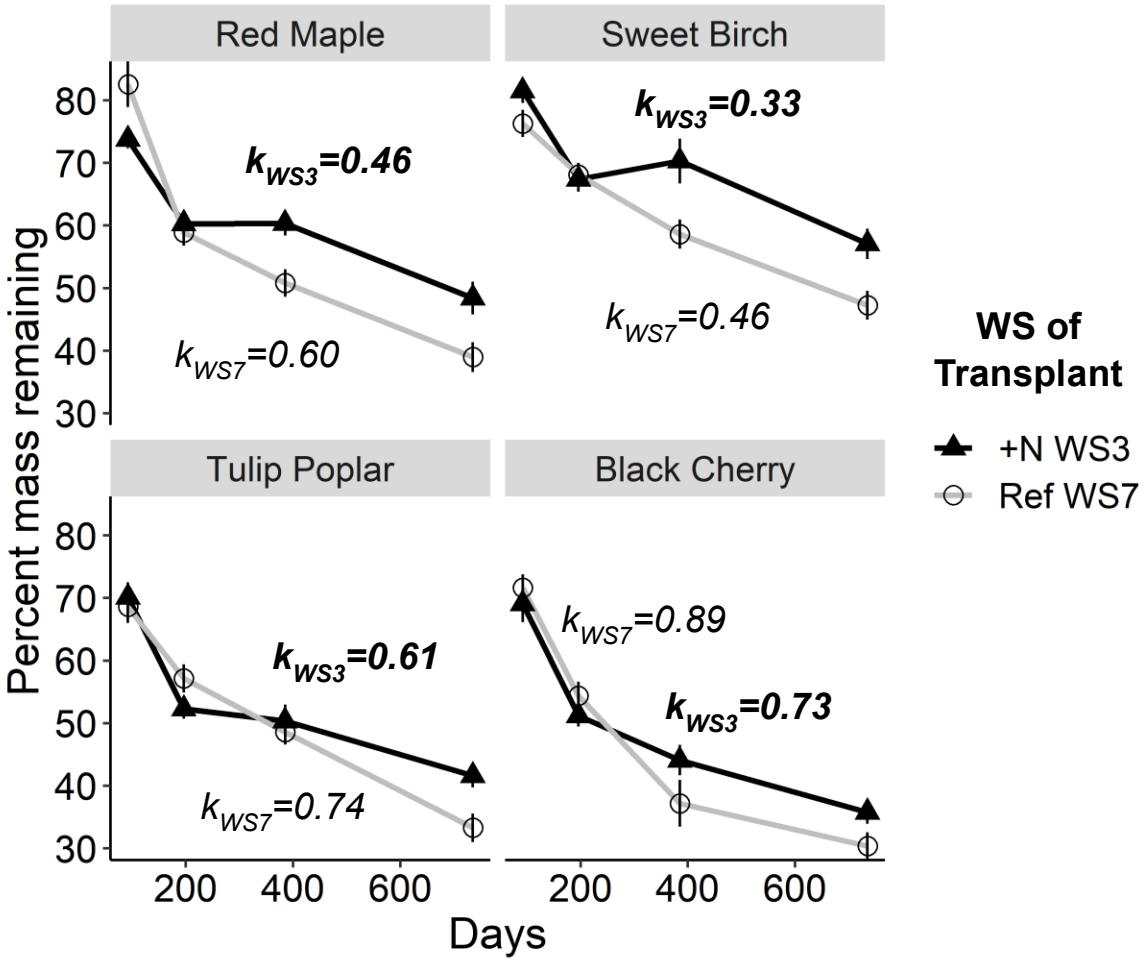

Figure 3-1. Percent of initial leaf litter mass remaining over two-year litter decomposition in the field for four dominant tree species. Mean +/- se of percent mass remaining for litter transplanted into the fertilized watershed (+N WS3; black triangles) and reference watershed (Ref WS7; open circles). Decomposition rates (*k*) displayed for each watershed and species combination. Decomposition rates (*k*) differed between watershed of transplant for all species, and there was no effect of watershed of litter origin on decomposition rates (but see Fig. S3-2).

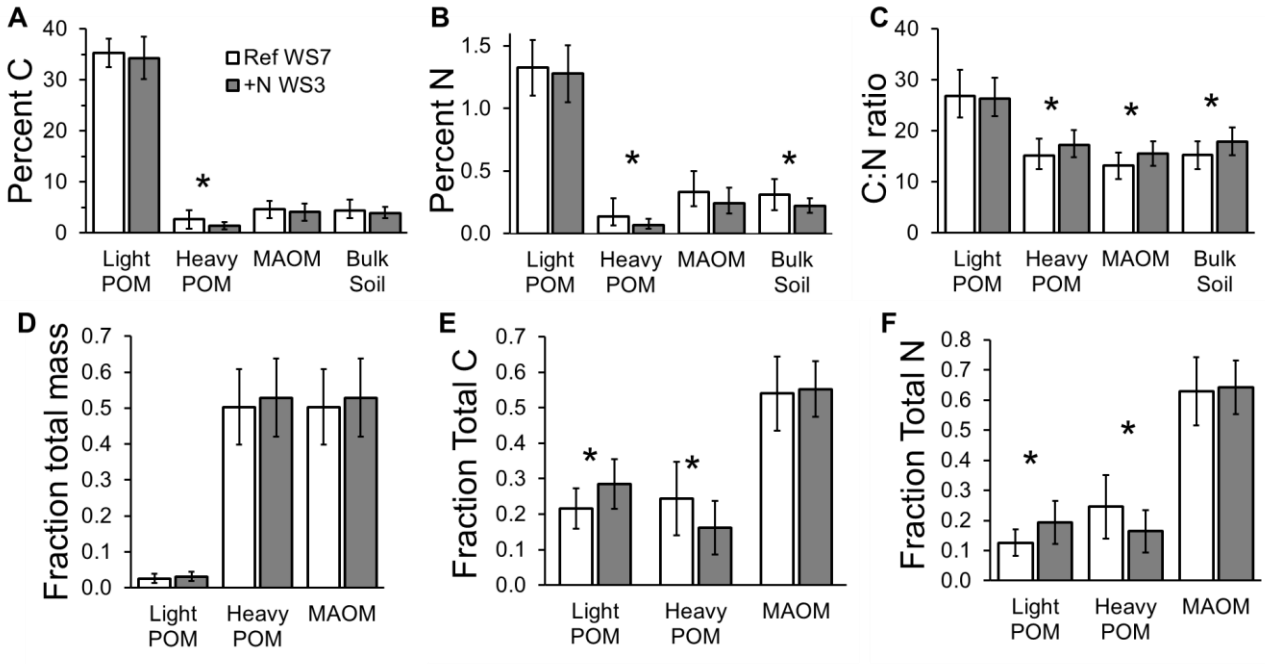

Figure 3-2. Soil density fractionation results for the reference watershed (Ref WS7, white bars) and fertilized watershed (+N WS3, gray bars). Mean (+/- se) of the percent C (**A**), percent N (**B**), and C:N ratio (**C**) of light particulate organic matter (POM), heavy POM, mineral-associated organic matter (MAOM) and bulk soil. The mean (+/- se) fraction of total bulk soil mass (**D**), carbon (**E**), and nitrogen (**F**) for the three soil fractions. Asterisks denote significant difference between watersheds (ANOVA, $P<0.05$).

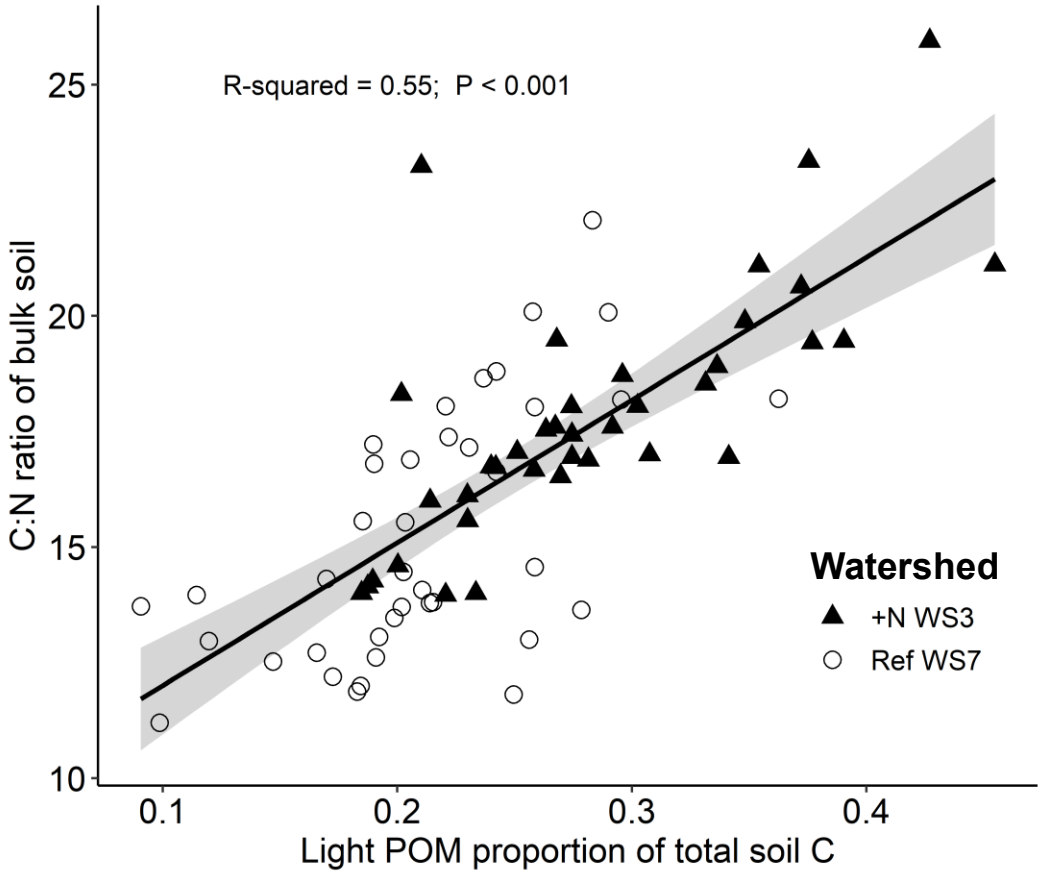

Figure 3-3. Significant and positive relationship between the proportion of total soil C in the light particulate organic matter (POM) fraction and the C:N ratio of bulk soil from the reference watershed (Ref WS7, open circles) and fertilized watershed (+N WS3, black triangles). Black line represents the linear regression with standard error (gray shading).

3.7 Literature Cited

Adair, E. C., Hobbie, S. E., Hobbie, R. K., 2010. Single-pool exponential decomposition models: potential pitfalls in their use in ecological studies. *Ecology* **91**, 1225-1236.

Adams, M.B., Angradi, T.R., 1996. Decomposition and nutrient dynamics of hardwood leaf litter in the Fernow Whole-Watershed Acidification Experiment. *Forest Ecology and Management* **83**, 61–69.

Adams, M.B., Burger, J., Zelazny, L., Baumgras, J., 2004. Description of the Fork Mountain Long-Term Soil Productivity Study: Site characterization. Newtown Square, PA, USA.

Adams, M.B., DeWalle, D.R., Hom, J.L. (Eds.), 2006. The Fernow Watershed Acidification Study, Environmental Pollution. Springer Netherlands, Dordrecht.

Adams, M.B., Edwards, P.J., Ford, W.M., Schuler, T.M., Thomas-Van Gundy, M., Wood, F., 2012. Fernow Experimental Forest: Research History and Opportunities. Washington, DC.

Angst, G., Mueller, K.E., Nierop, K.G.J., Simpson, M.J., 2021. Plant- or microbial-derived? A review on the molecular composition of stabilized soil organic matter. *Soil Biology & Biochemistry* **156**, 108189.

Argiroff, W.A., Zak, D.R., Upchurch, R.A., Salley, S.O., Grandy, A.S., 2019. Anthropogenic N deposition alters soil organic matter biochemistry and microbial communities on decaying fine roots. *Global Change Biology* **25**, 4369–4382.

Averill, C., Dietze, M.C., Bhatnagar, J.M., 2018. Continental-scale nitrogen pollution is shifting forest mycorrhizal associations and soil carbon stocks. *Global Change Biology* **24**, 4544–4553.

Bailey, V.L., Pries, C.H., Lajtha, K., 2019. What do we know about soil carbon destabilization? *Environmental Research Letters* **14**, 083004.

Berg, B., 1986. Nutrient release from litter and humus in coniferous forest soils-a mini review. *Scandinavian Journal of Forest Research* **1**, 359–369.

Blair, J. M., Crossley Jr, D. A., 1988. Litter decomposition, nitrogen dynamics and litter microarthropods in a southern Appalachian hardwood forest 8 years following clearcutting. *Journal of Applied Ecology* **25**, 683-698.

Blankinship, J.C., Berhe, A.A., Crow, S.E., Druhan, J.L., Heckman, K.A., Keiluweit, M., Lawrence, C.R., Marín-Spiotta, E., Plante, A.F., Rasmussen, C., *et al.*, 2018. Improving understanding of soil organic matter dynamics by triangulating theories, measurements, and models. *Biogeochemistry* **140**, 1–13.

Bradford, M.A., Wieder, W.R., Bonan, G.B., Fierer, N., Raymond, P.A., Crowther, T.W., 2016. Managing uncertainty in soil carbon feedbacks to climate change. *Nature Climate Change* **6**, 751–758.

Burnham, M.B., Cumming, J.R., Adams, M.B., Peterjohn, W.T., 2017. Soluble soil aluminum alters the relative uptake of mineral nitrogen forms by six mature temperate broadleaf tree species: possible implications for watershed nitrate retention. *Oecologia* **185**, 327–337.

Camenzind, T., Philipp Grenz, K., Lehmann, J., Rillig, M.C., 2021. Soil fungal mycelia have unexpectedly flexible stoichiometric C:N and C:P ratios. *Ecology Letters* **24**, 208–218.

Carrara, J.E., Walter, C.A., Hawkins, J.S., Peterjohn, W.T., Averill, C., Brzostek, E.R., 2018. Interactions among plants, bacteria, and fungi reduce extracellular enzyme activities under long-term N fertilization. Global *Change Biology* **24**, 2721–2734.

Carreiro, M.M., Sinsabaugh, R.L., Repert, D.A., Parkhurst, D.F., 2000. Microbial Enzyme Shifts Explain Litter Decay Responses to simulated nitrogen deposition. *Ecology* **81**, 2359–2365.

Castellano, M.J., Mueller, K., Olk, D.C., Sawyer, J.E., Six, J., 2015. Integrating plant litter quality, soil organic matter stabilization, and the carbon saturation concept. *Global Change Biology* **21**, 3200–3209.

Chen, J., Luo, Y., Van Groenigen, K.J., Hungate, B.A., Cao, J., Zhou, X., Wang, R. wu, 2018. A keystone microbial enzyme for nitrogen control of soil carbon storage. *Science Advances* **4**, 2–8.

Chen, J., Xiao, W., Zheng, C., Zhu, B., 2020. Nitrogen addition has contrasting effects on particulate and mineral-associated soil organic carbon in a subtropical forest. *Soil Biology & Biochemistry* **142**, 107708.

Ciais, P., Sabine, C., Bala, G., Bopp, L., Brovkin, V., Canadell, J., Chhabra, A., DeFries, R., Galloway, J., Heimann, M. *et al.*, 2013. The physical science basis. Contribution of working group to the fifth assessment report of the intergovernmental panel on climate change. *IPCC Climate Change Report*, 465-570.

Cordova, S.C., Olk, D.C., Dietzel, R.N., Mueller, K.E., Archontouilis, S.V., Castellano, M. J., 2018. Plant litter quality affects the accumulation rate, composition, and stability of mineral-associated soil organic matter. *Soil Biology & Biochemistry* **125**, 115–124.

Cotrufo, M.F., Ranalli, M., Haddix, M., Six, J., Lugato, E. 2019. Soil carbon storage informed by particulate and mineral-associated organic matter. *Nature Geoscience*, **12**, 989-994.

Cotrufo, M.F., Soong, J.L., Horton, A.J., Campbell, E.E., Haddix, M.L., Wall, D.H., Parton, W.J., 2015. Formation of soil organic matter via biochemical and physical pathways of litter mass loss. *Nature Geoscience* **8**, 776–779.

Cotrufo, M.F., Wallenstein, M.D., Boot, C.M., Denef, K., Paul, E., 2013. The Microbial Efficiency-Matrix Stabilization (MEMS) framework integrates plant litter decomposition with soil organic matter stabilization: Do labile plant inputs form stable soil organic matter? *Global Change Biology* **19,** 988–995.

Craine, J.M., Elmore, A.J., Wang, L., Aranibar, J., Bauters, M., Boeckx, P., Crowley, B.E., Dawes, M.A., Delzon, S., Fajardo, A., *et al.*, 2018. Isotopic evidence for oligotrophication of terrestrial ecosystems. *Nature Ecology and Evolution* **2**, 1735–1744.

DeForest, J.L., Zak, D.R., Pregitzer, K.S., Burton, A.J., 2004. Atmospheric Nitrate Deposition, Microbial Community Composition, and Enzyme Activity in Northern Hardwood Forests. *Soil Science Society of America Journal* **68**, 132-138.

Eastman, B.A., Adams, M.B., Brzostek, E.R., Burnham, M.B., Carrara, J.E., Kelly, C., McNeil, B.E., Walter, C.A., Peterjohn, W.T., 2021. Altered plant carbon partitioning enhanced forest ecosystem carbon storage after 25 years of nitrogen additions. *New Phytologist* **230**, 1435–1448.

Fanin, N., Fromin, N., Buatois, B., Hättenschwiler, S., 2013. An experimental test of the hypothesis of non-homeostatic consumer stoichiometry in a plant litter-microbe system. *Ecology Letters* **16**, 764–772.

Fowler, Z.K., Adams, M.B., Peterjohn, W.T., 2015. Will more nitrogen enhance carbon storage in young forest stands in central Appalachia? *Forest Ecology and Management* **337**, 144–152.

Frey, S.D., Ollinger, S., Nadelhoffer, K., Bowden, R., Brzostek, E., Burton, A., Caldwell, B.A., Crow, S., Goodale, C.L., Grandy, A.S., *et al.*, 2014. Chronic nitrogen additions suppress decomposition and sequester soil carbon in temperate forests. *Biogeochemistry* **121**, 305–316.

Friedlingstein, P., Meinshausen, M., Arora, V.K., Jones, C.D., Anav, A., Liddicoat, S.K., Knutti, R., 2014. Uncertainties in CMIP5 climate projections due to carbon cycle feedbacks. *Journal of Climate* **27**, 511–526.

Gill, A.L., Finzi, A.C., 2016. Belowground carbon flux links biogeochemical cycles and resource-use efficiency at the global scale. *Ecology Letters* **19,** 1419–1428.

Gilliam, F.S., Turrill, N.L., Aulick, S.D., Evans, D.K., Adams, M.B., 1994. Herbaceous layer and soil response to experimental acidification in a central Appalachian hardwood forest. *Journal of Environmental Quality* **23**, 835-844.

Gilliam, F.S., Yurish, B.M., Adams, M.B., 2001. Temporal and spatial variation of nitrogen transformations in nitrogen-saturated soils of a central Appalachian hardwood forest. *Revue Canadienne De Recherche Forestiere* **31**, 1768–1785.

Gregorich, E.G., Beare, M.H., McKim, U.F., Skjemstad, J.O., 2006. Chemical and biological characteristics of physically uncomplexed organic matter. *Soil Science Society of America Journal* **70**, 975–985.

Griscom, B.W., Adams, J., Ellis, P.W., Houghton, R.A., Lomax, G., Miteva, D.A., Schlesinger, W.H., Shoch, D., Siikamäki, J. V., Smith, P., *et al.*, 2017. Natural climate solutions. *Proceedings of the National Academy of Sciences* **114**, 11645–11650.

Groffman, P.M., Driscoll, C.T., Durán, J., Campbell, J.L., Christenson, L.M., Fahey, T.J., Fisk, M.C., Fuss, C., Likens, G.E., Lovett, *et al.*, 2018. Nitrogen oligotrophication in northern hardwood forests. *Biogeochemistry* **141**, 523-539.

Harmon, M.E., Silver, W.L., Fasth, B., Chen, H., Burke, I.C., Parton, W.J., Hart, S.C., Currie, W.S., Laundre, J., Wright, J., *et al.*, 2009. Long-term patterns of mass loss during the decomposition of leaf and fine root litter: An intersite comparison. *Global Change Biology* **15**, 1320–1338.

Helvey, J.D., Kunkle, S.H., 1986. Input-out budgets of selected nutrients on an experimental watershed near Parsons, West Virginia. Research Paper NE-584. US Department of Agriculture, Forest Service, Northeastern Forest Experiment Station, Broomall, PA, p. 7.

Hobbie, S.E., Eddy, W.C., Buyarski, C.R., Carol Adair, E., Ogdahl, M.L., Weisenhorn, P., 2012. Response of decomposing litter and its microbial community to multiple forms of nitrogen enrichment. *Ecological Monographs* **82**, 389–405.

Hocking, R. R. (1985), The analysis of linear models, Brooks/Cole Publishing Company Monteray, California.

Holtzapple, M.T. 2003. Cellulose. In: Caballero, B., Trugo, L.C., and Finglas, P.M (Eds.). Encyclopedia of food sciences and nutrition. Academic Press, Cambridge, MA, pp. 998-1007.

Hurlbert, S.H., 1984. Pseudoreplication and the Design of Ecological. *Ecological Monographs* **54,** 187–211.

Janssens, I.A. a., Dieleman, W., Luyssaert, S., Subke, J., Reichstein, M., Ceulemans, R., Ciais, P., Dolman, A.J., Grace, J., Matteucci, G., *et al*., 2010. Reduction of forest soil respiration in response to nitrogen deposition. *Nature Geoscience* **3**, 315–322.

Janzen, H.H., Entz, T., Ellert, B.H., 2002. Correcting mathematically for soil adhering to root samples. *Soil Biology & Biochemistry* **34**, 1965–1968.

Jenny, H., Gessel, S. P., Bingham, F. T., 1949. Comparative study of decomposition rates of organic matter in temperate and tropical regions. *Soil Science*, **68**, 419-432.

Kemner, J.E., Adams, M.B., Mcdonald, L.M., Peterjohn, W.T., Kelly, C.N., 2021. Fertilization and Tree Species Influence on Stable Aggregates in Forest Soil. *Forests* **12**, 39.

Kloke, J. and McKean, J.W., 2014. Nonparametric statistical methods using R. CRC Press.

Kloke, J.D., McKean, J., 2012. Rfit : Rank-based estimation for linear models. *The R Journal*.

Kochenderfer, J.N., 2006. Fernow and the Appalachian Hardwood Region, in: Adams, M.B., DeWalle, D.R., Hom, J.L. (Eds.), The Fernow Watershed Acidification Study. Springer, pp. 17–39.

Kochenderfer, J.N., Wendel, G.W., 1983. Plant succession and hydrologic recovery on a deforested and herbicided watershed. *Forest Science* **29**, 545-558.

Kölbl, A., Kögel-Knabner, I., 2004. Content and composition of free and occluded particulate organic matter in a differently textured arable Cambisol as revealed by solid-state 13C NMR spectroscopy. *Journal of Plant Nutrition and Soil Science* **167**, 45–53.

Lavallee, J.M., Soong, J.L., Cotrufo, M.F., 2020. Conceptualizing soil organic matter into particulate and mineral-associated forms to address global change in the 21st century. *Global Change Biology* **26**, 261-273.

Manzoni, S., Taylor, P., Richter, A., Porporato, A., Ågren, G.I., 2012. Environmental stoichiometric controls on microbial carbon-use efficiency in soils. *New Phytologist* **196**, 79-91.

Melillo, J.M., Aber, J.D., Linkins, A.E., Ricca, A., Fry, B., Nadelhoffer, K.J., 1989. Carbon and nitrogen dynamics along the decay continuum: Plant litter to soil organic matter, in: Clarholm, M., Bergstrom, L. (Eds.), *Ecology of Arable Land*. Kluwer Academic Publishers, pp. 53–62.

Melillo, J.M., Frey, S.D., DeAngelis, K.M., Werner, W.J., Bernard, M.J., Bowles, F.P., Pold, G., Knorr, M.A., Grandy, A.S., 2017. Long-term pattern and magnitude of soil carbon feedback to the climate system in a warming world. *Science* **358**, 101-105.

Midgley, M.G., Brzostek, E., Phillips, R.P., 2015. Decay rates of leaf litters from arbuscular mycorrhizal trees are more sensitive to soil effects than litters from ectomycorrhizal trees. *Journal of Ecology* **103**, 1454–1463.

Midgley, M.G., Phillips, R.P., 2016. Resource stoichiometry and the biogeochemical consequences of nitrogen deposition in a mixed deciduous forest. *Ecology* **97,** 3369-3377.

Mikutta, R., Turner, S., Schippers, A., Gentsch, N., Meyer-Stüve, S., Condron, L.M., Peltzer, D.A., Richardson, S.J., Eger, A., Hempel, G., *et al.*, 2019. Microbial and abiotic controls on mineral-associated organic matter in soil profiles along an ecosystem gradient. *Scientific Reports* **9**, 1–9.

Moore, J.A.M., Anthony, M.A., Pec, G.J., Trocha, L.K., Trzebny, A., Geyer, K.M., van Diepen, L.T.A., Frey, S.D., 2021. Fungal community structure and function shifts with atmospheric nitrogen deposition. *Global Change Biology* **27**, 1349-1364.

Mooshammer, M., Wanek, W., Zechmeister-Boltenstern, S., Richter, A., 2014. Stoichiometric imbalances between terrestrial decomposer communities and their resources: Mechanisms and implications of microbial adaptations to their resources. *Frontiers in Microbiology* **5**, 1–10.

Morrison, E.W., Frey, S.D., Sadowsky, J.J., van Diepen, L.T.A., Thomas, W.K., Pringle, A., 2016. Chronic nitrogen additions fundamentally restructure the soil fungal community in a temperate forest. *Fungal Ecology* **23**, 48–57.

Nave, L.E., Vance, E.D., Swanston, C.W., Curtis, P.S., 2009. Impacts of elevated N inputs on north temperate forest soil C storage, C/N, and net N-mineralization. *Geoderma* **153**, 231–240.

Nottingham, A. T., Meir, P., Velasquez, E., Turner, B. L., 2020. Soil carbon loss by experimental warming in a tropical forest. *Nature*, **584**, 234-237.

Ofiti, N. O., Zosso, C. U., Soong, J. L., Solly, E. F., Torn, M. S., Wiesenberg, G. L., Schmidt, M. W., 2021. Warming promotes loss of subsoil carbon through accelerated degradation of plant-derived organic matter. *Soil Biology & Biochemistry*, **156**, 108185.

Olsen, J.S., 1963. Energy storage and the balance of producers and decomposers in ecological systems. *Ecology* **44**, 322-331.

Pan, Y., Birdsey, R.A., Fang, J., Houghton, R., Kauppi, P.E., Kurz, W.A., Phillips, O.L., Shvidenko, A., Lewis, S.L., Canadell, J.G., *et al*., 2011. A large and persistent carbon sink in the world's forests. *Science* **333**, 988–93.

Phillips, R.P., Meier, I.C., Bernhardt, E.S., Grandy, A.S., Wickings, K., Finzi, A.C., 2012. Roots and fungi accelerate carbon and nitrogen cycling in forests exposed to elevated CO_2. *Ecology Letters* **15,** 1042-1049.

Pregitzer, K.S., Burton, A.J., Zak, D.R., Talhelm, A.F., 2008. Simulated chronic nitrogen deposition increases carbon storage in Northern Temperate forests. *Global Change Biology* **14,** 142–153.

Ramirez, K.S., Craine, J.M., Fierer, N., 2012. Consistent effects of nitrogen amendments on soil microbial communities and processes across biomes. *Global Change Biology* **18,** 1918–1927.

Schimel, J.P., Weintraub, M.N., 2003. The implications of exoenzyme activity on microbial carbon and nitrogen limitation in soil: A theoretical model. *Soil Biology & Biochemistry* **35**, 549–563.

Six, J., Bossuyt, H., Degryze, S., Denef, K., 2004. A history of research on the link between (micro)aggregates, soil biota, and soil organic matter dynamics. *Soil and Tillage Research* **79**, 7–31.

Sokol, N.W., Bradford, M.A., 2019. Microbial formation of stable soil carbon is more efficient from belowground than aboveground input. *Nature Geoscience* **12**, 46–53.

Sokol, N.W., Sanderman, J., Bradford, M.A., 2019. Pathways of mineral-associated soil organic matter formation: Integrating the role of plant carbon source, chemistry, and point of entry. *Global Change Biology* **25**, 12–24.

Sulman, B.N., Brzostek, E.R., Medici, C., Shevliakova, E., Menge, D.N.L., Phillips, R.P., 2017. Feedbacks between plant N demand and rhizosphere priming depend on type of mycorrhizal association. *Ecology Letters* **20**, 1043–1053.

Talbot, J.M., Treseder, K.K., 2012. Interactions among lignin, cellulose, and nitrogen drive litter chemistry-decay relationships. *Ecology* **93,** 345–354.

Talbot, J.M., Yelle, D.J., Nowick, J., Treseder, K.K., 2012. Litter decay rates are determined by lignin chemistry. *Biogeochemistry* **108**, 279–295.

Tan, X., Machmuller, M.B., Cotrufo, M.F., Shen, W., 2020. Shifts in fungal biomass and activities of hydrolase and oxidative enzymes explain different responses of litter decomposition to nitrogen addition. *Biology and Fertility of Soils* **56**, 423–438.

Terrer, C., Vicca, S., Stocker, B.D., Hungate, B.A., Phillips, R.P., Reich, P.B., Finzi, A.C., Prentice, I.C., 2017. Ecosystem responses to elevated CO 2 governed by plant-soil interactions and the cost of nitrogen acquisition. *New Phytologist* **217**, 347–355.

Treseder, K.K., 2004. A meta-analysis of mycorrhizal responses to nitrogen, phosphorus, and atmospheric CO2 in field studies. *New Phytologist* **164**, 347–355.

Van Soest, P., 1963. Use of detergents in the analysis of fibrous feeds. II. A rapid method for the determination of fiber and lignin. *Journal of the Association of Official Agricultural Chemists* **46**, 829-835.

Villarino, S.H., Pinto, P., Jackson, R.B., Piñeiro, G., 2021. Plant rhizodeposition : A key factor for soil organic matter formation in stable fractions. *Science Advances* **7**, eabd3176.

Von Lützow, M., Kögel-Knabner, I., Ludwig, B., Matzner, E., Flessa, H., Ekschmitt, K., Guggenberger, G., Marschner, B., Kalbitz, K., 2008. Stabilization mechanisms of organic matter in four temperate soils: Development and application of a conceptual model. *Journal of Plant Nutrition and Soil Science* **171**, 111–124.

Wallenstein, M.D., Peterjohn, W.T., Schlesinger, W.H., 2006. N Fertilization Effects on Denitrification and N Cycling. *Ecological Applications* **16,** 2168–2176.

Wang, J.-J., Bowden, R.D., Lajtha, K., Washko, S.E., Wurzbacher, S.J., Simpson, M.J., 2019. Long-term nitrogen addition suppresses microbial degradation, enhances soil carbon storage, and alters the molecular composition of soil organic matter. *Biogeochemistry* **142**, 299-313.

Waring, B.G., Sulman, B.N., Reed, S., Smith, A.P., Averill, C., Creamer, C.A., Cusack, D.F., Hall, S.J., Jastrow, J.D., Jilling, A., *et al.*, 2020. From pools to flow: The PROMISE framework for new insights on soil carbon cycling in a changing world. *Global Change Biology* **26**, 6631–6643.

Wilson, G.W.T., Rice, C.W., Rillig, M.C., Springer, A., Hartnett, D.C., 2009. Soil aggregation and carbon sequestration are tightly correlated with the abundance of arbuscular mycorrhizal fungi: results from long-term field experiments. *Ecology Letters* **12**, 452–461.

Winsome, T., Silva, L. C. R., Scow, K. M., Doane, T. A., Powers, R. F., and Horwath, W. R. 2017. Plant-microbe interactions regulate carbon and nitrogen accumulation in forest soils. *Forest Ecology and Management* **384**, 415–423.

Young, D., Zégre, N., Edwards, P., Fernandez, R., 2019. Assessing streamflow sensitivity of forested headwater catchments to disturbance and climate change in the central Appalachian Mountains region, USA. *Science of the Total Environment* **694**, 133382.

Zak, D.R., Argiroff, W.A., Freedman, Z.B., Upchurch, R.A., Entwistle, E.M., Romanowicz, K.J., 2019b. Anthropogenic N deposition, fungal gene expression, and an increasing soil carbon sink in the Northern Hemisphere. *Ecology* **100**, 1–8.

Chapter 4. Modeling forest carbon cycling with and without microbes: A model-data comparison using data from a long-term manipulation experiment

4.1 Abstract

A large uncertainty in land carbon (C) sink projections is the extent to which future conditions will lead to enhanced decomposition and loss of soil C stocks. Evidence suggests that the nitrogen (N) status of an ecosystem can directly and indirectly influence soil organic matter (SOM) decomposition, by affecting enzyme activity and plant-soil interactions. However, model representation of linked C-N cycles and SOM decay are not well-validated against experimental data. Here, we use extensive data from the Fernow Experimental Forest long-term, whole-watershed N fertilization study to compare the response to N perturbations of two soil models that represent decomposition dynamics differently (first-order decay versus microbially-explicit reverse Michaelis-Menten kinetics). These two soil models were coupled to a common vegetation model with identical input data. Key observations from the study site included reductions in soil respiration, accumulation of particulate organic matter (POM), and an increase in soil C:N ratios with N additions. Both models failed to capture these observed responses to N additions, except for simulated enhanced POM by the microbially-explicit model. Furthermore, the vegetation model did not capture the shift in allocation away from belowground C flux and in favor of wood production with N additions. We modified the models to force a shift in plant C allocation with N additions analogous to observations, and to further reduce decay rates of POM in the microbially-explicit model. With these modifications, the microbially-explicit model captured greater total soil C stocks and C:N ratios, but both modified models still failed to capture the observed reductions in soil respiration with N additions. Thus, while the soil models were restricted by the limitations of the vegetation model, neither soil model includes the mechanisms for the direct effect of reduced enzyme activity that is widely observed with N additions. This can lead to poor predictions of how the land C sink might respond to shifts in N cycling under future conditions of altered N inputs and increased soil temperatures.

4.2 Introduction

Northern temperate forests are a globally important carbon (C) sink (Galloway *et al.*, 2008; Pan *et al.*, 2011a), but are experiencing rapid changes to their environment that could impact their ability to sequester and store C. Predicting forest responses to environmental change over decadal time scales (or longer) is a challenge that will likely require the integration of long-term experimental manipulations and models that can detect and simulate changes in ecosystem patterns and processes. For example, many temperate forests have received decades of N deposition from the combustion of fossil fuels, which likely released them from N limitation and contributed to significant C sequestration (Vitousek and Howarth, 1991; Litton *et al*., 2007; Thomas *et al.*, 2010; Vicca *et al*., 2012; Du and de Vries, 2018). Additionally, many N enrichment studies report reductions in soil respiration rates and an accumulation of soil C, which are likely driven by plant reductions in belowground C allocation and lower soil microbial and enzyme activity (Janssens *et al.*, 2010; Schulte-Uebbing & de Vries, 2017b; Du & de Vries, 2018). While most existing models capture the enhancement in plant productivity with N additions, they fail to capture the reduction in soil respiration fluxes because these fluxes are positively related to plant productivity and litter inputs (Koven *et al.*, 2015; Wieder *et al.*, 2019b; Jian *et al.*, 2021). This shortcoming is especially concerning because, as N deposition declines and forest soil recover, the C the accumulated in these soils may become vulnerable to decomposition and loss. Furthermore, the response of soil heterotrophic respiration to global change will likely determine the overall magnitude of the land C sink (Bond-Lamberty *et al.*, 2018). Thus, to create meaningful emission reduction targets and mitigate climate change, it is of high priority to predict the drivers and fate of the soil C stock.

Recent theoretical advancements in the understanding of soil organic matter (SOM) formation and destabilization offer a framework for advancing the representation of soil C and N cycling in models (Cotrufo *et al.*, 2015; Lehmann & Kleber, 2015; Sokol *et al.*, 2019). These emerging views of soil biogeochemical processes highlight how plant productivity and belowground C allocation interact with soil microbial community composition and activity to regulate soil C persistence and heterotrophic respiration fluxes. Nonetheless, the Earth System Models (ESMs) we use to predict future C cycles and inform global change policy do not yet explicitly represent microbial physiology and are limited in their abilities to predict SOM dynamics under environmental change (Wieder *et al.*, 2015b; Varney *et al.*, 2022). These models typically represent soil C turnover as a linear process with first-order decay dynamics, and soil C formation is directly related to soil C inputs.

Recently, significant effort has gone towards incorporating explicit microbial communities and microbial physiology into soil models, which may improve the predictive ability of these models—especially under future conditions of environmental change—by incorporating additional mechanisms in the soil C cycle (Wieder *et al.*, 2013; Sulman *et al.*, 2018). For example, by explicitly representing microbial physiology, these models can simulate changes in the temperature sensitivity of decomposition and soil heterotrophic respiration as the microbial community shifts or microbial growth efficiency acclimates to soil warming (Wieder *et al.*, 2013). Furthermore, microbial models are structured to be able to capture the process of priming that occurs when fresh soil inputs lead to increased microbial demand for nutrients and, thus, accelerated microbial growth and decomposition of SOM. Reductions in root exudates and priming with N additions is an important mechanism behind the widely observed reduction in soil respiration with experimental N additions, and microbial models may have an advantage

over first-order decay models at predicting this response and the downstream impacts this has on soil C storage and cycling. However, few studies have compared the responses of first-order versus microbial models to N perturbations. Therefore, there is a need to combine modelling and empirical efforts to assess model performance in response to changes in N additions, and to identify any potential benefits of including additional soil C cycling mechanisms through explicit representation of microbes (Wieder *et al.*, 2019b).

The soil biogeochemical model testbed, developed by Wieder *et al.* (2018, 2019b), provides a framework to compare the performance of two structurally different soil C and N biogeochemical models by coupling them to a common vegetation model. The soil model testbed was originally developed to facilitate the comparison among three structurally distinct soil C models in their abilities to predict global soil C stocks and their responses to environmental change. Two of these three soil models in the testbed have been recently modified to include the N cycle and its interactions with the C cycle. The two soil models in the C and N version of the testbed include one first-order soil C and N model, the Carnegie-Ames-Stanford Approach (CASA; Potter *et al.*, 1993; Randerson *et al.*, 1996; Wang *et al.*, 2010) and one microbially explicit soil C and N model, MIcrobial-MIneral Carbon Stabilization (MIMICS) (Wieder *et al.*, 2014, 2015c; Kyker-Snowman *et al.*, 2020). The key difference between the CASA and MIMICS soil models is how these models represent SOM decomposition. The CASA model represents decomposition with linear first-order decay dynamics, and each litter and soil pool has a set turnover time. The MIMICS model explicitly represents two soil microbial communities (copiotrophic and oligotrophic), and decomposition is represented with reverse Michaelis-Menten kinetics. While both models were developed and parameterized to run

at the global scale, the testbed allows for the models to be run at single-point scale, for comparisons against site-level, empirical data.

In this study, we compare CASA and MIMICS model performance with a 30-year N perturbation experiment, and we validate models against the results from a long-term, whole-watershed N addition field experiment at the Fernow Experimental Forest (Fernow Forest) in West Virginia, USA. The duration and broad spatial scale of this field experiment provides a unique opportunity to validate the models and test model assumptions about soil biogeochemical responses to N enrichment. Observations from this long-term field manipulation found that N additions stimulated aboveground wood production and reduced total belowground C flux (Eastman *et al.*, 2021). Furthermore, this reduced belowground C allocation likely caused a reduction in soil microbial activity as observed through a decrease in soil respiration and leaf litter decomposition, lower rates of ligninolytic enzyme activity and mycorrhizal colonization, and an accumulation of particulate organic matter in surface mineral soils (POM; Carrara *et al.*, 2018; Eastman *et al.*, 2021, 2022). These responses are observed at other N addition studies, as well, and are likely difficult to capture with a first-order, linear decay soil model, because they are driven by shifts in microbial activity and plant-soil interactions—mechanisms not represented in microbially-implicit models like the CASA model.

The main objectives of this study were to assess the default model steady-state stocks as they compare to observations from the Fernow Forest, and to run three 30-year N addition modelling experiments. These three experiments were (1) default model responses to N additions; (2) modify models to shift plant C allocation with N additions, in accordance with field observations; (3) modify the MIMICS model to directly inhibit the decomposition of POM with N additions. Experiments (2) and (3) were a test of two hypotheses about the mechanisms

behind observed soil responses to chronic N enrichment at the Fernow Forest. By comparing model output to long-term experimental data, we compared the predictive abilities of a first-order (CASA) and a more mechanistic model representation of soil microbial physiology (MIMICS) of the transient ecosystem responses to N additions.

4.3 Methods

Site description

The Fernow Experimental Forest (Fernow Forest) is a broadleaf deciduous forest located in the Central Appalachian Mountains near Parsons, WV (39.03° N, 79.67° W). Elevations at the Fernow Forest range from 530-1,115 m with steep slopes between 20-50% grade. The predominant soils at the Fernow Forest are shallow (<1 m) Calvin channery silt loam (*Typic Dystrochrept*) underlain with fractured sandstone and shale parent material. Mean monthly temperatures range from about -18 °C in January to about 25 °C in July, and annual precipitation is about 146 cm with even distribution across seasons (Kochenderfer, 2006; See Table 1).

The Fernow Forest is the site of a long-term, whole-watershed, N-addition experiment. N additions to the experimental watershed catchment area (34 ha) were applied annually by aerial applications of 35.4 kg N ha^{-1} yr^{-1} as ammonium sulfate from 1989-2019 (30 years). The experimental N addition rate was about double the ambient N deposition measured in throughfall concentrations at the start of the experiment, and about 4x the rate of N deposition by the end of the experiment (https://nadp.slh.wisc.edu/; www.epa.gov/CASTNET). Aerial application of $(NH_4)_2SO_4$ was distributed in three applications per year to mimic the seasonal, ambient N deposition rates. An adjacent watershed of similar topography and forest age (24 ha) is used as a reference, receiving only ambient N deposition.

The vegetation at the Fernow Forest is classified as mixed mesophytic forest. The fertilized watershed (Watershed 3) was harvested using selection harvesting and patch-clearcutting from 1958-1968 before being clear-cut in 1970 and allowed to regrow naturally for 19 years before fertilization treatment began. The adjacent reference watershed (Watershed 7) was clear-cut in two sections, the upper half in 1963 and lower half in 1966. Following cutting, both sections of the reference watershed were kept barren with herbicide treatment until 1969 when it was allowed to regrow. No legacy effects of the herbicide treatment were observed ten years into regrowth (Kochenderfer & Wendel, 1983). The Fernow Forest has relatively diverse vegetation, and tree species compositions are similar in both watersheds, dominated by *Prunus serotina, Acer rubrum, Liriodendron tulipifera,* and *Betula lenta;* although, the fertilized watershed has a greater % basal area of *Prunus serotina* and less *Liriodendron tulipifera* than the reference watershed.

The observational data from the Fernow Forest used in this study were collected over various time scales and locations in the fertilized and reference watersheds, with most of these data described and summarized by Eastman *et al.* (2021). In summary, tree aboveground NPP measurements were estimated from 25 permanent growth plots per watershed, in which the aboveground biomass of all trees was estimated 6 times during the 30-year experiment using measurements of the diameter at breast height and allometric equations. Also at these plots, autumnal fine litterfall was measured annually from the start of the experiment (1989) through 2015, and in 20 additional plots per watershed from 2015-2017. Fine root biomass was measured several times throughout the experiment in various sets of plots using soil cores (ranging in depth from 0-10 cm to 0-45 cm), and fine root production (0-10 cm) was estimated in 2016-2017 using in-growth cores. Soil organic horizon C and N stocks were measured in 2012 and 2013, and

mineral soil C and N stocks were measured from soil pits (0-45 cm depth) in 2016. Soil respiration was measured at 80 locations per watershed approximately weekly during the growing season and monthly during the dormant season for two years (2016-2017) using an infrared gas analyzer. Stream inorganic N export has been monitored at the Fernow Forest from continuous streamflow measurements and weekly or biweekly streamwater chemistry samples since 1983 by the US Forest Service. Additionally, we used measurements of the partitioning of SOM into different soil density fractions in the fertilized and reference Fernow Forest watersheds to compare observed versus modelled SOM distributions and stoichiometry (Eastman *et al.*, 2022). These mineral soil samples were collected at 20 plots per watershed, in 4 subplots per plot, to a depth of 15 cm.

Soil biogeochemical model testbed description

The soil biogeochemical model testbed provided a mechanistic framework for comparing how a first-order decay model compared to a microbially-explicit model in their responses to elevated N inputs. After calibrating models to our study site, we ran three 30-year N addition experiments that simulated the long-term N addition study at The Fernow Forest. The first experiment was performed using the default models calibrated to the study site. In the second experiment, we addressed the assumptions in the common vegetation model about fixed plant allocation and added a root exudate flux. In the third experiment, we tested the mechanism that N additions can directly enzyme inhibition and the decomposition of recalcitrant SOM in the MIMICS model.

Overview

The soil biogeochemical model testbed was developed to investigate how model structural assumptions and parameterizations influence global-scale soil biogeochemical

projections over the historical record and in future climate change scenarios (Wieder *et al.*, 2018, 2019c). The testbed uses common environmental drivers and a shared vegetation model (CASA-CNP) to reduce uncertainties among soil models that are not directly related to their representation nor the parameterization of soil biogeochemical dynamics. The C and N version of the testbed includes the CASA and the MIMICS soil models. Both of these models have two litter pools—metabolic and structural—and three SOM pools with various turnover times and stoichiometry. The three SOM pools in CASA and MIMICS, respectively, include (1) the microbial or SOMa (microbially available) pool; (2) the slow or SOMc (chemically protected); and (3) the passive or SOMp (physicochemically protected) pool. In this study, we compare the relative abundance of the slow/SOMc and passive/SOMp to empirical measurements of particulate organic matter (POM) and mineral-associated organic matter (MAOM), respectively, from the Fernow Forest.

Key differences between the models are described in previous work (Wieder *et al.* 2018; 2019), but here we highlight differences in their representation of soil organic matter turnover and stoichiometry. Litter and SOM turnover in CASA occurs via an implicit representation of microbial activity, with decomposition controlled by linear, first-order dynamics. Soil C turnover times are defined by biome- and pool-specific decay constants that are modified by environmental scalars for soil temperature and soil moisture availability. The stoichiometry for each of the five organic matter pools in CASA is diagnostic (i.e., values are assigned), and are defined by pool- and biome- specific parameter values (Randerson *et al.*, 1996; Wang *et al.*, 2010; Fig 4-1a). Conversely, turnover of litter and SOM in MIMICS are determined via temperature sensitive reverse Michaelis-Menten kinetics so that organic matter turnover and heterotrophic respiration fluxes are dependent both on the size of the donor (substrate) and

receiver (microbial biomass) pools. MIMICS also represents two functionally distinct microbial communities that correspond to fast/copiotrophic and slow/oligotrophic growth strategies (or r- and K-type communities, MIC_r and MIC_K; Fig 4-1b). These microbial communities have different catabolic potential, anabolic traits, C:N ratios, and substrate affinities (Wieder *et al.* 2015; 2022; Kyker-Snowman *et al.* 2020; Fig. 4-1). The stoichiometries of the microbial biomass pools are parameterized in MIMICS (using C:N ratios of 6 and 10 for MICr and MICK, respectively), but the stoichiometries of litter and SOM pools are a diagnostic feature of the model. The testbed is typically run at the global scale, though it can also be run in a single-point configuration for the purpose of comparing the model to site-level observational data as a way to assess model performance and test ecological hypotheses.

Model forcing and initialization

The CASA-CNP model consists of coupled vegetation and soil models (Randerson *et al.*, 1996; Wang *et al.*, 2010). In the testbed used for this study, both the CASA soil component and the MIMICS soil model are coupled to the CASA-CNP vegetation model component. The vegetation component of CASA-CNP requires daily meteorological inputs, including air temperature, precipitation, and GPP. Both soil models (CASA & MIMICS) also need inputs for depth-weighted means of soil temperature and liquid and frozen soil moisture. The CASA-CNP vegetation model calculates net primary productivity, allocation to leaves, wood and roots, vegetation N demand and uptake (for C-N versions of the model), and litterfall fluxes. For this study, input data used to run the model were generated from simulations by the Community Land Model, version 5.0, with satellite phenology (CLM 5.0-SP), forced with GSWP3 climate reanalysis for the period 1900-2014 (Lawrence *et al.*, 2019). In contrast, previous work with the testbed used input data from an older version of CLM (CLM 4.5-SP) forced with Cru-NCEP

climate reanalysis data (Wieder *et al.* 2018; 2019). In the present study, input data beyond 2014 were generated by extending the CLM 5.0-SP simulation with an anomaly forcing (2015-2019) of atmospheric fields from projections made with the Community Earth System Model version 2 (CESM2, see Danabasoglu *et al.*, 2020; for methods, see also Wieder *et al.*, 2015a, 2019b, who used a similar approach with previous versions of CLM and CESM). Briefly, this anomaly forcing cycles over the last decade of the GSWP3 input and applies an anomaly based on a 3-member ensemble mean from CESM2 simulations that have been archived for the Coupled Model Intercomparison Project Phase 6 (CMIP6) experiment. This experiment was run under the SPP3-70 climate change scenario to generate data from 2015-2100 (http://www.earthsystemgrid.org). For this study we only present results through 2019.

From these global simulations we extracted data for the gridcell covering the Fernow Forest, and the daily CLM 5.0-SP output were then used as input boundary conditions for all simulations presented here. Because we ran the testbed in single-point mode, the CASA-CNP vegetation model was assigned one plant functional type (PFT) for our experiment: temperate deciduous forest. Some of the CASA-CNP vegetation parameters were also modified to better represent observations at the Fernow Forest when appropriate empirical observations were available (Table 4-1). The CASA-CNP vegetation model uses these inputs to produce NPP estimates and plant litterfall inputs that become inputs to both soil biogeochemical models (CASA & MIMICS). In all simulations, soil depth was set to 45 cm to allow for comparison with observations of soil C and N stocks.

Models were spun-up by cycling over meteorological input data (1901-1920) until C and N pools equilibrated. This took a spin-up period of 6,000 years for MIMICS and 8,000 years for CASA to ensure that soil stocks reached steady state. We also ran all simulations through a

historic period (1901-1988) using GSWP3 climate, N deposition taken from CLM5 simulation (Lawrence *et al.*, 2019), and atmospheric CO_2 data from the same period. Results from historic simulations were compared with observational data from the Fernow Forest (see **Site Description**) and used to complete the site-specific configuration of the testbed models.

Site-specific configuration of historic simulations

Based on preliminary results, we modified several parameters in the vegetation and soil model components so that historic simulations (through 1988) better matched observed ecosystem C and N stocks and fluxes at the Fernow Forest and were N limited (defined by a positive NPP response to N additions). All vegetation and soil parameter modifications for site-specific configuration are detailed in Tables 4-1, 4-2, 4-3, and these modifications are supported by observational data from the long-term experimental data (Eastman *et al.*, 2021). Briefly, changes in the CASA-CNP vegetation parameters were made to decrease vegetation C stocks and increase the baseline N limitation in the model, which was defined by a positive NPP response to N additions (Table 4-1).

Modifications to CASA soil component parameters reduced the soil C:N ratio and total soil C stocks, again better capturing observed values (Table 2; Eastman *et al.*, 2021, 2022). In contrast, modifications to the MIMICS soil parameters were needed to increase total soil C:N ratios and total C stocks, to better reflect observed values and reduce model-to-model differences (Table 4-3; Eastman *et al.*, 2021, 2022). After both CASA and MIMICS soil model parameters were calibrated to the Fernow Forest site for the end of the historic period, the models with these calibrated parameters became the "default" models that were used in experimental simulations (1989-2019) that are the main focus of this study.

Experimental design: N enrichment experimental simulations

Our three experimental testbed simulations were run to coincide with the experimental N additions at the Fernow Forest (1989-2019). Similar to historic simulations, experimental simulations used GSWP3 climate and atmospheric CO_2 data that was extended with an anomaly forcing for years 2015-2019. Control simulations received ambient N deposition rates used in CLM 5.0, while the fertilized, +N simulation, received an additional 3.5 g N m^{-2} y^{-1}, distributed evenly across every day of year. This annual rate of additional N deposition matched the annual rate of experimental N additions at the Fernow Forest whole-watershed fertilization experiment (Adams *et al.*, 2006). In the first experiment, the N perturbations were the only modifications made to the default, site-calibrated models.

In the second experiment, we made modifications to the CASA-CNP vegetation model to address assumptions about plant C allocation. With N enrichment, the default models accurately captured an increase in vegetation NPP and soil C stocks, but did not capture an increase in wood biomass, a greater soil C:N ratio, nor a reduction in soil heterotrophic respiration. It is well established that more nutrient availability leads to less belowground C flux, and thus increases aboveground NPP (Litton *et al.*, 2007; Vicca *et al.*, 2012; Fernández-Martínez *et al.*, 2017), but this dynamic allocation pattern in response to nutrient enrichment is one that some models, like the CASA-CNP vegetation model, do not capture (Thomas *et al.*, 2015; Wieder *et al.*, 2019b). To improve model representation of observed ecosystem responses at the Fernow, and to test our hypothesis that reduced soil heterotrophic respiration was due to shifts in plant allocation away from belowground C inputs (and enhanced wood production), we adjusted vegetation parameters in CASA-CNP in two ways (Fig. 4-1a). First, we added a "root exudate" flux, which was implemented as a C-only flux to the metabolic litter pool set to 10% of GPP C under ambient conditions, and we adjusted the root exudate flux rate with elevated N deposition: decreasing root exudate C from 10% of GPP C under ambient N deposition conditions (control) to 5% of

GPP C (+N). Additionally, we adjusted the fixed allocation scheme in the CASA-CNP vegetation model to shift 10% of GPP C away from roots and to wood production under conditions of +N.

In the third experiment, we used the microbially-explicit MIMICS soil model to test the direct enzyme inhibition mechanism: that reduced microbial enzyme activity from elevated soil N led to an accumulation of particulate organic matter and subsequent increase in the mineral soil C:N ratio. In the MIMICS model, this could be approached multiple ways (see Wieder *et al.*, 2015a), but here we focus on the direct effects that N additions may have by suppressing ligninolytic enzyme activity, which is supported by observations at the Fernow Forest and other sites (Carreiro *et al.*, 2000; Xia *et al.*, 2017; Carrara *et al.*, 2018; Tan *et al.*, 2020). MIMICS represents an analogous transition of chemically protected SOM (SOM_c which we equate with POM) to microbially available SOM (SOM_a). This transition from SOMc to SOMa in MIMICS follows reverse Michaelis-Menten kinetics but is not parameterized as a function of soil N availability. To represent potential nitrogen inhibition on POM decomposition, therefore, we increased the half saturation constant for the oxidation of the chemically protected SOM pool, essentially reducing rates of decomposition of this pool (Fig. 4-1b). Results from the experiment are presented here and referred to as "*veg & mic mod*" models and simulations hereafter.

Model-data comparisons

To compare the sensitivity of observed and modelled responses to N enrichment we calculated response ratios for different C and N pools and fluxes following 30 years of N additions. Response ratios were calculated for key observations and model outputs, using the most recent observed values and the annual mean value from the last 10 years of the experimental simulations. Response ratios were estimated by dividing the ambient (control)

observed or modelled value by the +N watershed or modelled value. Thus, a response ratio of 1 meant that there was no effect of N additions on the pool/flux, whereas a response ratio greater than or less than one indicates an increase or decrease in that flux/pool with N additions, respectively.

4.4 Results

Experiment 1: Default model responses to N additions

Both default versions of the models accurately represented an increase in NPP with N additions but to varying degrees (Fig. 4-2a). The magnitude of the NPP response to N fertilization in CASA was much weaker than observed. In contrast, the magnitude of the NPP response to N fertilization in MIMICS better matched observations at the Fernow, suggesting that the greater N limitation generated by MIMICS (Table 4-1) may be more realistic. Both of the default models favored leaf and fine root production over wood C growth, contrary to observations at the Fernow (Figure 4-2).

Similar to vegetation responses, the simulated soil responses to N additions of default model versions were stronger in the MIMICS model than the CASA model, though the two models responded in similar manners. Specifically, soil heterotrophic respiration increased, while soil C:N ratios decreased with N enrichment in both models (Fig. 4-2b). Total soil C stocks increased in MIMICS but did not change in the CASA model with N additions (Fig. 4-2b). The negligible change and slight increase in soil C stocks simulated by CASA and MIMICS, respectively, were within the observed range for both models. However, the positive soil respiration responses were opposite to what was observed (Fig. 4-2b). Additionally, the total soil C:N ratio decreased slightly with N enrichment in both models, in contrast to the positive response of the mean soil C:N ratio observed in the field experiment (Fig. 4-2b). Observed soil

responses to N additions (i.e., reduced soil respiration, increased soil C stocks and C:N ratio) were driven by a reduction in decomposition and accumulation of POM (Figs. 4-3, 4-4). Despite a slight increase in soil C stocks with N additions in MIMICS and slight decreases in the soil C:N ratio of both models, the relative abundance of SOM distributed across MAOM (PASS/SOMp) and POM (SLOW/SOMc) pools was not sensitive to N additions for either the CASA nor MIMICS default models (Fig. 4-3a). Rather, all SOM pools in MIMICS increased by similar magnitudes, and the C:N ratios of these pools were not altered by N additions (Fig. 4-3b).

Experiment 2: Plant allocation shifts with N additions

In an attempt to rectify a positive NPP response with a negative soil respiration response to N additions in the models, we made modifications to plant C allocation in the CASA-CNP vegetation model. The modifications were intended to slow the overall turnover time of C in the ecosystem by reducing the flux of C to soil by fast-turnover and microbially available pool (root exudates) and increasing the production of a slow-turnover and recalcitrant pool (woody biomass). As expected, the modifications to vegetation parameters improved model predictions of the enhanced woody biomass C stock with N additions in both models (Fig. 4-2a), but also caused some diverging vegetation responses between models and unexpected heterotrophic respiration responses.

Considering the vegetation responses, one key difference between *vegmod* simulations was that these modifications reduced fine root C stocks in the CASA model, while magnifying the positive response of fine root C stocks in the MIMICS model (Fig. 4-2a). Additionally, the MIMICS *vegmod* simulations had much stronger positive NPP and leaf and wood C stock responses compared to the default, all of which exceeded the positive response observed in the field experiment (Fig. 4-2a). This overestimation in plant productivity in MIMICS *vegmod* was,

in large part, due to an increase in the overall vegetation carbon use efficiency (defined here as the quotient of NPP and GPP). By increasing allocation to wood, relative to fine roots and leaves, vegetation N demand decreased, which allowed greater overall biomass production in response to N enrichment (Fig. 4-2a). These differences in vegetation responses were also reflected in some diverging soil responses between models.

Notably, the CASA *vegmod* model responded to +N with a very slight reduction in heterotrophic respiration (- 2%) and a decrease in the total C stock, driven by reductions in fine root C pools (~20 % reduction) and fluxes to soil (Fig. 4-2). On the other hand, MIMICS *vegmod* simulated increases in heterotrophic respiration and soil C stocks similar to results from Experiment 1, as the reduced root exudate C flux to soil was counteracted by increased leaf and fine root litter fluxes (Fig. 4-2). The soil C:N ratio decreased with N additions in CASA *vegmod*—like in Experiment 1—but increased with N additions in the MIMICS *vegmod* simulation, more similar to the mean observed response (Fig. 4-2b). While vegetation allocation shifts did not influence the distribution nor CLN ratio of the three SOM pools, the MIMICS *vegmod* model generated a greater relative abundance of MAOM (SOMp) under ambient N deposition conditions compared to the default MIMICS version (Experiment 1). And with N additions, MIMICS *vegmod* simulated a small shift in the distribution of SOM pools to a greater fraction of POM (SOMc) and less MAOM (SOMp; Fig 4-3a). The change in SOM pool distribution captured by MIMICS was a similar pattern but lesser magnitude of change compared to observations (Fig. 4-3).

Experiment 3: Microbial inhibition of decomposition with N additions

Based on observed increases in light particulate organic matter (POM) and soil C:N ratios with N additions in the surface soil at the Fernow Forest (Eastman *et al.*, 2022), we examined

whether the MIMICS model could capture this pattern with an additional parameter modification—reducing soil enzyme activity—with the elevated N perturbation (Fig. 4-1b; MIMICS *veg & mic mod*). In Experiment 3, we kept the modifications to plant C allocation from *vegmod*, and we increased the half-saturation constant controlling oxidation of SOMc (POM) in MIMICS model in attempt to reduce soil respiration rates and promote the accumulation of SOMc/POM (Fig. 4-1b).

The MIMICS *veg & mic mod* experiment generated similar plant productivity responses as in the *vegmod* simulation: significant positive responses of NPP and plant component pools (Fig. 4-2a). Interestingly, despite this strong, positive plant productivity response and subsequent soil C inputs in MIMICS *veg & mic mod*, this simulation generated a more moderate positive response of soil respiration than by the default version (+ 8% versus + 13%, respectively; Fig. 4-2b). Additionally, by reducing the rate of oxidation of SOMc/POM, MIMICS *veg & mic mod* produced a greater increase in the relative abundance of SOMc/POM with N additions than in the *vegmod* only simulation (Fig. 4-3a). These results aligned better with observed increases in POM with N additions and are reflected in the greater increase in total soil C and C:N ratio simulated by the MIMICS *veg & mic mod* (Fig. 4-2b).

Similar to observations, the positive response of the bulk soil C:N ratio that occurred with N additions was concurrent to an increase in the relative abundance of the SOMc/POM pools in modified MIMICS simulations (Fig. 4-3b; Fig. 4-4). However, these increases in bulk soil C:N ratios with N additions that were captured by the MIMICS model were weak compared to the differences in soil C:N ratio between watersheds at the Fernow Forest (Figs. 4-2b, 4-4). The weak relationship between POM abundance and bulk soil C:N ratios was due to the low C:N ratios of the SLOW/SOMc pools in CASA and MIMICS models (Fig. 4-3b).

4.5 Discussion

Current land C models have simplistic representations of soil organic matter formation and decomposition that do not include microbial physiology and enzyme kinetics, creating challenges in modeling and predicting future soil C stocks under environmental changes, such as elevated N deposition, that alter plant-soil interactions (Wieder *et al.*, 2013). Here we use a soil model testbed to explore whether a more complex and realistic representation of soil biogeochemistry—through the inclusion of explicit microbial communities and physiology—influences model estimation of the C cycle response to N additions. Our results show that neither the simplistic (CASA) nor microbially-explicit (MIMICS) models accurately captured both an increase in aboveground plant productivity and a decrease in soil heterotrophic respiration with N additions, as observed in the long-term N addition experiment at the Fernow Forest (Fig. 4-2). However, we also show that model modifications that increase the overall turnover time of vegetation C and directly inhibit microbial activity helped to move the model predictions closer to observed responses to N additions (Eastman *et al.*, 2021; Fig. 4-2). Given the widespread occurrence of reduced soil respiration and microbial activity with N additions (Janssens *et al.*, 2010), as well as the importance of this C flux for the future of the land C sink (Bond-Lamberty *et al.*, 2018), validating model assumptions against long-term experimental data is a necessary step to improve our predictions of the land C sink to global change.

Implications of a fixed allocation vegetation model

While both the CASA and MIMICS models accurately predicted increases in NPP with N additions, the magnitude of this response was often outside the range of observations (Fig. 4-2a), and the often-observed shift in allocation to favor wood biomass production over belowground C flux (Zak *et al.*, 2008; de Vries *et al.*, 2014; Fernández-Martínez *et al.*, 2014; Frey *et al.*, 2014)

was not captured within the fixed allocation framework of the CASA-CNP vegetation model. Even after modifying the allocation scheme of the CASA-CNP vegetation model (Fig. 4-1), the increased plant carbon use efficiency that resulted from greater allocation to wood (and less N and respiration requirements) increased leaf litter and fine root production with N additions (in MIMICS) beyond the range of observed responses (Fig. 2a). Because the CASA-CNP vegetation model did not accurately predict the observed vegetation response to N additions, it limits our ability to assess how the soil models respond to augmented N. Indeed, soil biogeochemistry responds to shifts in vegetation productivity and inputs, such as reduced microbial activity and, thus, soil respiration with less belowground C flux in nutrient-rich environments (Janssens *et al.*, 2010; Gill & Finzi, 2016). Evidence from the Fernow Forest of shifting N acquisition and C allocation strategies with N enhancements is similar to results from other studies suggesting that forests will respond to other global changes, such as CO_2 enrichment and changes in precipitation, with similar strategies (Reich, 2014; Terrer *et al.*, 2017b; Fleischer *et al.*, 2019). Therefore, considering how nutrient acquisition strategies and plant C allocation and turnover are represented in vegetation models can be as important for predicting soil C cycling as the structure of the soil models themselves.

Comparing modelled responses to N additions

Despite limitations brought forth by the CASA-CNP vegetation model structure (e.g., static allocation scheme, N fixation, leaching rates, and stoichiometry), the testbed still proved a valuable tool for identifying key model differences that impact their predicted ecosystem responses to N additions. Notably, the large differences in N limitation status between MIMICS and CASA contributed significantly to their differing vegetation responses to N additions and the downstream responses of soil C and N cycling. The strong N limitation in the MIMICS model

was reflected in the much larger positive vegetation response to N additions compared to CASA (Fig. 4-2). Furthermore, the modified CASA and MIMICS models in Experiments 2 & 3 simulated opposite N addition responses of total soil C, soil C:N; the increase in these ecosystem properties simulated by MIMICS better reflected observed shifts in soil C and C:N ratios with a shift in plant allocation (Fig. 4-2). High soil N availability encourages shifts in plant nutrient acquisition strategies by reducing belowground C flux to mycorrhizae that is typically required for nutrient acquisition (Gill & Finzi, 2016; Eastman *et al.*, 2021). These shifts in nutrient acquisition strategy and C allocation lead to reduced mycorrhizal colonization, reduced rates of SOM decomposition, and an accumulation of soil C. While vegetation allocation modifications did influence some soil biogeochemical processes as desired in the MIMICS models, the apparent importance of direct effects of N additions (enzyme inhibition) on SOM processing led us to modify the enzyme kinetics in the MIMICS model (Experiment 3). This modification further improved model predictions of soil responses to N additions, particularly by further increasing to soil C stock and C:N ratio and further moderating the positive soil respiration response (Fig. 4-2b).

Despite efforts to modify the models to better reflect the observed vegetation response and produce a decrease in soil respiration, none of the model simulations captured the strong (~13%) reduction in soil respiration with N additions. Decreases in soil respiration rates are consistently reported under conditions of N enhancement, even with greater NPP and litter inputs (Janssens *et al.*, 2010), and the soil respiration flux is a large, globally important flux of C from land to atmosphere that may drive the magnitude of the future land C sink (Bond-Lamberty *et al.*, 2018). Heterotrophic respiration fluxes in models are typically proportional to NPP or litter C inputs. Thus, a common response of ecosystem models to N additions (or enhanced

productivity and greater C inputs from vegetation to the soil, in general) is an increase in rates of soil respiration (Koven *et al.*, 2015; Sulman *et al.*, 2019; Wieder *et al.*, 2019b). Thus, the large increases in heterotrophic respiration in the MIMICS model reflects the enhanced vegetation productivity with N additions. While we considered the accurate simulation of soil heterotrophic respiration to be a high priority, considering the balance between soil C inputs and outputs can be equally valuable as they ultimate determine the overall change in the soil C pool. With N additions, CASA *vegmod* predicted a small increase in NPP (of wood, despite decreased root production) and slight decrease in soil respiration, but still resulted in a decrease in soil C (Fig. 4-2b). Whereas MIMICS modified models predicted large increases in NPP (over 50%) of all plant components and increases in soil respiration (+ 8-13%), but still captured an accumulation of total soil C (+13 % in MIMICS *veg & mic mod;* Fig. 4-2b). The increase in soil C with N addition predicted by the MIMICS models were remarkably similar to the mean enhancement in surface mineral soil (0-15 cm) at the Fernow Forest (Eastman *et al.*, 2021), as well as increases in surface soil C stocks at other long-term N addition experiments (Zak *et al.*, 2008; Frey *et al.*, 2014). These results highlight the differences in how C was allocated among vegetation components, as well as how SOM turnover is represented by the two models. The first order decay dynamics in models like CASA more closely links soil C input fluxes to soil C stocks (see Friend *et al.*, 2014; Koven *et al.*, 2015), so a decrease in fine root production likely drove decreased soil C stocks. In contrast the microbially-explicit decay in MIMICS better represents SOM turnover as independent from overall C inputs (live plant C turnover), and decay rates increased to prevent an exaggerated increase in soil C.

Soil organic matter distribution and stoichiometry

In addition to accurately predicting changes in the total soil C stocks and fluxes, the distribution of SOM among POM and MAOM pools is of high important for understanding the future land C sink response to environmental change. Changes in the distribution of these SOM pools may impact overall soil stoichiometry (e.g., Eastman *et al.,* 2021), which exerts controls on important soil C and nutrient cycling processes, such as net N mineralization rates (Aber *et al.,* 2003; Venterea *et al.,* 2004). Additionally, a recent global analysis by Hartley *et al.* (2021) found evidence for greater vulnerability of POM decomposition under conditions of soil warming compared to MAOM. Here, default models (Experiment 1) do not capture a shift in either the distribution of SOM into these distinct pools, nor a shift in the overall C:N ratio of bulk soil (Fig. 4-3; 4-4). However, the modified model simulations allowed us to explore two hypotheses about how N additions indirectly and directly lead to the accumulation of light POM. Indirectly, shifts in allocation—through the reduction of root exudate C flux and increasing the production of recalcitrant woody material—can limit microbial growth, reduce overall rates of SOM decay (Kuzyakov, 2010; Sulman *et al.*, 2017; Craig *et al.*, 2022), and increase the amount of recalcitrant organic matter flux into the POM pools at decadal timescales (Eastman *et al.,* 2022). This plant allocation shift mechanism was tested with the *vegmod* simulations in Experiment 2. Directly, N additions can inhibit oxidative enzyme activity, reducing recalcitrant plant litter decomposition and increasing the amount of SOM formed as particulate matter (Xia *et al.,* 2017; Bonner *et al.,* 2019). This direct enzyme inhibition mechanism was tested with the MIMICS *veg & mic mod* simulation in Experiment 3.

Our results from Experiments 2 and 3 showed an accumulation of POM with N additions in the modified MIMICS models only, especially the MIMICS *veg & mic mod* (Fig. 4-4). These

differences between the CASA and MIMICS models are reflective of model structure and representation of SOM decay. Because the CASA model has prescribed turnover times for each SOM pool, any change in the distribution of these pools must originate from changes in input fluxes of labile versus recalcitrant plant litter. The CASA model did not produce the expected increase in POM with greater wood production and belowground C flux (Figs. 4-3, 4-4), perhaps because the slow turnover time of wood might cause a delay in the SOM pool responses beyond the 30-year experiment. In MIMICS, the decomposition of SOM pools is determined by soil conditions, soil community composition, and the quality of litter inputs using reverse Michaelis-Menten kinetics. Thus, the shift in plant C allocation, especially the reduction in root exudate flux, increased the flow of litter inputs (i.e., structural litter) to the SOMc pool and reduced the flow of litter inputs (i.e., metabolic litter) to the MAOM pool. Regardless of differences in SOM decomposition dynamics between models, both models assume a much longer turnover time of MAOM than POM, an assumption that is challenged by studies of N addition that suggest augmented N can increase the turnover time of the POM pool through reduced oxidative enzyme activity and less microbial priming (Craine *et al.*, 2007; Von Lützow *et al.*, 2008; Chen *et al.*, 2018; Eastman *et al.*, 2022).

An increase in the relative proportion of POM constituting SOM stocks in the fertilized watershed at the Fernow Forest raises compelling questions about the future of C and N stocks that may have accumulated due to chronic N additions. Greater POM abundance can lead to greater bulk soil C:N ratios, yet POM is more vulnerable to decomposition under certain environmental and land use changes (Gregorich *et al.*, 2006; Hartley *et al.*, 2021). POM represents plant-like organic matter with minimal microbial processing and observed POM C:N ratios are similar to the C:N ratios of fine roots and slightly lower than that of leaf litter (Eastman *et al.*, 2022). As such, observed C:N ratios of POM are ~25, whereas the C:N ratios in CASA

and MIMICS were between ~14-20. One explanation for the differences between model responses of different SOM pools and soil C:N ratio to N additions is the difference in how stoichiometry is represented in the models. In the CASA model, there was little difference in the C:N ratios between SOM pools or bulk soil (Fig. 4-3b). Because the C:N ratios of SOM pools in CASA are prescribed as parameters, they do not respond to environmental changes like N additions. One potential advantage the MIMICS model has over CASA is that the C:N ratios of SOM pools are not prescribed, but instead rely on the environmental conditions, input stoichiometry, and microbial community composition. Additionally, the reverse Michaelis-Menten representation of decomposition in MIMICS offers some added flexibility—compared to the simpler, first-order model—for testing mechanisms that may drive observed responses to N additions, such as reduced microbial biomass and activity with reduced belowground C allocation by plants and reduced oxidative enzyme activity under conditions of high N addition

. On the other hand, there still appears to be some uncertainty in how these dynamics should be parameterized and how they are functionally related to environmental changes, such as the direct effect of reduced enzyme activity with N additions. Given the widespread empirical evidence for a reduction in lignin-degrading enzyme activity with elevated N inputs (Treseder, 2004; Pregitzer *et al.*, 2008; Frey *et al.*, 2014; Carrara *et al.*, 2018), it would be meaningful to identify a threshold or relationship between the level of soil N additions, or N availability, and rates of decomposition of this chemically-protected litter and SOM pool with which to impose controls on the MIMICS-CN model. Capturing the accumulation of POM with N additions can have important implications for the future N cycling and C storage in forest ecosystems that have experienced historically high rates of N deposition. For example, under environmental changes, such as elevated N deposition, the stoichiometry of these SOM pools shift and impact downstream processes such as oxidation of POM (SOMc), net N mineralization, and N leaching

(Aber *et al.*, 2003; Venterea *et al.*, 2004; Lovett & Goodale, 2011). A negative relationship between lignin enzyme activity and bulk soil C:N and POM abundance has been observed across many N addition experiments (Chen *et al.*, 2018). This common observation begs the question of how this N-induced shift in the nature and stoichiometry of SOM will impact forest recovery from N deposition and progressive N limitation under elevated CO_2 conditions (Groffman *et al.*, 2018; Craine *et al.*, 2018; Norby *et al.*, 2010).

Conclusions

As atmospheric CO_2 levels rise, forest C sequestration and productivity will depend on the nutrient availability and nutrient acquisition strategies of plants in the ecosystem (Sulman *et al.*, 2017; Terrer *et al.*, 2017b, 2019a). Concurrently, as forests recover from N deposition (which is declining in the US and Europe but continuing to increase in Eastern Asian temperate forests), any N-induced soil C accumulation may become subject to destabilization, as plants allocate more C belowground and microbes mineralize more soil C to access and meet a greater N demand (Finzi *et al.*, 2015; Bailey *et al.*, 2017; Wurzburger & Brookshire, 2017). It is unknown how the forest C stores and sinks will recover from N deposition, and in order to make solid predictions, we must first be able to accurately model how forests have responded to chronic N deposition in the past. Currently, the two models tested in this study were unable to capture some key ecosystem responses to N additions: notably, a shift in plant C allocation to favor wood biomass over belowground allocation, decreased soil respiration, and an accumulation of POM with high C:N ratios (Eastman *et al.*, 2021, 2022). We suspect that because of the indirect and direct impacts that N deposition has on C cycling by altering plant-soil interactions, a more microbially explicit model has a greater potential to capture these complex responses to N enrichment and predict ecosystem recovery from N additions compared

to first-order relationships that have been commonly used in the past. However, there are still some key mechanisms driving the N addition response that are not included or parameterized to empirical data, such as direct enzyme inhibition and increased turnover time of POM. Because some of the ecosystem responses to N additions take decades to play out, such as changes in the size and stoichiometry of soil pools, the integration of long-term experimental data can aid in the effort to improve our modelling of past and future couple C and N cycles.

4.6 Tables and Figures

Table 4-1. Parameter modifications made to CASA-CNP vegetation model for site-specific configuration during spin-up and historical runs.

CASA-CNP Vegetation Model				
Parameter	**Default**	**Modified**	**Source**	**Description**
Fine root mean age *(years)*	10	1.45	Eastman & Peterjohn, *upublished data*	reduce fine root biomass to better match observations
Allocation of GPP C (leaf, wood, froot)	0.3, 0.2, 0.5	0.3, 0.3, 0.4	Eastman *et al.,* 2021	Increase wood C stocks and decrease fine root C stocks
Wood respiration *($year^{-1}$)*	6	3	Eastman *et al.,* 2021	Adjust NPP and wood C stocks to match observed
Leaf C:N	50	42	Eastman *et al.,* 2021	Match observed
Leaf N:C (min, max)	0.02, 0.024	0.0222, 0.02439		Capture modified target leaf C:N
Fine root C:N	41	35	Adams, 1991	Match observed
Fine root N:C (min, max)	0.02439, 0.029268	0.025, 0.032258		Capture modified target fine root C:N
N:C ratio CWD (max)	0.006857	0.00625	Eastman *et al.,* 2021	Increase C:N of CWD, decrease N availability
N leach rate *(g N m^{-2} y^{-1})*	0.01	0.15	Adams *et al.,* 2006	Closer to observed rates; Increase N limitation under ambient N deposition
Max fine litter pool *(g C m^{-2})*	887	1527	Greatest value of all CASA PFTs	Increases N limitation
Max CWD pool *(g C m^{-2})*	1164	1918	Greatest value of all CASA PFTs	Increases N limitation
xkNlimiting (min, max)	0.5, 2	3.4, 5.6 (CASA only)		Increases N limitation in CASA model, to be more similarly N limited as the MIMICS model

Table 4-2. Soil parameter modifications made to CASA-CN for site-specific configuration during spin-up and historical runs. Soil C and N stocks and C:N ratios were compared against observations from Eastman *et al.* (2021, 2022).

CASA-CN			
Parameter	**Default**	**Modified**	**Justification**
MIC soil pool mean age *(years)*	0.137	0.30688	Decrease total soil C:N ratio
SLOW soil pool mean age *(years)*	5	3	Decrease SLOW soil pool, total soil C:N ratio, and soil C and N stocks
PASSIVE soil pool mean age *(years)*	222.22	621	Increase PASSIVE soil pool; decrease total soil C:N ratio
MIC pool C:N (target, min, max)	8, 6.69, 8	7, 6, 10	Decrease total soil C:N ratio
SLOW pool C:N (target, min, max)	30, 16.2, 30	14, 12, 16	Decrease total soil C:N ratio
PASSIVE pool C:N (target, min, max)	30, 16.2, 30	13, 10, 15	Decrease total soil C:N ratio

Table 4-3. Soil parameter modifications made to MIMICS-CN for site-specific configuration during spin-up and historical runs. Default values are those used by Kyker-Snowman *et al.* (2020). Some parameters used were sourced from the C-only global simulation of the tesbed (Wieder *et al*., 2015), and denoted as such. Soil C and N stocks and C:N ratios were compared against observations from Eastman *et al*. (2021, 2022).

MIMICS-CN				
Parameter	**Default**	**Modified**	**Description**	**Justification**
a_V	4.8×10^{-7}	8×10^{-8}	Tuning coefficient	Increases decomposition rates of all pools; Wieder *et al.,* 2015
K_{slope} $ln(mg\ C\ cm^{-3})\circ C^{-1}$	0.017-0.027	0.025	Regression coefficient	Wieder *et al.,* 2015
a_K	0.5	10	Tuning coefficient	Wieder *et al.,* 2015
V_{mod} (k2)	2.25	2.5	Modifies V_{max} for fluxes from LITs to MICk	Increases decomposition of structural litter
τ_r (h^{-1})	0.00024, 0.3	0.000624, 0.6	Controls r-type microbial biomass turnover rate	Increases turnover of r-type microbial biomass
τ _k (h^{-1})	0.00011, 0.1	0.000288, 0.1	Controls k-type microbial biomass turnover rate	Increases turnover of K-type microbial biomass
τ Mod (min, max)	0.6, 1.3	1, 1	Modifies microbial biomass turnover rate	Wieder *et al.,* 2015; (no modification)
f_p (r)	0.015, 1.3	0.2, 1.3	Fraction of τ (r) partitioned to SOMp $0.2 \times e^{1.3(fclay)}$	Increases fraction of r-type microbial biomass partitioned to SOMp
f_p (k)	0.01, 0.8	0.2, 0.8	Fraction of τ (k) partitioned to SOMp $0.2 \times e^{0.8(fclay)}$	Increases fraction of K-type microbial biomass partitioned to SOMp (Wieder *et al.,* 2015)
D (h^{-1})	1.0×10^{-6}, -4.5	1.0×10^{-6}, -1.5	Desorption rate from SOMp to SOMa $10^{-6} \times e^{-1.5(fclay)}$	Increase desorption rate from SOMp to SOMa (Wieder *et al.,* 2015)
f_l (met)	0.05	0.3	Fraction of metabolic litter inputs transferred to SOMp	Increase total soil C stocks, increase SOMp
f_l (struc)	0.3	0.35	Fraction of structural litter inputs transferred to SOMc	Increase SOMc, increase total soil C:N ratio
f_{met}	0.85—0.013	0.65—0.013	Partitioning of inputs to metabolic pool	Reduce fraction of inputs partitioned to metabolic pool (Wieder *et al.,* 2015)
NUE (1, 2, 3, 4) $(mg\ mg^{-1})$	0.85, 0.85, 0.85, 0.85	0.8, 0.7, 0.8, 0.7	Proportion of mineralized N captured by microbes (1) LITmN or SOMaN to MICrN; (2) LITsN to MICrN; (3) LITmN or SOMaN to MICkN; (4) LITsN to MICkN	By reducing NUE, we reduced the microbial competitive advantage over plants for N and N limitation. Reducing NUE more for structural litter fluxes increased soil C:N
CN_r, CN_k	6 10	8 12	C:N ratio of r-type microbes C:N ratio of k-type microbes	Increase soil C:N; reduce microbial N demand & N limitation
fracDINavailMIC	0.5	0.2	Fraction of dissolved inorganic N available to microbes	Reduce N limitation by decreasing microbial N uptake
Soil Depth *(cm)*	100	45	Total soil depth	Observed values are measured to a depth of 45 cm

(a) **CASA-CN model and vegetation modifications**

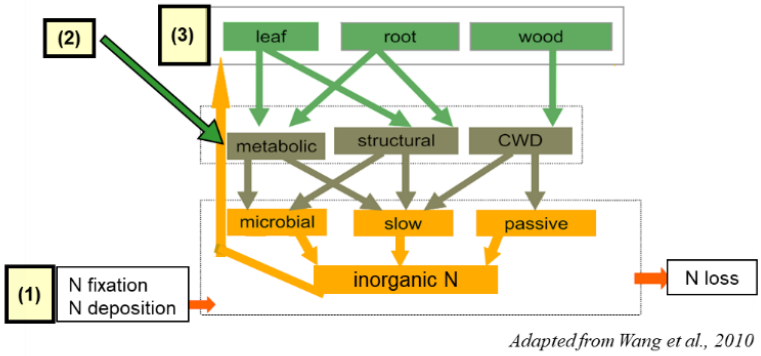

Adapted from Wang et al., 2010

CASA-CNP Modification	Default (calibrated to site)	Modified control/ambient	Modified +N
(1) N deposition	Ambient (from CLM5)	Ambient (from CLM5)	Ambient + 3.5 g N m^{-2} y^{-1}
(2) Root exudation flux	None	0.10 * GPP-C	0.05 * GPP-C
(3) Allocation of GPP-C	leaf : root : wood 0.3 : 0.4 : 0.3	leaf : root : wood 0.3 : 0.4 : 0.3	leaf : root : wood 0.3 : 0.3 : 0.4

(b) **MIMICS-CN model and microbial modification**

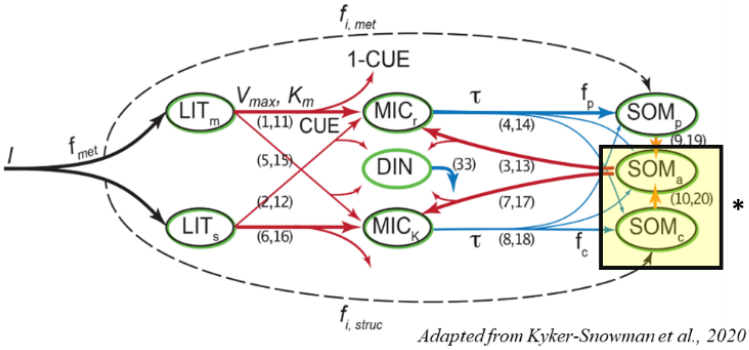

Adapted from Kyker-Snowman et al., 2020

* **Oxidation of SOMc to SOMa**

$$SOM_{c,C}\_SOM_{a,C} = \left(\frac{MIC_{r,C} \times V_{max[r2]} \times SOM_{c,C}}{(KO_{[r]} \times K_{m[r2]} + SOM_{c,C})}\right) + \left(\frac{MIC_{K,C} \times V_{max[K2]} \times SOM_{c,C}}{(KO_{[K]} \times K_{m[K2]} + SOM_{c,C})}\right)$$

MIMICS-CN Modification	Default (calibrated to site)	Modified control/ambient	Modified +N
(*) KO	6	6	8

Figure 4-1. Conceptual diagram of the CASA-CNP coupled vegetation and soil model (a) and MIMICS soil model component (b) along with key modifications made to models to test nitrogen response hypotheses (right). Key modifications made in the CASA-CNP vegetation model (a) included: (1) addition of a belowground C exudate flux that decreased with N additions; (2) modifying C allocation to plant tissues to increase wood production with N additions; (3) altering inputs of N through N fixation to reduce N limitation; and (4) increasing the rate of annual N deposition to match experimental N additions. A theoretically and empirically-supported modification to microbial physiology made to the MIMICS-CN model (b) was an increase in the KO_r and KO_k parameters that modifies the half-saturation constant (K_m) to reduce overall rates of oxidation of chemically protected SOM by both microbial communities (*).

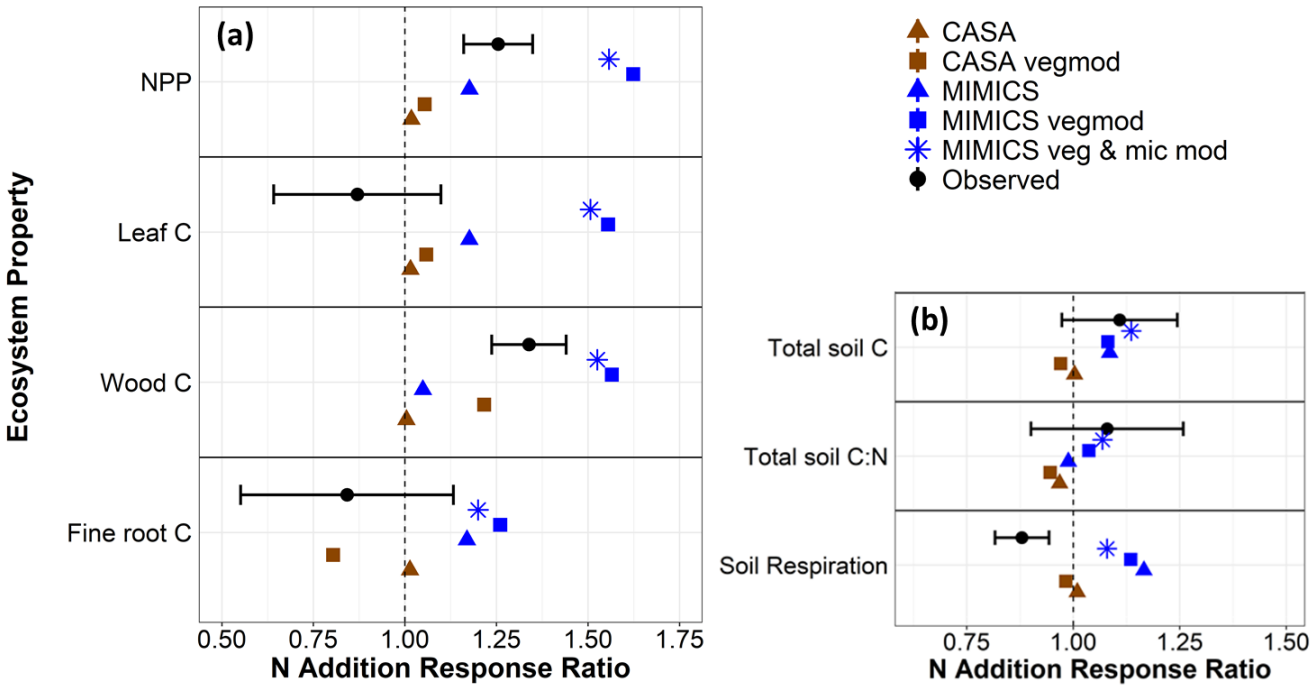

Figure 4-2. Observed (black circles) and simulated response ratios of nitrogen additions on select C and N pools and fluxes. Observations show the mean (+/- se) values from a synthesis of a whole-watershed fertilization study at the Fernow Forest (Eastman *et al.*, 2021). Modelled responses include the CASA-CN (brown) and MIMICS-CN (blue) default models (triangles), modified vegetation models (*vegmod*; square) and the MIMICS-CN modified vegetation and microbial physiology model (veg & mic mod; asterisk). The vertical dashed line represents no effect of N additions. Observed NPP does not include fine root NPP. Observed soil respiration includes autotrophic + heterotrophic, whereas modelled soil respiration includes only heterotrophic. Total soil pools include organic and mineral horizons, to a depth of 45 cm for both modelled and observed values.

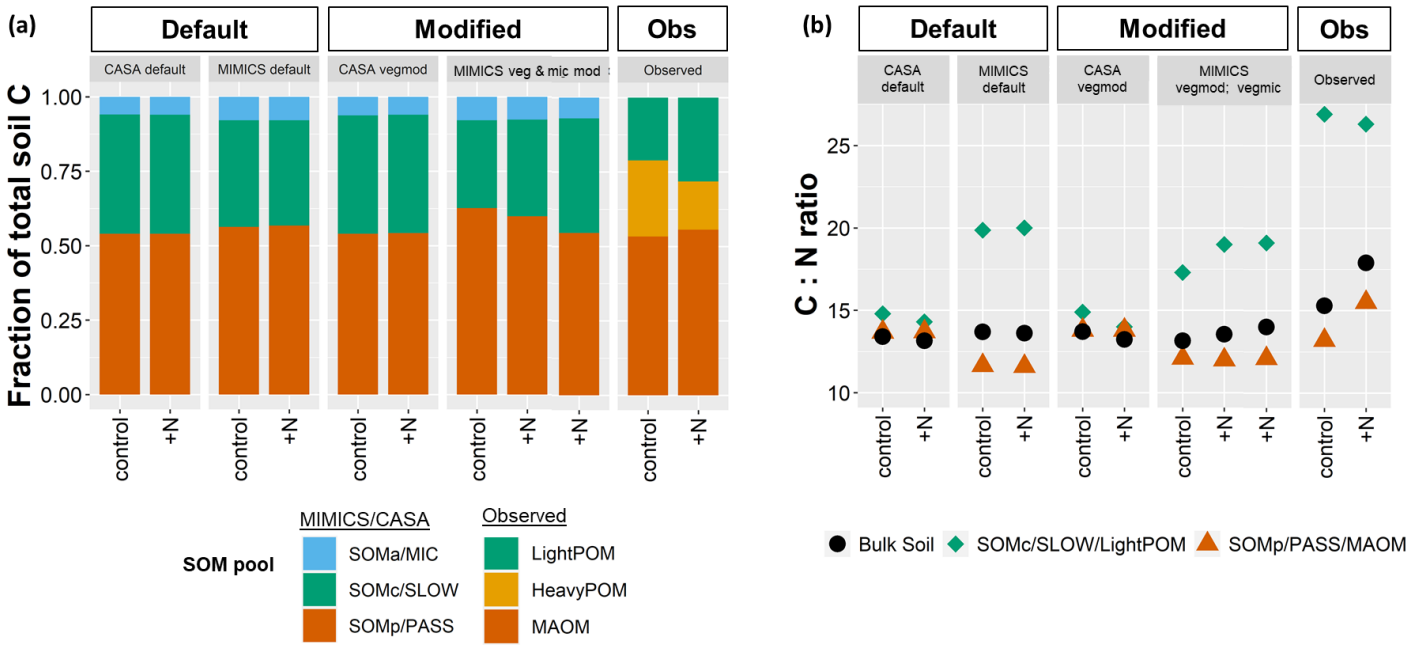

Figure 4-3. Variation in the relative distribution of SOM pools **(a)** and total mineral soil C:N ratios **(b)** across model simulations and observations. **(a)** The relative fraction of SOM C in microbial or microbially available (SOMa) pools (light blue); chemically protected, SLOW, or light particulate organic matter (green); and physicochemically protected, PASSIVE, or mineral associated organic matter (orange). The observed fractions of mineral associated organic matter (MAOM) are separated into heavy particulate and MAOM based on particulate size.

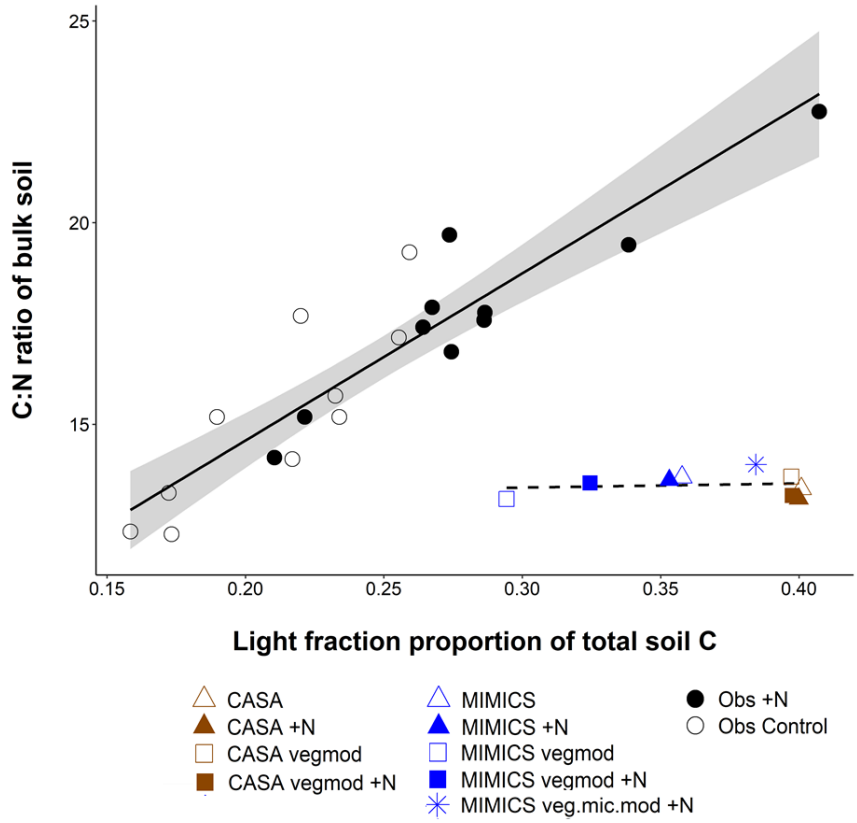

Figure 4-4. Relationship between the relative proportion of light particulate SOM (SOMc and SLOW pools in MIMICS and CASA, respectively) and the C:N ratio of bulk mineral soil in observed (black circles) and modeled (brown=CASA, blue=MIMICS) ambient (open shapes) and +N (solid shapes) conditions. Figure adapted from Eastman *et al.* (2022). Observed points represent the mean of four soil samples per plot (n=20 plots per watershed). Linear regression (standard error in gray shading) for observed (solid black) and modelled (dashed) values.

4.7 Literature Cited

Adams MB, DeWalle DR, Hom JL (Eds.). 2006. *The Fernow Watershed Acidification Study*. Dordrecht: Springer Netherlands.

Bailey VL, Bond-Lamberty B, DeAngelis K, Grandy AS, Hawkes C V., Heckman K, Lajtha K, Phillips RP, Sulman BN, Todd-Brown KEO, *et al.* 2017. Soil carbon cycling proxies: Understanding their critical role in predicting climate change feedbacks. *Global Change Biology* **24**: 895–905.

Bond-Lamberty B, Bailey VL, Chen M, Gough CM, Vargas R. 2018. Globally rising soil heterotrophic respiration over recent decades. *Nature* **560**: 80–83.

Bonner MT, Castro D, Schneider AN, Sundström G, Hurry V, Street NR, Näsholm T. 2019. Why does nitrogen addition to forest soils inhibit decomposition? *Soil Biology and Biochemistry* **137**: 107570.

Carrara JE, Walter CA, Hawkins JS, Peterjohn WT, Averill C, Brzostek ER. 2018. Interactions among plants, bacteria, and fungi reduce extracellular enzyme activities under long-term N fertilization. *Global Change Biology* **24**: 2721–2734.

Carreiro MM, Sinsabaugh RL, Repert DA, Parkhurst DF. 2000. Microbial Enzyme Shifts Explain Litter Decay Responses to simulated nitrogen deposition. *Ecology* **81**: 2359–2365.

Chen J, Luo Y, Van Groenigen KJ, Hungate BA, Cao J, Zhou X, Wang R wu. 2018. A keystone microbial enzyme for nitrogen control of soil carbon storage. *Science Advances* **4**: 2–8.

Cotrufo MF, Soong JL, Horton AJ, Campbell EE, Haddix ML, Wall DH, Parton WJ. 2015. Formation of soil organic matter via biochemical and physical pathways of litter mass loss. *Nature Geoscience* **8**: 776–779.

Craig ME, Geyer KM, Beidler K V., Brzostek ER, Frey SD, Stuart Grandy A, Liang C, Phillips RP. 2022. Fast-decaying plant litter enhances soil carbon in temperate forests but not through microbial physiological traits. *Nature Communications* **13**: 1–10.

Craine JM, Elmore AJ, Wang L, Aranibar J, Bauters M, Boeckx P, Crowley BE, Dawes MA, Delzon S, Fajardo A, *et al*. 2018. Isotopic evidence for oligotrophication of terrestrial ecosystems. *Nature Ecology and Evolution* **2**: 1735–1744.

Craine JM, Morrow C, Fierer N. 2007. Microbial nitrogen limitation increases decomposition. *Ecology* **88**: 2105–2113.

Danabasoglu G, Lamarque JF, Bacmeister J, Bailey DA, DuVivier AK, Edwards J, Emmons LK, Fasullo J, Garcia R, Gettelman A, *et al.* 2020. The Community Earth System Model Version 2 (CESM2). *Journal of Advances in Modeling Earth Systems* **12**: 1–35.

Du E, de Vries W. 2018. Nitrogen-induced new net primary production and carbon sequestration in global forests. *Environmental Pollution* **242**: 1476–1487.

Eastman BA, Adams MB, Peterjohn WT. 2022. The path less taken: Long-term N additions slow leaf litter decomposition and favor the physical transfer pathway of soil organic matter formation. *Soil Biology and Biochemistry* **166**: 108567.

Eastman BA, Adams MB, Brzostek ER, Burnham MB, Carrara JE, Kelly C, McNeil BE, Walter CA, Peterjohn WT. 2021. Altered plant carbon partitioning enhanced forest ecosystem carbon storage after 25 years of nitrogen additions. *New Phytologist* **230**: 1435–1448.

Fernández-Martínez M, Vicca S, Janssens IA, Ciais P, Obersteiner M, Bartrons M, Sardans J, Verger A, Canadell JG, Chevallier F, *et al.* 2017. Atmospheric deposition, CO2, and change in the land carbon sink. *Scientific Reports* **7**: 9632.

Fernández-Martínez M, Vicca S, Janssens IA, Sardans J, Luyssaert S, Campioli M, Chapin III FS, Ciais P, Malhi Y, Obersteiner M, *et al.* 2014. Nutrient availability as the key regulator of global forest carbon balance. *Nature Climate Change* **4**: 471–476.

Finzi AC, Abramoff RZ, Spiller KS, Brzostek ER, Darby BA, Kramer MA, Phillips RP. 2015. Rhizosphere processes are quantitatively important components of terrestrial carbon and nutrient cycles. *Global Change Biology* **21**: 2082–2094.

Fleischer K, Rammig A, De Kauwe MG, Walker AP, Domingues TF, Fuchslueger L, Garcia S, Goll DS, Grandis A, Jiang M, *et al.* 2019. Amazon forest response to CO2 fertilization dependent on plant phosphorus acquisition. *Nature Geoscience* **12**: 736–741.

Frey SD, Ollinger S, Nadelhoffer K, Bowden R, Brzostek E, Burton A, Caldwell BA, Crow S, Goodale CL, Grandy AS, *et al.* 2014. Chronic nitrogen additions suppress decomposition and sequester soil carbon in temperate forests. *Biogeochemistry* **121**: 305–316.

Friend AD, Lucht W, Rademacher TT, Keribin R, Betts R, Cadule P, Ciais P, Clark DB, Dankers R, Falloon PD, *et al.* 2014. Carbon residence time dominates uncertainty in terrestrial vegetation responses to future climate and atmospheric CO_2. *Proceedings of the National Academy of Sciences* **111**:3280–3285.

Galloway JN, Trends R, Townsend AR, Erisman JW, Bekunda M, Cai Z, Freney JR, Martinelli LA, Seitzinger SP, Sutton MA. 2008. Transformation of the Nitrogen Cycle : Potential Solutions. *Science* **320**: 889–892.

Gill AL, Finzi AC. 2016. Belowground carbon flux links biogeochemical cycles and resource-use efficiency at the global scale. *Ecology Letters* **19**: 1419–1428.

Gregorich EG, Beare MH, McKim UF, Skjemstad JO. 2006. Chemical and biological characteristics of physically uncomplexed organic matter. *Soil Science Society of America Journal* **70**:975–985.

Groffman PM, Driscoll CT, Durán J, Campbell JL, Christenson LM, Fahey TJ, Fisk MC, Fuss C, Likens GE, Lovett G, *et al.* 2018. Nitrogen oligotrophication in northern hardwood forests. *Biogeochemistry* **141**: 523–539.

Hartley IP, Hill TC, Chadburn SE, Hugelius G. 2021. Temperature effects on carbon storage are controlled by soil stabilisation capacities. *Nature Communications* **12**: 6713.

Janssens IA a., Dieleman W, Luyssaert S, Subke J, Reichstein M, Ceulemans R, Ciais P, Dolman AJ, Grace J, Matteucci G, *et al.* 2010. Reduction of forest soil respiration in response to nitrogen deposition. *Nature Geoscience* **3**: 315–322.

Jian J, Bond-Lamberty B, Hao D, Sulman BN, Patel KF, Zheng J, Dorheim K, Pennington SC, Hartman MD, Warner D, *et al*. 2021. Leveraging observed soil heterotrophic respiration fluxes as a novel constraint on global-scale models. *Global Change Biology* **00**: 1–12.

Kochenderfer JN. 2006. Fernow and the Appalachian Hardwood Region. In: Adams MB, DeWalle DR, Hom JL, eds. *The Fernow Watershed Acidification Study*. Springer, 17–39.

Kochenderfer JN, Wendel GW. 1983. Plant succession and hydrologic recovery on a deforested and herbicided watershed. *Forest Science* **29**: 545–558.

Koven CD, Chambers JQ, Georgiou K, Knox R, Negron-Juarez R, Riley WJ, Arora VK, Brovkin V, Friedlingstein P, Jones CD. 2015. Controls on terrestrial carbon feedbacks by productivity versus turnover in the CMIP5 Earth System Models. *Biogeosciences* **12**: 5211–5228.

Kuzyakov Y. 2010. Priming effects: Interactions between living and dead organic matter. *Soil Biology and Biochemistry* **42**: 1363–1371.

Kyker-Snowman E, Wieder W, Frey S, Grandy AS. 2020. Stoichiometrically coupled carbon and nitrogen cycling in the MIcrobial-MIneral Carbon Stabilization model (MIMICS-CN). *Geoscientific Model Development Discussions* **13**: 4413–4434.

Lawrence DM, Fisher RA, Koven CD, Oleson KW, Swenson SC, Bonan G, Collier N, Ghimire B, van Kampenhout L, Kennedy D, *et al.* 2019. The Community Land Model Version 5: Description of New Features, Benchmarking, and Impact of Forcing Uncertainty. *Journal of Advances in Modeling Earth Systems* **11**: 4245–4287.

Lehmann J, Kleber M. 2015. The contentious nature of soil organic matter. *Nature* **528**: 60–68.

Litton CM, Raich JW, Ryan MG. 2007. Carbon allocation in forest ecosystems. *Global Change Biology* **13**: 2089–2109.

von Lützow M, Kögel-Knabner I, Ludwig B, Matzner E, Flessa H, Ekschmitt K, Guggenberger G, Marschner B, Kalbitz K. 2008. Stabilization mechanisms of organic matter in four

temperate soils: Development and application of a conceptual model. *Journal of Plant Nutrition and Soil Science* **171**:111–124.

Pan Y, Birdsey RA, Fang J, Houghton R, Kauppi PE, Kurz WA, Phillips OL, Shvidenko A, Lewis SL, Canadell JG, et al. 2011. A large and persistent carbon sink in the world's forests. *Science* **333**: 988–993.

Potter CS, Randerson JT, Field CB, Matson PA, Vitousek PM, Mooney HA, Klooster SA. 1993. Terrestrial ecosystem production: A process model based on global satellite and surface data. *Global Biogeochemical Cycles* **7**: 811–841.

Pregitzer KS, Burton AJ, Zak DR, Talhelm AF. 2008. Simulated chronic nitrogen deposition increases carbon storage in Northern Temperate forests. *Global Change Biology* **14**: 142–153.

Randerson JT, Thompson M V., Malmstrom CM, Field CB, Fung IY. 1996. Substrate limitations for heterotrophs: Implications for models that estimate the seasonal cycle of atmospheric CO_2. *Global Biogeochemical Cycles* **10**: 585–602.

Reich PB. 2014. The world-wide 'fast-slow' plant economics spectrum: A traits manifesto. *Journal of Ecology* **102**: 275–301.

Schulte-Uebbing L, de Vries W. 2017. Global-scale impacts of nitrogen deposition on tree carbon sequestration in tropical, temperate, and boreal forests: A meta-analysis. *Global Change Biology* **24**: 416–431.

Sokol NW, Sanderman J, Bradford MA. 2019. Pathways of mineral-associated soil organic matter formation: Integrating the role of plant carbon source, chemistry, and point of entry. *Global Change Biology* **25**: 12–24.

Sulman BN, Shevliakova E, Brzostek ER, Kivlin SN, Malyshev S, Menge DNL, Zhang X. 2019. Diverse Mycorrhizal Associations Enhance Terrestrial C Storage in a Global Model. *Global Biogeochemical Cycles* **33**: 501–523.

Sulman BN, Moore J, Abramoff R, Averill C, Kivlin S, Georgiou K, Sridhar B, Hartman M, Wang G, Wieder W, *et al.* 2018. Multiple models and experiments underscore large uncertainty in soil carbon dynamics. *Biogeochemistry* **141**: 109–123.

Sulman BN, Brzostek ER, Medici C, Shevliakova E, Menge DNL, Phillips RP. 2017. Feedbacks between plant N demand and rhizosphere priming depend on type of mycorrhizal association. *Ecology Letters* **20**: 1043–1053.

Tan X, Machmuller MB, Cotrufo MF, Shen W. 2020. Shifts in fungal biomass and activities of hydrolase and oxidative enzymes explain different responses of litter decomposition to nitrogen addition. *Biology and Fertility of Soils* **56**: 423–438.

Terrer C, Jackson RB, Prentice IC, Keenan TF, Kaiser C, Vicca S, Fisher JB, Reich PB, Stocker BD, Hungate BA, *et al*. 2019. Nitrogen and phosphorus constrain the CO_2 fertilization of global plant biomass. *Nature Climate Change* **9**: 684–689.

Terrer C, Vicca S, Stocker BD, Hungate BA, Phillips RP, Reich PB, Finzi AC, Prentice IC. 2017. Ecosystem responses to elevated CO_2 governed by plant-soil interactions and the cost of nitrogen acquisition. *New Phytologist* **217**: 347–355.

Thomas RQ, Brookshire ENJ, Gerber S. 2015. Nitrogen limitation on land: How can it occur in Earth system models? *Global Change Biology* **21**: 1777–1793.

Treseder KK. 2004. A meta-analysis of mycorrhizal responses to nitrogen, phosphorus, and atmospheric CO_2 in field studies. *New Phytologist* **164**: 347–355.

Varney RM, Chadburn SE, Burke EJ, Cox PM. 2022. Evaluation of soil carbon simulation in CMIP6 Earth System Models. [preprint]

Vicca S, Luyssaert S, Peñuelas J, Campioli M, Chapin FS, Ciais P, Heinemeyer A, Högberg P, Kutsch WL, Law BE, *et al.* 2012. Fertile forests produce biomass more efficiently. *Ecology Letters* **15**: 520–526.

Vitousek PM, Howarth RW. 1991. Nitrogen Limitation on Land and in the Sea : How Can It Occur? *Biogeochemistry* **13**: 87–115.

de Vries W, Du E, Butterbach-Bahl K. 2014. Short and long-term impacts of nitrogen deposition on carbon sequestration by forest ecosystems. *Current Opinion in Environmental Sustainability* **9**: 90–104.

Wang YP, Law RM, Pak B. 2010. A global model of carbon , nitrogen and phosphorus cycles for the terrestrial biosphere. *Biogeosciences* **7**: 2261–2282.

Wieder WR, Lawrence DM, Fisher RA, Bonan GB, Cheng SJ, Goodale CL, Grandy AS, Koven CD, Lombardozzi DL, Oleson KW, *et al.* 2019a. Beyond static benchmarking: Using experimental manipulations to evaluate land model assumptions. *Global Biogeochemical Cycles* **33**: 1289–1309.

Wieder WR, Sulman BN, Hartman MD, Koven CD, Bradford MA. 2019b. Arctic Soil Governs Whether Climate Change Drives Global Losses or Gains in Soil Carbon. *Geophysical Research Letters* **46**: 14486–14495.

Wieder WR, Hartman MD, Sulman BN, Wang YP, Koven CD, Bonan GB. 2018. Carbon cycle confidence and uncertainty: Exploring variation among soil biogeochemical models. *Global Change Biology* **24**: 1563–1579.

Wieder WR, Cleveland CC, Lawrence DM, Bonan GB. 2015a. Effects of model structural uncertainty on carbon cycle projections: Biological nitrogen fixation as a case study. *Environmental Research Letters* **10**: 044016.

Wieder WR, Cleveland CC, Smith WK, Todd-Brown K. 2015b. Future productivity and carbon storage limited by terrestrial nutrient availability. *Nature Geoscience* **8**: 441–444.

Wieder WR, Grandy AS, Kallenbach CM, Taylor PG, Bonan GB. 2015c. Representing life in the Earth system with soil microbial functional traits in the MIMICS model. *Geoscientific Model Development* **8**: 1789–1808.

Wieder WR, Grandy AS, Kallenbach CM, Bonan GB. 2014. Integrating microbial physiology and physio-chemical principles in soils with the MIcrobial-MIneral Carbon Stabilization (MIMICS) model. *Biogeosciences* **11**: 3899–3917.

Wieder WR, Bonan GB, Allison SD. 2013. Global soil carbon projections are improved by modelling microbial processes. *Nature Climate Change* **3**:909–912.

Wurzburger N, Brookshire ENJ. 2017. Experimental evidence that mycorrhizal nitrogen strategies affect soil carbon. *Ecology* **38**: 42–49.

Xia M, Talhelm AF, Pregitzer KS. 2017. Long-term simulated atmospheric nitrogen deposition alters leaf and fine root decomposition. *Ecosystems* **21**: 1–14.

Zak DR, Holmes WE, Burton AJ, Pregitzer KS, Talhelm AF. 2008. Simulated atmospheric NO^{3-} deposition increases organic matter by slowing decomposition. *Ecological Applications* **18**: 2016–2027.

Chapter 5. Conclusion: Advancing our understanding of integrated plant-soil responses to global change

My heart is moved by all I cannot save:
so much has been destroyed

I have to cast my lot with those
who age after age, perversely,

with no extraordinary power,
reconstitute the world

- **Adrienne Rich**

Summary of results

This dissertation explored how long-term experimental N additions impacted the storage and cycling of C in a temperate forest ecosystem, and how this long-term experiment can inform and refine soil biogeochemical models. To do this, I used three different approaches: I synthesized a diverse set of observational data from the study site, I created a targeted short-term experiment of litter decomposition and soil density fractionation, and I performed a model-data comparison.

Overall, I found evidence that many of the changes in C cycling and storage that occurred with N additions were driven by a shift in the tree's N acquisition strategies. Results from my dissertation supported the ecological theory that plants allocate less C belowground for nutrient acquisition under conditions of high nutrient availability (Vicca *et al.*, 2012; Bloom *et al.*, 2013). Consequently, plant-soil interactions weakened, contributing to changes in microbial activity and increasing the importance of particulate organic matter (POM) in total soil C stocks. Such weakened connections in the tightly coupled C and N cycles and plant-soil continuum proved challenging to represent in heuristic computational models, as many biogeochemical models rely on consistent connections between above- and below-ground processes, as well as C and N cycles.

The findings of this dissertation highlighted the importance and value of long-term and broad spatial scale experiments, as some of the changes in soil biogeochemistry we detected may take decades to emerge (e.g., soil C accrual). Additionally, I discovered how environmental changes, such as elevated N deposition, can alter some key relationships and connections of plant-soil interaction and C-N cycling that require treating our understanding of the past and predictions of the future differently. Thus, this knowledge highlights the need to integrate

observational, experimental, and theoretical knowledge to improve our predictions and reduce uncertainties in the land C sink. More specifically, the methods I implemented for my dissertation allowed me to answer three broad questions:

(1) How do potential changes in nutrient acquisition strategies due to chronic N additions impact the forest C sink?

(2) What effects does over 25 years of N additions have on the decomposition and fate of soil organic matter?

(3) To what extent does soil biogeochemical model structure (first-order decay dynamics vs. microbially explicit) impact model performance in response to N additions?

Chapter 2. How do potential changes in nutrient acquisition strategies due to chronic N additions impact the forest C sink?

In *Chapter 2,* I synthesized a broad range of observational data that was collected at various spatial and temporal scales throughout the duration of the 30-year, whole-watershed fertilization experiment. Key takeaways from this synthesis included how N additions resulted in greater woody biomass production, less total belowground C flux, lower rates of soil respiration, greater mineral soil C:N ratios, and an apparent accumulation of C in the surface mineral soil. Considered together, these key findings suggest that plants shifted their C allocation away from belowground C flux, allowing for greater wood production. Under N limitation, plants allocate a significant proportion of total fixed C belowground for the acquisition of nutrients (Bloom *et al.*, 1985; Kivlin *et al.*, 2013; Bae *et al.*, 2015). And with

augmented N availability, this C can instead be used towards the next limiting resource (e.g., to produce more woody biomass to access light; Reich, 2014).

Additionally, reduced belowground C flux had many cascading effects on soil biogeochemistry. Observations of reduced soil respiration, greater C:N ratios and greater C stocks in the surface mineral soil suggest that rates of organic matter decay decreased with N additions. This is supported by previous observations of slower leaf litter decay (Adams & Angradi, 1996), and reduced oxidative enzyme activity in the fertilized watershed (Carrara *et al.*, 2018, 2022), as well as similar observations at other forest N addition experiments (Treseder, 2004; Pregitzer *et al.*, 2008; Zak *et al.*, 2008; Frey *et al.*, 2014). It is easy for increases in soil C to go undetected, as it is such a large pool and changes very slowly. The long-term nature and broad spatial scale of this experiment allowed for the detection of C accrual in the soil, which can have important implications for the evaluation and prediction of the land C sink. Nonetheless, questions remained about the nature of this soil C, which seemed to be shifting giving the greater C:N ratio, and whether it would persist into the future as the climate warms, atmospheric CO_2 increases, and N deposition declines. This led me to ask the question:

Chapter 3. What effects does over 25 years of N additions have on the decomposition and fate of soil organic matter?

In *Chapter 3*, I designed and performed a targeted, short-term experiment to test the impacts of chronic N additions on the pathway of plant litter inputs to becoming soil organic matter (SOM). To do so, I used a reciprocal-transplant litter decomposition design to isolate the effects of litter quality versus the soil matrix on the rates of leaf litter decay, and I fractionated SOM by density to evaluate the distribution of organic matter along a microbial decomposition gradient. Results of this experiment supported the hypothesis that microbial activity was directly

inhibited by N additions, as soil matrix effects on reduced litter decay overwhelmed any changes in the leaf litter chemistry with N additions. Furthermore, we detected an accumulation of POM in the soils of the fertilized watershed, and the proportion of total SOC in the POM fraction was strongly correlated with the bulk soil C:N ratio.

This shift in the nature of SOM appears to favor the "physical transfer" pathway of SOM formation under chronic N additions (Cotrufo *et al.*, 2015; Mikutta *et al.*, 2019), as opposed to SOM formation via microbial processing (Kallenbach *et al.*, 2016). Also, this pattern challenges the assumption that microbial processing of organic matter followed by mineral-association is the most important pathway for SOM formation (Schmidt *et al.*, 2011; Cotrufo *et al.*, 2013), while supporting more recent arguments of the importance of plant-like SOM persistence (Angst *et al.*, 2019; Mikutta *et al.*, 2019). A change in the distribution and composition of SOM after 25+ years of N additions can have important implications for the future of soil C stocks and the land C sink.

The results from this experiment and other studies at this site suggest that the observed increases in the C:N ratio and relative abundance of POM is in fact due to some combination of the direct inhibition of enzyme activity with N additions and reduced microbial priming as plants allocate less C belowground (Ramirez *et al.*, 2012; Averill & Waring, 2017; Chen *et al.*, 2018). As forests recover from chronic N deposition and experience a warmer, CO_2-rich world, they will likely shift their nutrient acquisition strategies again, perhaps promoting the decomposition of this accumulated POM through microbial priming (Groffman, *et al.*, 2018; Finzi *et al.*, 2015; Craine *et al.*, 2018). Furthermore, there is limited evidence that enzyme activity under some tree species (but not all) recovered quickly when experimental N additions ceased (Carrara *et al.*, 2022). Yet, our current modeled predictions of the land C sink under future conditions does not account for the impacts that N deposition and recovery have on soil C stocks. Because soil

microbial responses to future changes will determine whether forests are a C sink or source in the future (Bond-Lamberty *et al.*, 2018), I sought to evaluate whether soil biogeochemical models can capture the observed changes in the coupled soil C-N cycles. Specifically, I asked:

Chapter 4. To what extent does soil biogeochemical model structure (first-order decay dynamics vs. microbially explicit) impact model performance in response to N additions?

In *Chapter 4*, I used a soil biogeochemical model ensemble that consisted of a first-order decay soil model and a microbially explicit soil model to assess how model structure influences the representation of how the forest C and N cycle responsds to N perturbation. I compared model output to the extensive observational and experimental data from the Fernow whole-watershed fertilization study (results from Chapters 2 and 3). Through this modeling exercise, I was able to identify the strengths and limitations of how models represent coupled soil C and N cycles, and I evaluated the benefits and uncertainties that come with incorporating microbial physiology into soil biogeochemical models.

The results from this study highlighted the strong linear relationship between vegetation productivity and soil heterotrophic respiration rates (and SOM decomposition). However, with N additions, this relationship is broken—N additions lead to enhanced vegetation productivity and reduced rates of soil respiration (Hyvönen *et al.*, 2008; Pregitzer *et al.*, 2008; Janssens *et al.*, 2010; Frey *et al.*, 2014). Thus, we made modifications to the allocation of C by vegetation under conditions of N addition that reduced belowground C allocation and increased woody biomass production. These changes weakened the relationship between vegetation productivity and heterotrophic respiration, but it was still challenging to capture both of the observed (and disparate) responses of NPP and heterotrophic respiration. The microbially explicit model

presented some potential advantages over the first-order model, such as the ability to target key decomposition kinetic parameters that reflect the inhibition of oxidative enzyme activity with N additions. Nonetheless, there is a clear gap in our knowledge of the functional relationships between environmental changes and fine-scale levers of SOM formation and destabilization.

Future directions and science policy

In this dissertation, I used a long-term, whole-watershed experiment to test important emerging theories and ideas about soil C cycling. The broad range of methods used and experiences gained in this process has led to the development of a diverse toolbox including synthesizing research, applying forest ecological data to model predictions, and considering how the results from these studies fit into the greater context of our scientific understanding of forest C cycling. I plan to use these skills to shift to a career in science policy. I hope to apply the foundational knowledge and research skillsets I have gained, while incorporating my social science and environmental justice interests, to analyze and propose equitable climate change solutions.

Much of the motivation behind my research and interest in forest C cycling at the Fernow originated from my curiosity of how forests will mediate some of the negative impacts of climate change. Little did I know, today, emerging C credit markets are sweeping across the world's forests, promoting sustainable forest management to maximize C sequestration and offset some of our anthropogenic, CO_2-equivalent greenhouse gas emissions (Griscom *et al.*, 2017). However, many of these forest C crediting markets and programs do not consider how soil C accrues, and how management strategies impact the sequestration of soil C. There is some evidence that tree biomass harvesting can lead to large losses in soil C, sometimes offsetting the accumulation of new wood growth for decades following harvests (Hamburg *et al.*, 2019).

Furthermore, detecting a small change in this large, heterogeneous soil C pool over short time scales (years to decades) can prove challenging to infeasible, necessitating the development of new methods and modelling efforts for evaluating soil C accrual (Bautista *et al.*, 2021). It is critical to address these key gaps and uncertainties to assure that climate solutions being enacted are truly effective. We, as a scientific community, have the methods and data available to answer some of the questions about forest C sequestration, as well as address the shortcomings of C crediting protocols. Thus, I intend to contribute to this effort by offering the scientific expertise behind forest (especially soil) C sequestration and working alongside economists and social scientists to evaluate the options that provide the best ecological, economic, and social benefits to our society.

Literature cited

Adams MB, Angradi TR. 1996. Decomposition and nutrient dynamics of hardwood leaf litter in the Fernow Whole-Watershed Acidification Experiment. *Forest Ecology and Management* **83**: 61–69.

Angst G, Mueller KE, Eissenstat DM, Trumbore S, Freeman KH, Hobbie SE, Chorover J, Oleksyn J, Reich PB, Mueller CW. 2019. Soil organic carbon stability in forests: Distinct effects of tree species identity and traits. *Global Change Biology* **25**: 1529–1546.

Averill C, Waring B. 2017. Nitrogen limitation of decomposition and decay: how can it occur? *Global Change Biology* 13980: 1–11.

Bae K, Fahey TJ, Yanai RD, Fisk M. 2015. Soil nitrogen availability affects belowground carbon allocation and soil respiration in northern hardwood forests of New Hampshire. *Ecosystems* **18**: 1179–1191.

Bautista N, Marino BDV, William Munger J. 2021. Science to commerce: a commercial-scale protocol for carbon trading applied to a 28-year record of forest carbon monitoring at the harvard forest. *Land* **10:** 1–22.

Bloom AJ, Chapin FS, Mooney HA. 1985. Resource limitation in plants-An economic analogy. *Annual Review of Ecology and Systematics* **16**: 363–392.

Bloom AJ, Chapin FS, Mooney HA. 2013. Plants-an Economic Analogy. Annual Review of *Ecology and Systematics* **16**: 363–392.

Bond-Lamberty B, Bailey VL, Chen M, Gough CM, Vargas R. 2018. Globally rising soil heterotrophic respiration over recent decades. *Nature* **560**: 80–83.

Carrara JE, Fernandez IJ, Brzostek ER. 2022. Mycorrhizal type determines root–microbial responses to nitrogen fertilization and recovery. *Biogeochemistry* **157**: 245–258.

Carrara JE, Walter CA, Hawkins JS, Peterjohn WT, Averill C, Brzostek ER. 2018. Interactions among plants, bacteria, and fungi reduce extracellular enzyme activities under long-term N fertilization. *Global Change Biology* **24**: 2721–2734.

Chen J, Luo Y, Van Groenigen KJ, Hungate BA, Cao J, Zhou X, Wang R wu. 2018. A keystone microbial enzyme for nitrogen control of soil carbon storage. *Science Advances* **4**: 2–8.

Cotrufo MF, Soong JL, Horton AJ, Campbell EE, Haddix ML, Wall DH, Parton WJ. 2015. Formation of soil organic matter via biochemical and physical pathways of litter mass loss. *Nature Geoscience* **8**: 776–779.

Cotrufo MF, Wallenstein MD, Boot CM, Denef K, Paul E. 2013. The Microbial Efficiency-Matrix Stabilization (MEMS) framework integrates plant litter decomposition with soil organic matter stabilization: Do labile plant inputs form stable soil organic matter? *Global Change Biology* **19:** 988–995.

Craine JM, Elmore AJ, Wang L, Aranibar J, Bauters M, Boeckx P, Crowley BE, Dawes MA, Delzon S, Fajardo A, *et al.* 2018. Isotopic evidence for oligotrophication of terrestrial ecosystems. *Nature Ecology and Evolution* **2**: 1735–1744.

Finzi AC, Abramoff RZ, Spiller KS, Brzostek ER, Darby BA, Kramer MA, Phillips RP. 2015. Rhizosphere processes are quantitatively important components of terrestrial carbon and nutrient cycles. *Global Change Biology* **21**: 2082–2094.

Frey SD, Ollinger S, Nadelhoffer K, Bowden R, Brzostek E, Burton A, Caldwell BA, Crow S, Goodale CL, Grandy AS, *et al*. 2014. Chronic nitrogen additions suppress decomposition and sequester soil carbon in temperate forests. *Biogeochemistry* **121**: 305–316.

Griscom BW, Adams J, Ellis PW, Houghton RA, Lomax G, Miteva DA, Schlesinger WH, Shoch D, Siikamäki J V., Smith P, *et al*. 2017. Natural climate solutions. *Proceedings of the National Academy of Sciences of the United States of America* **114**: 11645–11650.

Groffman PM, Driscoll CT, Durán J, Campbell JL, Christenson LM, Fahey TJ, Fisk MC, Fuss C, Likens GE, Lovett G, *et al.* 2018. Nitrogen oligotrophication in northern hardwood forests. *Biogeochemistry* **141:** 523–539.

Hamburg SP, Vadeboncoeur MA, Johnson CE, Sanderman J. 2019. Losses of mineral soil carbon largely offset biomass accumulation 15 years after whole-tree harvest in a northern hardwood forest. *Biogeochemistry* **144**: 1–14.

Hyvönen R, Persson T, Andersson S, Olsson B, Ågren GI, Linder S. 2008. Impact of long-term nitrogen addition on carbon stocks in trees and soils in northern Europe. *Biogeochemistry* **89**: 121–137.

Janssens IA a., Dieleman W, Luyssaert S, Subke J, Reichstein M, Ceulemans R, Ciais P, Dolman AJ, Grace J, Matteucci G, *et al.* 2010. Reduction of forest soil respiration in response to nitrogen deposition. *Nature Geoscience* **3**: 315–322.

Kallenbach CM, Frey SD, Grandy AS. 2016. Direct evidence for microbial-derived soil organic matter formation and its ecophysiological controls. *Nature Communications* **7:** 1–10.

Kivlin SN, Emery SM, Rudgers JA. 2013. Fungal symbionts alter plant responses to global change. *American Journal of Botany* **100**: 1445–1457.

Mikutta R, Turner S, Schippers A, Gentsch N, Meyer-Stüve S, Condron LM, Peltzer DA, Richardson SJ, Eger A, Hempel G, *et al.* 2019. Microbial and abiotic controls on mineral-associated organic matter in soil profiles along an ecosystem gradient. *Scientific Reports* **9**: 1–9.

Pregitzer KS, Burton AJ, Zak DR, Talhelm AF. 2008. Simulated chronic nitrogen deposition increases carbon storage in Northern Temperate forests. *Global Change Biology* **14:** 142–153.

Ramirez KS, Craine JM, Fierer N. 2012. Consistent effects of nitrogen amendments on soil microbial communities and processes across biomes. *Global Change Biology* **18**: 1918–1927.

Reich PB. 2014. The world-wide 'fast-slow' plant economics spectrum: A traits manifesto. *Journal of Ecology* **102**: 275–301.

Schmidt MWI, Torn MS, Abiven S, Dittmar T, Guggenberger G, Janssens I a., Kleber M, Kögel-Knabner I, Lehmann J, Manning D a. C, *et al.* 2011. Persistence of soil organic matter as an ecosystem property. *Nature* **478**: 49–56.

Treseder KK. 2004. A meta-analysis of mycorrhizal responses to nitrogen, phosphorus, and atmospheric CO_2 in field studies. *New Phytologist* **164**: 347–355.

Vicca S, Luyssaert S, Peñuelas J, Campioli M, Chapin FS, Ciais P, Heinemeyer A, Högberg P, Kutsch WL, Law BE, *et al.* 2012. Fertile forests produce biomass more efficiently. *Ecology Letters* **15**: 520–526.

Zak DR, Holmes WE, Burton AJ, Pregitzer KS, Talhelm AF. 2008. Simulated atmospheric NO_3^- deposition increases organic matter by slowing decomposition. *Ecological Applications* **18**: 2016–2027.

Appendix A. Supplementary Tables

Table S2-1. Mean (+/- se) tree wood carbon and nitrogen concentrations in the outer 1 cm of bolewood, and sample sizes (*n*) for the reference WS7 and fertilized WS3. Results from 2-way ANOVA with Watershed and Species as main effects: bold values differed between watersheds ($p<0.05$) and superscripts of different letters were different among species ($p<0.05$; Tukey HSD test).

Watershed	Species	%C	%N	*n*
Reference WS7				
	Acer rubrum	**46.51 (0.08)**	0.145 (0.008)^{ab}	10
	Betula lenta	**46.21 (0.07)**	0.125 (0.013)^{a}	10
	Liriodendron tulipifera	**46.17 (0.08)**	0.189 (0.018)^{b}	8†
	Prunus serotina	**45.97 (0.08)**	0.110 (0.005)^{a}	10
Fertilized WS3				
	Acer rubrum	**47.53 (0.19)**	0.129 (0.007)^{ab}	10
	Betula lenta	**47.39 (0.26)**	0.107 (0.011)^{a}	10
	Liriodendron tulipifera	**47.05 (0.15)**	0.160 (0.014)^{b}	10
	Prunus serotina	**47.45 (0.10)**	0.098 (0.004)^{a}	10

†Two outliers removed for unusually high values.

Table S2-2. Mean (+/- se) leaf litter carbon and nitrogen concentrations, C:N ratios, mass (g m-2) and sample size (*n*) for the reference WS7 and fertilized WS3.

Watershed	Species	Year	%C	%N	C:N ratio	litter mass (g m-2)	*n*†
Reference WS7	*Acer rubrum*	2015	47.2 (0.2)	1.09 (0.09)	46.7 (4.3)	44 (18)	10
		2016	48.4 (0.3)	0.89 (0.05)	56.2 (3.2)	41 (16)	10
		2017	47.8 (0.1)	0.99 (0.07)	50.6 (3.6)	48 (17)	10
	Betula lenta	2015	49.5 (0.6)	1.41 (0.03)	35.2 (0.9)	87 (12)	10
		2016	51.2 (1.5)	1.3 (0.04)	40.7 (1.3)	69 (14)	10
		2017	50.3 (0.9)	1.34 (0.03)	37.8 (1.0)	114 (51)	10
	Liriodendron tulipifera	2015	47.5 (0.3)	1.38 (0.04)	34.8 (1.2)	60 (12)	10
		2016	49.5 (0.8)	1.02 (0.02)	48.9 (1.2)	87 (19)	10
		2017	48.5 (0.5)	1.20 (0.02)	40.7 (1.1)	93 (23)	10
	Prunus serotina	2015	50.7 (1.0)	1.13 (0.04)	45.2 (1.5)	42 (9)	10
		2016	49.0 (0.7)	1.31 (0.05)	37.9 (1.3)	37 (9)	10
		2017	49.9 (0.7)	1.22 (0.03)	41.1 (1.0)	37 (8)	10
	Quercus rubra	2015	48.8 (0.6)	0.82 (0.03)	60.6 (2.7)	48 (20)	10
		2016	51.4 (2.4)	0.87 (0.05)	59.6 (3.1)	22 (9)	7
		2017	49.8 (1.0)	0.85 (0.02)	58.9 (1.3)	28 (12)	9
Fertilized WS3	*Acer rubrum*	2015	45.9 (1.8)	1.37 (0.07)	34.4 (2.3)	72 (13)	10
		2016	48.1 (0.2)	0.88 (0.04)	55.9 (2.6)	64 (16)	10
		2017	47.0 (0.8)	1.12 (0.05)	42.6 (2.1)	65 (14)	10
	Betula lenta	2015	48.5 (0.4)	1.82 (0.12)	27.6 (1.6)	31 (6)	10
		2016	49.9 (0.7)	1.38 (0.04)	36.3 (1.2)	31 (7)	10
		2017	49.2 (0.4)	1.60 (0.07)	31.2 (1.4)	45 (12)	10
	Liriodendron tulipifera	2015	47.2 (0.4)	1.77 (0.26)	29.3 (3.2)	6 (4)	7
		2016	49.2 (0.4)	1.38 (0.09)	36.7 (2.1)	9 (4)	9
		2017	48.2 (0.1)	1.53 (0.10)	32.6 (1.8)	21 (14)	10
	Prunus serotina	2015	49.8 (0.3)	1.42 (0.08)	36.1 (2.1)	105 (13)	10
		2016	51.7 (1.0)	1.68 (0.05)	31.0 (0.9)	68 (9)	10
		2017	50.7 (0.6)	1.55 (0.04)	33.0 (0.9)	135 (35)	10
	Quercus rubra	2015	48.6 (0.6)	1.18 (0.12)	44.4 (3.7)	41 (11)	10
		2016	49.4 (0.4)	1.11 (0.06)	45.2 (2.0)	39 (8)	10
		2017	49.0 (0.3)	1.15 (0.06)	43.5 (1.9)	35 (9)	10

†Sample size for litter chemistry based on plot-level litter collection baskets. If n<10, there were no leaves of that species collected from one or more litter baskets (plots) that year.

Table S2-3. Methods for fine root measurements at the Fernow Experimental Forest Watershed Fertilization Experiment.

Organic horizon				
Date	**Sampling scheme**	**Sample dimensions**		**Sample processing**
June 2012	2 subsamples from two locations in 7 plots	25 x 25 cm square divided in half by steel frame		Fine roots (<2mm diameter) were picked by hand and dried at 65'C for >48 hours.
June 2013	2 subsamples from two locations in 7 plots	25 x 25 cm square divided in half by steel frame		Fine roots (<2mm diameter) were picked by hand, dried at 65'C for >48 hours, and ground in mill to #20 mesh for %C and %N analysis
June, July & August 2015[a]	1 sample in 10 plots	10 x 10 cm		Fine roots (<2 mm diameter) were picked by hand, washed in deionized water, and dried
Mineral horizon				
Date	**Sampling scheme**	**Core diameter (cm)**	**Depth (cm)**	**Sample processing**
May & September 1991[b]	1 soil core in 17 plots	5.08	45.72	Fine roots were picked by hand and washed with water. Live roots were separated into fine (<2mm diameter) and coarse (>2mm diameter). Roots were oven dried at 70'C for 24 hours
June 2013	2 subsamples in 7 plots where O-horizon was sampled	4	15	Fine roots (<2mm diameter) were picked by hand, dried at 65'C for >48 hours, and ground in mill to #20 mesh for %C and %N analysis
June, July & August 2015[a]	3 subsamples in 10 plots where O horizons sampled	5	15	Fine roots (<2mm diameter) were picked by hand, washed in deionized water, and dried
June 2016	6 subsamples in 10 plots	4.5	10	Fine roots (<2mm diameter) were picked by hand, washed with deionized water, dried at 65'C for >48 hours, and ground to #20 mesh for %C and %N analysis

[a]From Carrara et al., 2018

[b]From Adams, 2016

Table S2-4. Mean (+/- se) pre-senescence foliar carbon and nitrogen concentrations and C:N ratios and sample size (*n*) for the reference WS7 and fertilized WS3.

Watershed	Species	%C	%N	C:N ratio	*n*
Reference WS7					
	Acer rubrum	49.7 (0.47)	2.19 (0.03)	22.8 (0.35)	30
	Betula lenta	49.7 (0.41)	2.93 (0.05)	17.1 (0.27)	30
	Liriodendron tulipifera	49.0 (0.47)	3.25 (0.08)	15.3 (0.36)	30
	Prunus serotina	49.4 (0.32)	2.93 (0.06)	17.1 (0.38)	30
	Quercus rubra[†]	49.8 (0.40)	2.87 (0.12)	17.6 (0.66)	8
Fertilized WS3					
	Acer rubrum	48.6 (0.16)	2.24 (0.04)	21.8 (0.36)	30
	Betula lenta	49.0 (0.15)	2.93 (0.05)	16.8 (0.28)	30
	Liriodendron tulipifera	47.9 (0.21)	3.46 (0.09)	14.1 (0.43)	30
	Prunus serotina	49.4 (0.13)	3.04 (0.08)	16.6 (0.51)	30
	Quercus rubra[†]	48.1 (0.72)	2.40 (0.10)	20.3 (0.97)	11

[†]All leaves sampled in July 2012 except *Quercus rubra* leaves were sampled in July 2016

Table S3-1. Two-way ANOVA table for chemical composition of initial, freshly-fallen leaf litter from four dominant tree species and two source watersheds. 7 and 3 refer to source watersheds of reference watershed 7 and +N watershed 3, respectively. Bold terms were significant effects at α=0.05. Species codes: ACRU red maple, BELE sweet birch, LITU tulip poplar, and PRSE black cherry.

Property	Effect	DF	SS	MS	F	$p < 0.05$
% N	**Source Watershed (S_WS)**	**1**	**0.0295**	**0.0295**	**4.199**	**0.0471**
	Species (Spp)	**3**	**1.881**	**0.6294**	**89.57**	**<0.0001**
	S_WS * Spp	**3**	**0.2579**	**0.0860**	**12.23**	**<0.0001**
	Error	40	0.2811	0.0070		
% C	Source Watershed	1	0.0770	0.0770	0.1460	0.7047
	Species	**3**	**18.08**	**6.026**	**11.42**	**<0.0001**
	S_WS * Spp	**3**	**12.44**	**4.147**	**7.866**	**0.0003**
	Error	40	21.09	0.5270		
C:N ratio	**Source Watershed**	**1**	**224**	**224**	**14.48**	**0.0005**
	Species	**3**	**4665**	**1555**	**100.7**	**<0.0001**
	S_WS * Spp	**3**	**732**	**243.9**	**15.80**	**<0.0001**
	Error	40	618	15.40		
% Cellulose	Source Watershed	1	0.0006	0.0006	0.4970	0.4865
	Species	**3**	**0.0252**	**0.0084**	**7.097**	**0.0010**
	S_WS * Spp	3	0.0010	0.0003	0.2810	0.8388
	Error	30	0.0355	0.0012		
Property	Robust ANOVA Table	DF	RD	Mean RD	F	$p < 0.05$
% Lignin	Source Watershed	1	0.0811	0.0811	3.755	0.0621
	Species	**3**	**0.5752**	**0.1917**	**8.881**	**0.0002**
	S_WS * Spp	3	0.0920	0.0307	1.420	0.2563
LCI	Source Watershed	1	0.0404	0.0404	1.053	0.3130
	Species	**3**	**0.7025**	**0.2342**	**6.104**	**0.0023**
	S_WS * Spp	3	0.0859	0.0286	0.7463	0.5330
Lignin:N	**Source Watershed**	**1**	**71.62**	**71.62**	**35.22**	**<0.0001**
	Species	**3**	**278.2**	**92.72**	**45.60**	**<0.0001**
	S_WS * Spp	3	13.15	4.383	2.155	0.0942

Table S3-2. Three-way ANOVA table for chemical composition of final leaf litter, decomposed in the field for two years, from four dominant tree species, two source watersheds, and two watersheds of transplant. Bold terms were significant effects at α=0.05. Species codes: ACRU red maple, BELE sweet birch, LITU tulip poplar, and PRSE black cherry.

Property	Robust ANOVA Table	DF	RD	Mean RD	F	p < 0.05
% N	**Source Watershed (S_WS)**	**1**	**0.0325**	**0.0325**	**16.80**	**<0.0001**
	Watershed of transplant (WS_T)	**1**	**0.0405**	**0.0405**	**20.95**	**<0.0001**
	Species (Spp)	**3**	**0.2743**	**0.0914**	**47.27**	**<0.0001**
	S_WS * WS_T	1	0.0028	0.0028	1.466	0.2263
	S_WS * Spp	3	0.0016	0.0005	0.2812	0.8390
	WS_T * Spp	3	0.0005	0.0002	0.0813	0.9702
	S_WS * WS_T * Spp	3	0.0006	0.0002	0.1107	0.9539
C:N ratio	**S_WS**	**1**	**36.34**	**36.34**	**20.50**	**<0.0001**
	WS_T	**1**	**32.06**	**32.06**	**18.09**	**<0.0001**
	Spp	**3**	**174.1**	**58.04**	**32.74**	**<0.0001**
	S_WS * WS_T	1	4.099	4.099	2.312	0.1288
	S_WS * Spp	3	0.2012	0.0671	0.0378	0.9902
	WS_T * Spp	3	2.946	0.9820	0.5539	0.6456
	S_WS * WS_T * Spp	3	1.133	0.3777	0.2130	0.8874

Property	Effect	DF	SS	MS	F	*p* < 0.05
% Cellulose	**S_WS**	**1**	**0.0037**	**0.0037**	**6.882**	**0.0132**
	WS_T	**1**	**0.0025**	**0.0025**	**4.744**	**0.0369**
	Spp	**3**	**0.0117**	**0.0039**	**7.265**	**0.0008**
	S_WS * WS_T	1	0.0002	0.0002	0.3920	0.5356
	S_WS * Spp	3	0.0029	0.0010	1.790	0.1688
	WS_T * Spp	3	0.0008	0.0003	0.5160	0.6744
	S_WS * WS_T * Spp	3	0.0033	0.0011	2.040	0.1279
	Error	32	0.0172	0.0005		
% Lignin	S_WS	1	0.0008	0.0008	0.3900	0.5368
	WS_T	**1**	**0.0133**	**0.0133**	**6.559**	**0.0154**
	Spp	**3**	**0.0922**	**0.0307**	**15.15**	**<0.0001**
	S_WS * WS_T	1	0.0000	0.0000	0.0030	0.9533
	S_WS * Spp	3	0.0002	0.0001	0.0320	0.9922
	WS_T * Spp	3	0.0048	0.0016	0.7900	0.5086
	S_WS * WS_T * Spp	3	0.0026	0.0008	0.4190	0.7406
	Error	32	0.0649	0.0020		
LCI	**S_WS**	**1**	**0.0085**	**0.0085**	**9.131**	**0.0049**
	WS_T	1	0.0000	0.0000	0.0450	0.8330
	Spp	**3**	**0.0318**	**0.0106**	**11.42**	**<0.0001**
	S_WS * WS_T	1	0.0004	0.0004	0.4360	0.5138
	S_WS * Spp	3	0.0039	0.0013	1.408	0.2584
	WS_T * Spp	3	0.0005	0.0002	0.1660	0.9182
	S_WS * WS_T * Spp	3	0.0029	0.0010	1.042	0.3871
	Error	32	0.0297	0.0009		
Lignin:N	S_WS	1	0.6800	0.6800	0.1470	0.7043
	WS_T	1	1.490	1.490	0.3210	0.5748
	Spp	**3**	**124.7**	**41.55**	**8.945**	**0.0002**
	S_WS * WS_T	1	0.2200	0.2200	0.0460	0.8308
	S_WS * Spp	3	2.270	0.7600	0.1630	0.9208
	WS_T * Spp	3	19.60	6.530	1.407	0.2588
	S_WS * WS_T * Spp	3	5.820	1.940	0.4180	0.7414
	Error	32	148.7	4.650		

Table S3-3. Mean(se) chemical composition and decay rates (*k*) of final leaf litter (decomposed for two years in field) summarized by leaf litter source watershed. Bold values indicate difference between source watershed means (at α=0.05).

Source watershed	% N *n = 396*	C:N ratio *n = 396*	% cellulose *n=24*	% lignin *n=24*	lignocellulose index *n=24*	lignin:N ratio *n=24*	*k* (year^{-1}) *n=76-77*
Ref WS7	**2.20(0.1)**	**23.1(0.01)**	**17.1(0.14)**	34.3(0.24)	**0.67(0.001)**	13.4(0.10)	0.57(0.02)
+N WS3	**2.30(0.1)**	**21.8(0.02)**	**15.3(0.10)**	35.1(0.28)	**0.69(0.001)**	13.7(0.11)	0.55(0.02)

Table S3-4. Three-way ANOVA results for source watershed, watershed of transplant, species, and their interactive effects on leaf litter decomposition rates (*k*). Bold terms were significant effects at α=0.05.

Effect	DF	SS	MS	F	P < 0.05
Source Watershed (S_WS)	1	0.027	0.027	1.17	0.281
Watershed of Transplant (WS_T)	**1**	**0.199**	**0.199**	**8.60**	**0.004**
Species (Spp)	**3**	**2.12**	**0.707**	**30.6**	**<0.001**
S_WS * WS_T	1	0.001	0.001	0.051	0.822
S_WS * Spp	3	0.031	0.010	0.442	0.724
WS_T * Spp	3	0.122	0.041	1.75	0.159
S_WS * WS_T * Spp	3	0.013	0.004	0.189	0.904
Error	137	3.17	0.023		

Appendix B. Supplementary Figures

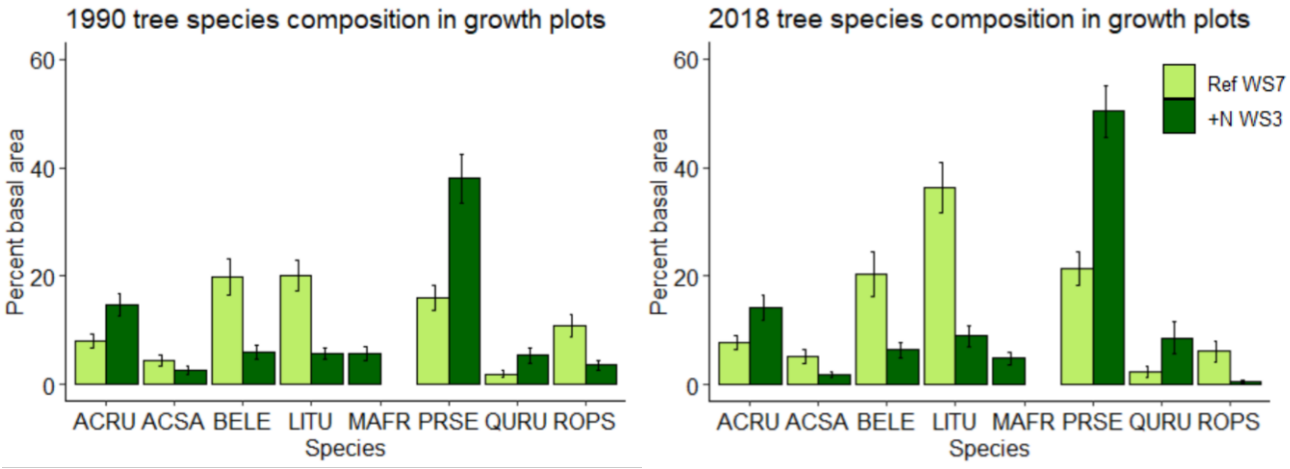

Figure S2-1 Mean percent basal area of eight dominant species in the reference watershed (light green) and the fertilized watershed (dark green) at the beginning of the experiment (1990-1991) and end of the experiment (2018). Data are from 25 permanent growth plots that were censused in 1990-1991 and 2018 (see Fig 1 and methods). Error bars represent +/- 1 se. Species codes: ACRU *Acer rubra*, ACSA *Acer saccharum*, BELE *Betula lenta*, LITU *Liriodendron tulipifera*, MAFR *Magnolia fraseri*, PRSE *Prunus serotina*, QURU *Quercus rubrum,* and ROPS *Robinia psuedoacacia* (symbiotic N fixer).

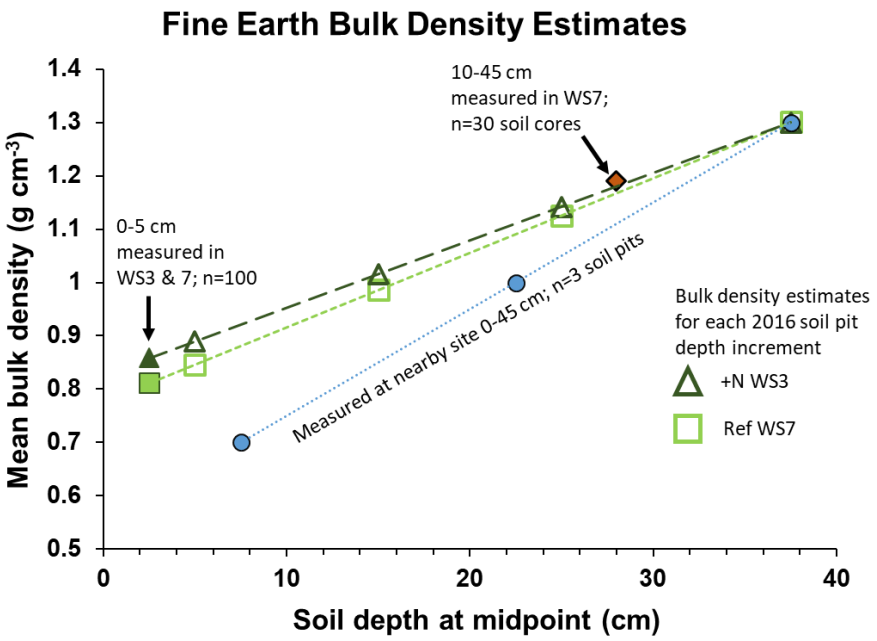

Figure S2-2 Mean measurements and estimates of fine earth soil bulk density. Measured (solid symbols) and estimated (open symbols) of fine earth bulk density in +N WS3 (dark green), Ref WS7 (light green), and a nearby site at the Fernow (blue). Estimates of fine earth bulk density were constructed using a linear relationship between mean measured bulk density and soil depth at 0-5 cm and 30-45 cm depths. The orange diamond is an additional mean measurement made in Ref WS7 using soil cores in 30 locations (Kelly, 2010) and shows that the linear regression matches this measurement and is likely a reasonable approach to estimate bulk density in the absence of robust measurements in both watersheds.

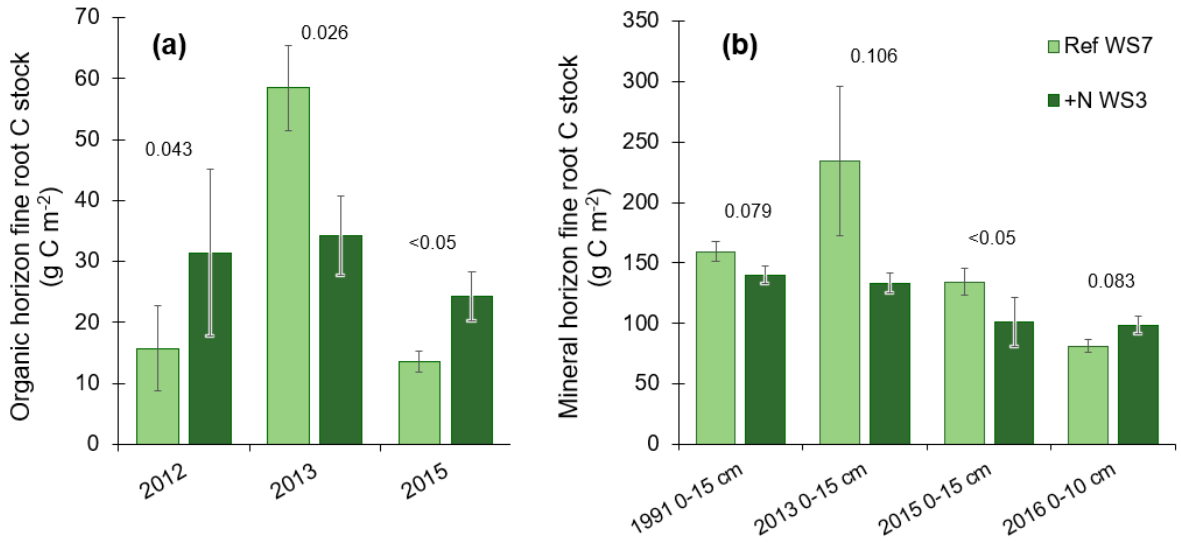

Figure S2-3 Mean fine root C stocks in the organic horizon (a) and surface mineral soil (b) were variable across 5 different years of measurement in the reference WS7 (light green) and +N WS3 (dark green). Error bars represent +/- one standard error. Labels above bars are p-values comparing watershed root stocks for each year and soil depth (t-one-way ANOVA). 1991 values are from Adams et al. (2006); 2015 values are adapted from Carrara et al. (2018).

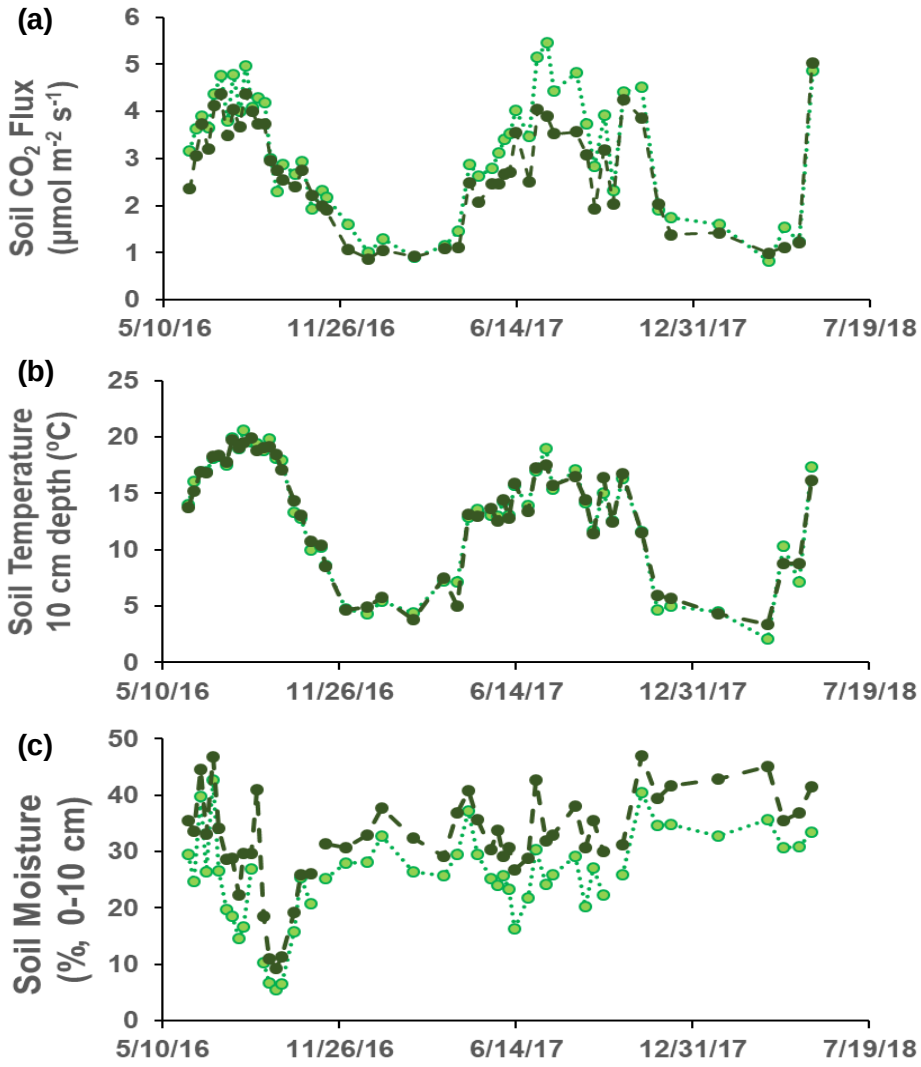

Figure S2-4 Time series of soil respiration, temperature, and moisture data from 2016-2017 at the Fernow Watershed Fertilization study. Mean (a) soil respiration rates, (b) soil temperature at 10 cm soil depth, and (c) soil percent moisture at 0-10 cm soil depth for Ref WS7 (light green, dotted lines) and +N WS3 (dark green, dashed lines) (n=40) over two years (x-axis date format: month/day/year).

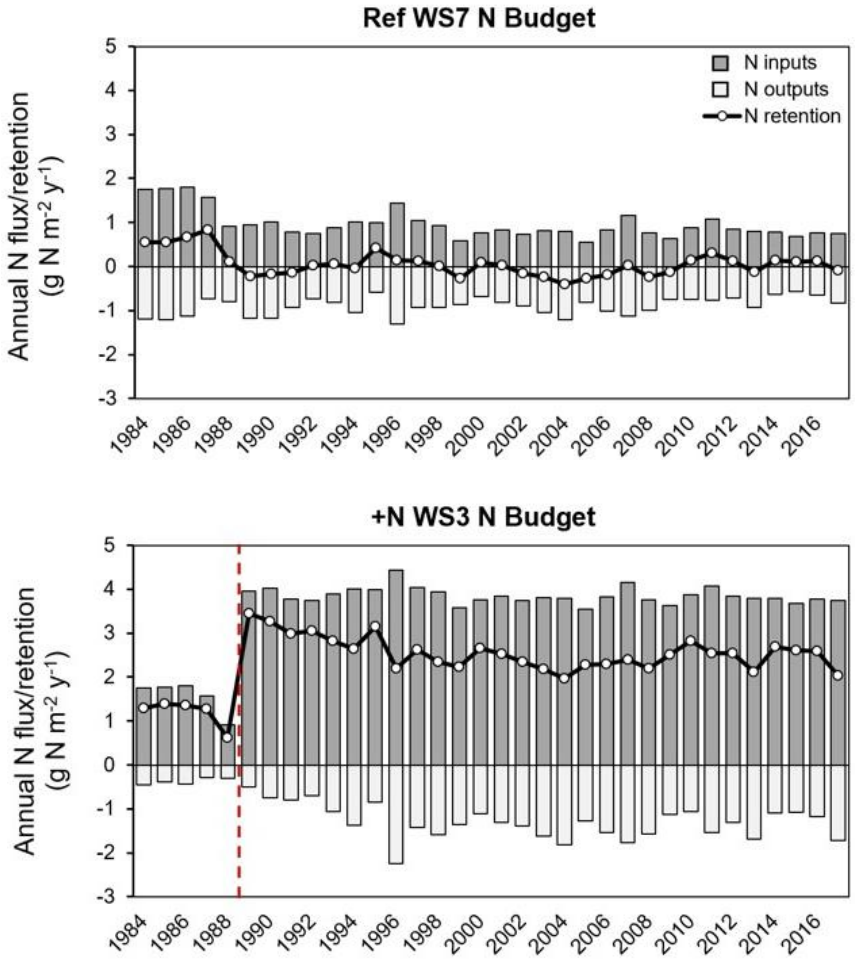

Figure S2-5 Hydrologic inorganic N budgets for reference watershed 7 (left) and fertilized watershed 3 (right) over 34 calendar years. N inputs (dark gray) include total ambient N deposition (CASTNET, NADP) and experimental N additions (for +N WS3). N outputs (light gray) include total NO3- -N and NH4+-N discharged in streamwater. The apparent N retention (black lines) is the difference between inputs and outputs. The red, dashed line indicates the start of experimental N additions to +N WS3. Watershed-scale N budgets reveal enhanced losses of inorganic N in streamwater, as well as significant levels of N retention (~3 g N m-2 y-1) in the fertilized watershed that have persisted for more than 25 years.

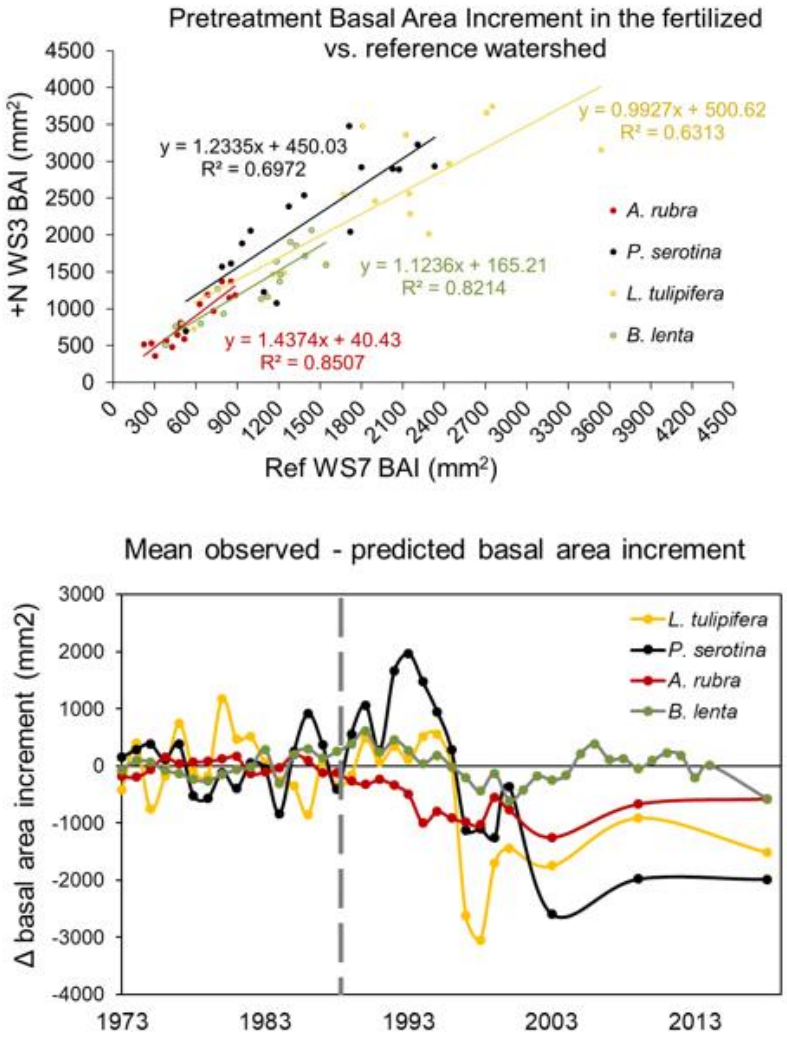

Figure S2-6 Top: Basal area increment (BAI; mm2) of four dominant species in +N WS3 vs. Ref WS7 during pretreatment years (1973-1988) suggest faster growth (regression slopes >1) in all species in +N WS3 except *Liriodendron tulipifera* prior to the start of fertilizer application. Bottom: Mean observed minus mean predicted BAI for four dominant species in +N WS3 show an enhancement in growth early in N addition experiment, followed by relative decrease in tree growth later in the experiment. Predicted BAI was estimated from pretreatment relationships of BAI between watersheds, as determined from increment cores (Top). Observed BAI was estimated from increment cores and permanent growth plot data. Method and pretreatment data through 2000 for *Acer rubra*, *Prunus serotina* and *L. tulipifera* were from DeWalle *et al.* (2006). Data past 2000 from permanent growth plot data. All increment core data for *Betula lenta* from M.B. Burnham & W.T. Peterjohn, unpublished.

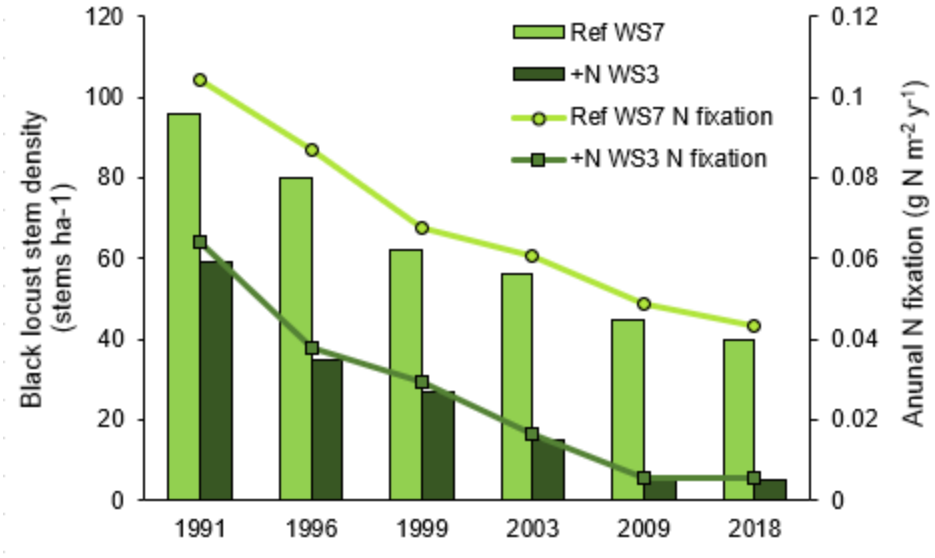

Figure S2-7 Mean black locust (*Robinia pseudoacia*) stem density and annual estimated N fixation flux from black locust in Ref WS7 (light green) and +N WS3 (dark green). Mean stem densities are reported as measured at each growth plot census (1991-2018, n=25). Annual N fixation rates were estimated from N fixation rates and stem densities reported by Boring and Swank (1984). N fixation rates were assumed to be proportional to black locust stem density.

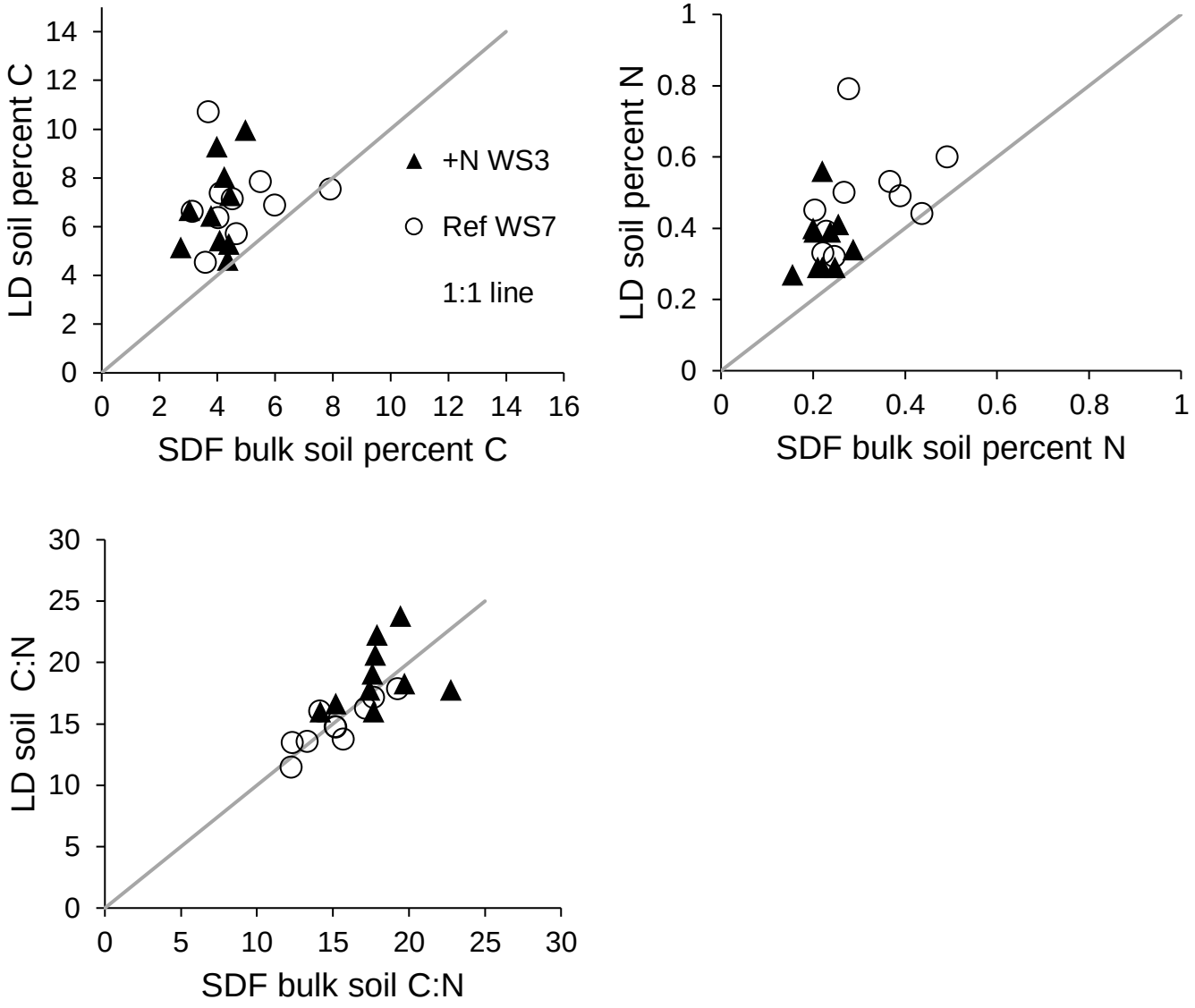

Figure S3-2. Comparison of %C (A), %N (B), and C:N (C) of mineral soil sampled for the soil density fractionation (SDF) analysis (0-15 cm; x-axis) and from the leaf litter decomposition (LD) plots (0-5 cm; y-axis) from the reference watershed (Ref WS7; open circles) and fertilized watershed (+N WS3; black triangles). Each point represents the mean soil property from one plot (n=3 replicates per plot from LD study; n=4 replicates per plot from SDF study). Solid gray lines indicate a 1:1 relationship.

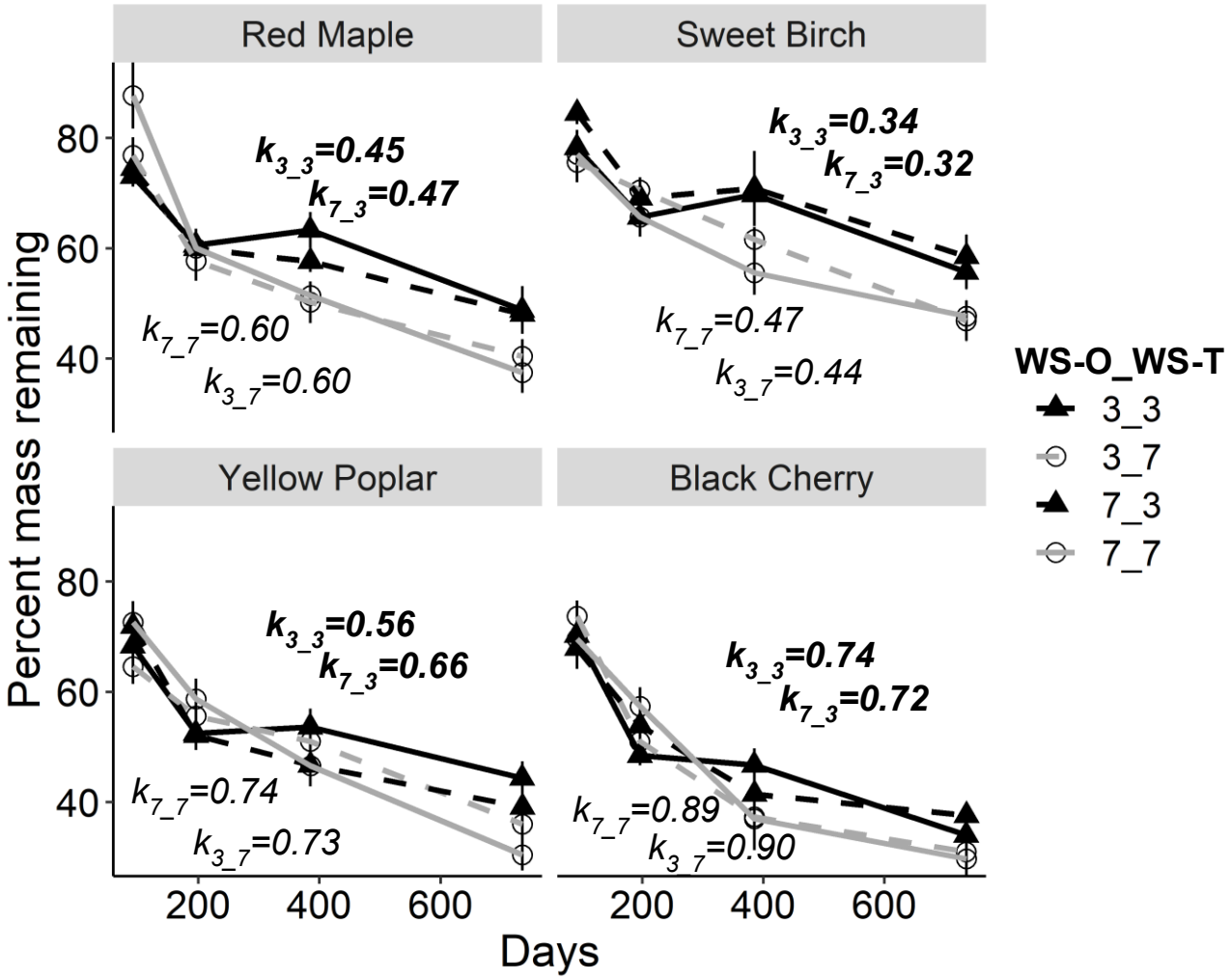

Figure S3-1. Percent of initial leaf litter mass remaining over two-year litter decomposition in the field for four dominant tree species. Mean +/- s.e. of percent mass remaining for litter transplanted into +N WS3 (black triangle) and Ref WS7 (open circles). Solid lines indicate litterbags transplanted into the watershed of origin; dotted lines indicate litterbags transplanted into the reciprocal watershed. Decay rates (*k*) displayed for each watershed and species combination. Differences in decomposition rates were detected between watershed of transplant, but not watershed of origin.

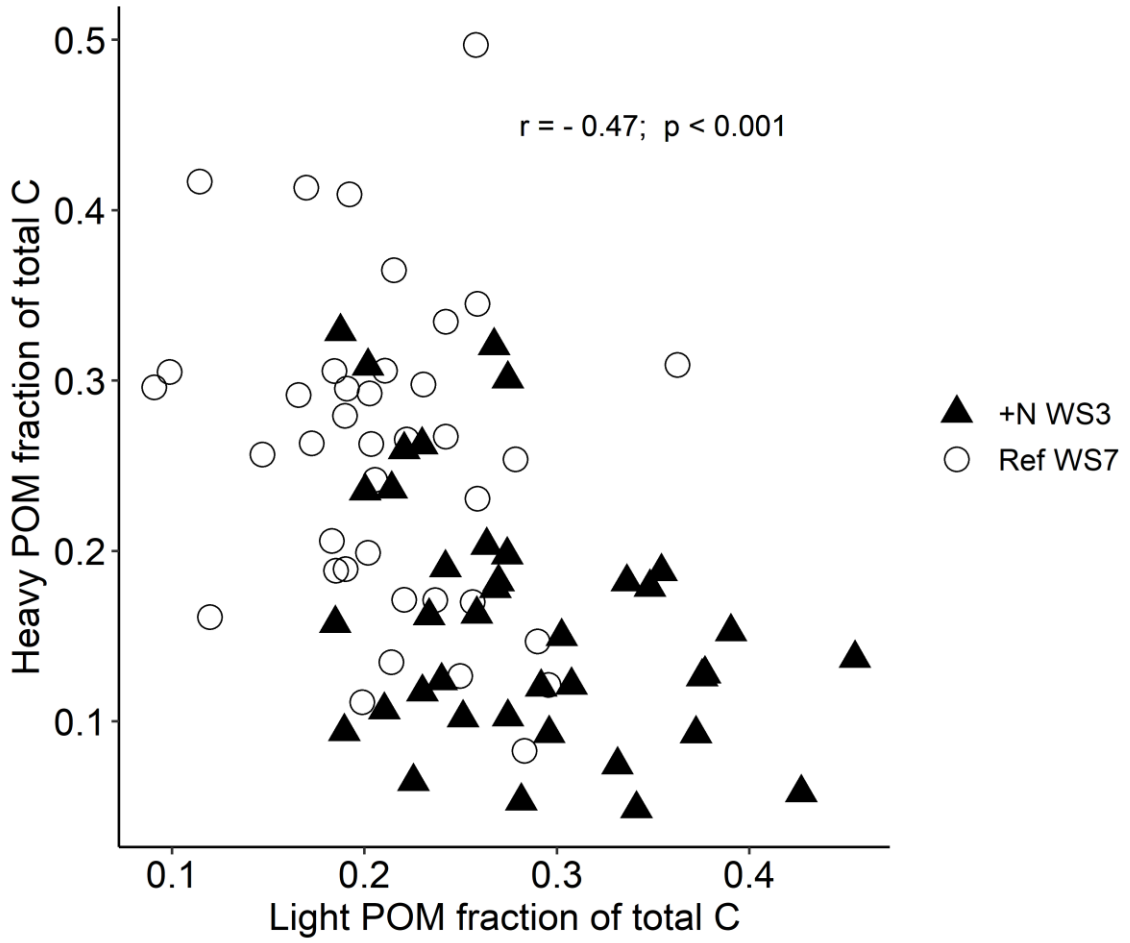

Figure S3-3. The fraction of total soil C in the heavy POM fraction is negatively correlated with the fraction of total soil C in the light POM fraction. Each point represents one plot per watershed (n=20) in the N-fertilized watershed (+N WS3; black triangles) and reference watershed (Ref WS7; open circles). Rho and p-values are the Pearson's correlation analysis results.

Appendix C. Supplementary Text

Supplementary Methods S2-1

Methods for propagating error when combining datasets across various years or plots.

Standard errors were propagated analytically following the methods of Lehrter & Cebrian (2010). such that when means are added or subtracted, $z = x + y$, errors ($\delta x, \delta y$) are summed in quadrature:

$$\delta z = \sqrt{\delta x^2 + \delta y^2} \quad \text{Eq.1}$$

and when means are multiplied or divided, $z = x * y$, fractional errors ($\delta x/x, \delta y/y$) are summed in quadrature:

$$\frac{\delta z}{z} = \sqrt{\left(\frac{\delta x}{x}\right)^2 + \left(\frac{\delta y}{y}\right)^2} \quad \text{Eq. 2}$$

Supplementary Methods S2-2

Leaf litterfall collection and chemical analysis for 2015-2017.

Leaf litter collections baskets were placed in the center of 10 plots in each of the reference (Ref WS7) and fertilized (+N WS3) watersheds (Fig. 2-1). Litter collection baskets were 0.56 m x 0.40 m (0.224 m2). Litter from baskets were collected in the autumns of 2015-2017 every one or two weeks from September through the first week in November. Leaves were air dried in 2015 for over 5 days, and oven-dried at 65°C in 2016 and 2017 for over 48 hours. In all three years, dried leaves were separated by species, weighed, and leaves of five species (*Acer rubrum, Betula lenta, Liriodendron tulipifera, Prunus serotina, and Quercus rubra*) were ground and analyzed for C and N concentrations with Dumas combustion using an elemental analyzer (NA 1500 Series 2, Carlo Erba Instruments). We estimated plot-level estimates of total C and N litterfall for each year using the species-level mass and C and N concentrations, and for those species from which C and N concentrations were not measured, we applied the mean plot C and N concentrations to this remaining (other species) mass. Summarized data are presented in **Table S2-2**. These C and N fluxes were applied to the long-term leaf litterfall mass data. Litter trap sizes and litter pickup schedule were similar between the long-term traps (Adams, 2008) and the 10 additional traps. The locations of the 10 additional traps were selected to correspond with the location of soil respiration and other soil measurements (see Fig. 2-1).

Supplementary Methods S2-3

Green foliage collection and chemical analysis.

Green canopy leaves were collected with a shotgun in July of 12 from ten plots in Ref WS7 and +N WS3. At each plot, three leaves were collected from one canopy tree from each of four species (*Acer rubrum, Betula lenta, Liriodendron tulipifera, and Prunus serotina*) at the high, mid, and low canopy. Leaf samples were kept on ice and stored in a cold room for transportation back to the lab and before analysis (~24 hours after collection). Leaves were dried at 65°C for 48 hours and ground through a # 20 mesh screen (0.841 m) prior to C and N analysis using an elemental analyzer (NA 1500 Series 2, Carlo Erba Instruments). Values from the three canopy leaves per tree were averaged and considered one observation. In the July of 2016, green foliage from an additional species (Quercus rubra) was collected with a shotgun from 8 canopy trees in Ref WS7 and 11 canopy trees in +N WS3. Leaves were dried at 60°C for 48 hours, ground through a #40 mesh screen (0.425 mm) before analysis for C and N using Dumas combustion elemental analyzer (NC 2500, Carlo Erba Instruments) at the University of Maryland Central Appalachian Stable Isotope Facility. Summarized data for all foliage are presented in **Table S2-3**.

Supplementary Methods S2-4

Soil respiration measurements and annual CO2 efflux estimates

Estimates of annual soil CO_2 efflux used soil respiration measurements that were made year-round from June 2016-May 2017 at four respiration collars in each of 10 plots per watershed (Fig. 2-1), for a total of 40 measurements per treatment on each measurement date. Respiration collars (10 cm diameter, 5 cm height PVC) were inserted 2.5 cm into the soil approximately one week before the first respiration measurement. Soil respiration (μmol CO_2 m^{-2} s^{-1}) was measured with an infrared gas analyzer (LI-8100A, LI-COR®, Inc., Lincoln, NE) weekly during the growing season, and biweekly to monthly during the non-growing season and snow-free period. In tandem with soil respiration measurements, soil temperature at 5- and 10-cm depths and soil moisture to a depth of 10 cm was measured. Additionally, buried soil temperature loggers at a depth of 5 cm in the center of each plot recorded soil temperature every hour over the course of the 2-year measurement period (HOBO Pendant® Temperature Data Logger, Onset Computer Corporation, Bourne, MA). These continuous soil temperature measurements were used to model annual respiration, using a first-order exponential relationship (ae^{bT}, T= soil temperature, and *a* and *b* are parameters optimized to each watershed using Guass-Newton optimization; van't Hoff 1898). All analyses were done in R (version 3.0.2) and SAS JMP (JMP® Pro ver. 12.2.0).

Supplementary Literature Cited

Adams MB. 2008. Long-term leaf fall mass from three watersheds on the Fernow Experimental Forest, West Virginia. 16th Central Hardwoods Forest Conference, USDA Forest Service **304**: 179–186.

Adams MB. 2016. Fernow Experimental Forest Watershed Acidification Root Data, 1991. Parsons, WV, USA: Department of Agriculture, Forest Service, North Central Research Station.

Adams MB, DeWalle DR, Hom JL (Eds.). 2006. The Fernow Watershed Acidification Study. Springer Netherlands, Dordrecht.

Boring LR, Swank WT. 1984. Symbiotic nitrogen fixation in regenerating black locust (*Robinia pseudoacacia* L.) stands. *Forest Science* **30**: 528–537.

Carrara JE, Walter CA, Hawkins JS, Peterjohn WT, Averill C, Brzostek ER. 2018. Interactions among plants, bacteria, and fungi reduce extracellular enzyme activities under long-term N fertilization. *Global Change Biology* **24**:2721–2734.

DeWalle DR, Kochenderfer JN, Adams MB, Miller GW, Gilliam FS, Wood F, Odenwald-Clemens SS, Sharpe WE. 2006. Vegetation and Acidification. In: Adams MB, Dewalle DR, Hom JL, eds. The Fernow Watershed Acidification Study. Netherlands: Springer, 137–188.

Kelly CN. 2010. Carbon and nitrogen cycling in watersheds of contrasting vegetation types in the Fernow Experimental Forest, West Virginia. Doctoral dissertation, Virginia Tech.

Lehrter JC, Cebrian J. 2010. Uncertainty propagation in an ecosystem nutrient budget. *Ecological Applications* **20**: 508–524.

van't Hoff JH. 1898. Lectures on theoretical and physical chemistry. Chemical Dynamics Part I. 224-229. Edward Arnold, London.